# The first genotypic fitness network in a vertebrate reveals that hybridization increases access to novel fitness peaks

Austin H. Patton[1,2], Emilie J. Richards[1,2], Katelyn J. Gould[3], Logan K. Buie[3], Christopher H. Martin[1,2]

[1]*Department of Integrative Biology, University of California, Berkeley, CA*

[2]*Museum of Vertebrate Zoology, University of California, Berkeley, CA*

[3]*Department of Biology, University of North Carolina, Chapel Hill, NC*

**Keywords:** fitness landscape; genotypic fitness network adaptive radiation; introgression; standing genetic variation; *de novo* mutation

**Correspondence:** chmartin@berkeley.edu

**Abstract**

Estimating the complex relationship between fitness and genotype or phenotype (i.e. the adaptive landscape) is one of the central goals of evolutionary biology. Empirical fitness landscapes have now been estimated for numerous systems, from phage to proteins to finches. However, adaptive walks connecting genotypes to organismal fitness, speciation, and novel ecological niches are still poorly understood and the process by which fitness valleys are crossed remains controversial. One outstanding system for addressing these connections is a recent adaptive radiation of ecologically and morphologically novel pupfishes (a generalist, molluscivore, and scale-eater) endemic to San Salvador Island, Bahamas. Here, we leveraged whole-genome sequencing of 139 hybrids from two independent field fitness experiments to identify the genomic basis of fitness, visualize the first genotypic fitness networks in a vertebrate system, and measure the accessibility of adaptive walks on the fitness landscape. We identified 132 SNPs that were significantly associated with fitness in field enclosures. Six fitness-associated regions contained differentially expressed genes and fixed SNPs between trophic specialists; one gene (*mettle21e*) was also misexpressed in hybrids, suggesting a potential intrinsic genetic incompatibility. We then constructed genotypic fitness networks from adaptive alleles and showed that scale-eating specialists are most isolated on these networks. Furthermore, only introgressed and *de novo* variants, not standing genetic variation, increased the accessibility of genotypic fitness paths from generalist to specialists. Our results suggest that adaptive introgression and *de novo* mutations provided key connections in adaptive walks necessary for crossing fitness valleys and triggering the evolution of novelty during adaptive radiation.

**Significance**

*The fitness landscape describes the complex relationship between genotype or phenotype and fitness and is the conceptual bridge between micro- and macroevolution. There are many studies of phenotypic fitness landscapes across a range of animal and plant taxa, but studies of the genotypic fitness landscape remain limited to microbial systems and the function of individual proteins. Here, we conducted the first study investigating the genotypic fitness landscape for organismal fitness in an exceptionally young vertebrate adaptive radiation including a generalist algivore, molluscivore, and scale-eating pupfish. We show that hybridization and de novo mutations increase the availability of accessible pathways to new fitness peaks on the fitness landscape, enabling the evolution of novelty.*

## Introduction

First conceptualized by Sewell Wright in 1932, the adaptive landscape describes the complex relationship between genotype or phenotype and fitness (1). The landscape is a concept, metaphor, and an empirical measurement that exerts substantial influence over all evolutionary dynamics (2–6). Fitness landscapes were originally depicted as high-dimensional networks spanning genotypic space in which each genotype is associated with fitness (1). Simpson (7) later described phenotypic evolution of populations through time on a rugged landscape, in which isolated clusters of fitness peaks represent 'adaptive zones' relative to adjacent regions of low fitness (8). Lande and Arnold formalized the analysis of selection and estimation of phenotypic fitness landscapes (9–11), leading to empirical studies of fitness landscapes in numerous empirical systems (12–18). Fitness surfaces are also central components of speciation models and theory (19–21). Speciation can result from divergent selection (22), either on static landscapes or through negative frequency-dependent disruptive selection (23–28).

A fundamental concept in fitness landscape theory is that not all genotypic trajectories are accessible (5, 29, 30). Rather, only paths that monotonically increase in fitness at each mutational step are evolutionarily accessible, an expectation stemming from Fisher's fundamental theorem (31). These accessible genotypic trajectories can thus be considered potential adaptive walks under Fisher's geometric model (31, 32). There are a growing number of experimental studies of adaptive walks in nature, including the evolution of toxin resistance in monarch butterflies (33), alcohol tolerance in Drosophila (34, 35), and host-shift in aphids (36). Likewise, the accessibility of genotypic fitness networks has now been explored in numerous microbial systems, including the evolution of antibiotic resistance (29) and metabolism (37), citrate exploitation (38), and glucose limitation in *E. coli* (39), as well as adaptation to salinity in

83 yeast via evolution of heat shock protein *Hsp90* (40). However, these studies are still limited to
84 the investigation of specific coding substitutions and their effects on fitness in laboratory
85 environments. Nosil et al. (41) estimated genotypic fitness networks for *Timema* stick insects
86 based on a field experiment. However, this study still focused on a single large-effect locus
87 underlying dimorphic coloration between ecotypes. To our knowledge, no study has estimated
88 genotypic fitness landscapes in a vertebrate system among multiple species as originally
89 envisioned by Wright (1) despite the clear utility of this framework in bridging micro- and
90 macroevolutionary dynamics.

91 One promising system for estimating fitness landscapes is a recent adaptive radiation of
92 *Cyprinodon* pupfishes (17, 18, 42, 43). This radiation is comprised of two endemic specialists, a
93 molluscivore (durophage: *Cyprinodon brontotheroides*) and a scale-eater (lepidophage: *C.*
94 *desquamator*), derived from a Caribbean-wide generalist ancestor (*C. variegatus*). These three
95 species all occur in sympatry in the hypersaline lakes of San Salvador Island, Bahamas (Fig 1A).
96 Originating less than 10,000 years ago (based on geological age estimates for the lakes: (44)), the
97 functional and trophic novelty harbored within this radiation is the product of exceptional rates
98 of craniofacial morphological evolution (45–49). Furthermore, species boundaries appear to
99 persist across multiple lake populations, despite persistent admixture among species (50, 51). We
100 previously estimated fitness landscapes in these hypersaline lakes from two independent field
101 experiments measuring the growth and survival of hybrids placed in field enclosures. Selection
102 analyses revealed a stable, multi-peaked fitness landscape across lake populations, year of study,
103 and manipulation of the frequency of rare hybrid phenotypes (Fig. 1B: (17, 18, 43)). One of the
104 strongest and most persistent trends across studies and treatments was the apparent isolation of
105 hybrid phenotypes resembling the scale-eater by a large fitness valley from the other two species

(17, 18). Hybrids resembling the generalist occupied a fitness peak and were isolated by a smaller fitness valley from hybrids resembling the molluscivore in a second region of high fitness. Understanding how an ancestral generalist population crossed these fitness valleys is key to understanding the origins of novelty in this system, particularly given the rare evolution of lepidophagy (scale-eating), a niche occupied by less than 0.3% of all fishes (52, 53).

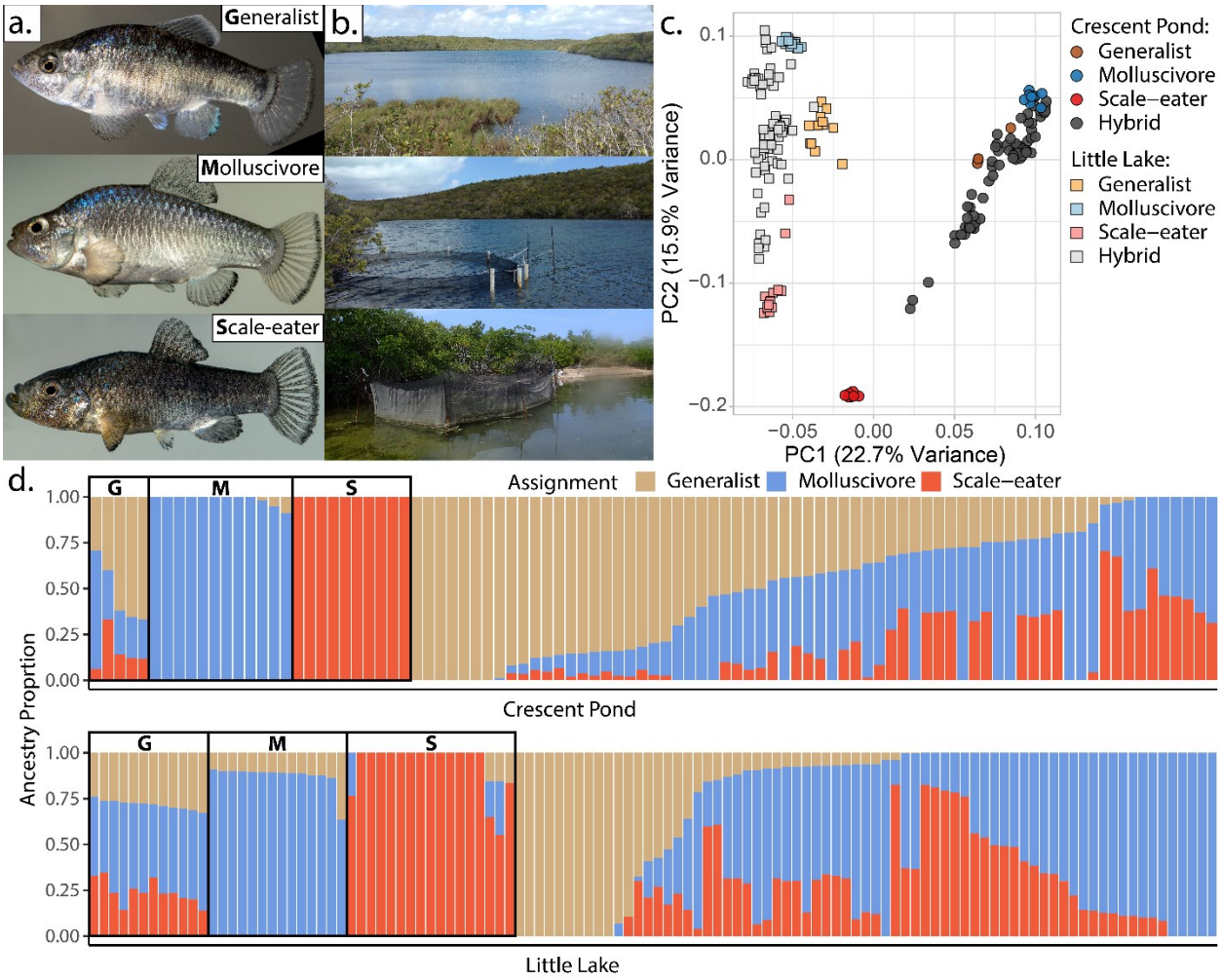


**Figure 1. San Salvador Island pupfishes and their hybrids. a.** From top to bottom: the generalist, *Cyprinodon variegatus*, the molluscivore *C. brontotheroides*, and the scale-eater *C. desquamator.* **b.** Representative images of experimental field enclosures. **c.** Principal component analysis of 1,129,771 SNPs genotyped in hybrids and the three parental species. **d.** ADMIXTURE analyses for Crescent Pond (top) and Little Lake (bottom). G, M and S indicate individual samples of Generalists (G), Molluscivores (M), and Scale-eaters (S), respectively, followed by all resequenced hybrid individuals from field experiments. Colors correspond to probability of assignment to one of three assumed populations/species (K = 3 in this analysis).

121 The relative contributions of standing genetic variation, *de novo* mutation, and
122 introgression to the tempo and mode of adaptive radiation are now of central interest to the field
123 of speciation genomics (54–59). Yet to date, no study has investigated the relative influence of
124 each on the accessibility of the fitness landscape, a critical determinant of the dynamics of
125 speciation. The adaptive radiation of San Salvador Island pupfishes, like many others (60–64),
126 appears to have resulted from a complex interplay of abundant standing genetic variation,
127 adaptive introgression from neighboring islands, and several *de novo* substitutions and deletions
128 found only in the scale-eater (51, 65). We have now identified many adaptive alleles showing
129 evidence of hard selective sweeps in each of the trophic specialists (51). Notably, both specialists
130 harbor numerous introgressed adaptive alleles in the regulatory regions of known craniofacial
131 genes (51, 65). In contrast, hard selective sweeps of *de novo* mutations only appear in the scale-
132 eating species, *C. desquamator*; many of these novel mutations also fall in or near craniofacial
133 genes, such as a single non-synonymous fixed substitution in the transcription factor and
134 oncogene *twist1* (51). Here, we leverage whole genome sequencing of 139 hybrids used in these
135 field experiments to identify the genomic basis of fitness differences, infer genotypic fitness
136 networks, and quantify the accessibility of novel fitness peaks and the influence of each source
137 of genetic variation on these adaptive walks.
138

139 **Results and Discussion**

140 *Population structure and ancestry association with fitness*

141 We resequenced 139 hybrids (86 survivors, 56 deaths (Table S1)) from two independent field
142 experiments across a total of six field enclosures and two lake populations (2011: two high-
143 density 3 m diameter enclosures for three months: Crescent Pond n = 796; Little Lake = 875 F2
144 hybrids (17); 2014/2015: four high-density 4 m diameter enclosures: three months in Crescent

Pond n = 923 F4/F5 hybrids; eleven months in Little Lake = 842 F4/F5 hybrids (66)). We then characterized patterns of genetic variation among parental species in each lake and their lab-reared hybrids used in field experiments. We genotyped 1,129,771 SNPs with an average coverage of 9.79x per individual. Principal components analysis (PCA) of genetic variation strongly differentiated pupfishes sampled from Little Lake/Osprey Lake and Crescent Pond (PC1: 22.7% variance explained) and among species within each lake (PC2: 15.9% variance explained: Fig. 1D; Fig. S1-S2). These results were supported by ADMIXTURE analyses (67, 68) (Fig. 1E). However, some hybrids were genotypically transgressive, falling outside the genotypic distributions of the three parental species (Fig. S2), leading ADMIXTURE to attribute the third population to these hybrids, rather than generalists which often contain segregating variation found in the trophic specialists (67).

Neither scale-eater nor molluscivore ancestry estimated by ADMIXTURE analysis was significantly associated with hybrid composite fitness (Fig. S3A, Table S2: Scale-eater $P$ = 0.164; molluscivore $P$ = 0.595), survival probability (Fig. S3B: Scale-eater $p$ = 0.804; molluscivore $P$ = 0.313), or growth (Fig. S3C: Scale-eater $P$ = 0.283; molluscivore $P$ = 0.328), while controlling for effects of lake and experiment. Similarly, neither PC1 nor PC2 was associated with composite fitness (Table S2). Furthermore, pairwise genetic distance did not predict pairwise morphological distance (Fig. S4). Therefore, in contrast to previous studies (70–72), in this system genome-wide ancestry is not associated with fitness, highlighting the complex nonlinear relationship between genotype, phenotype, and fitness within this nascent adaptive radiation. We must look to local ancestry to understand fitness relationships (e.g. (73)).

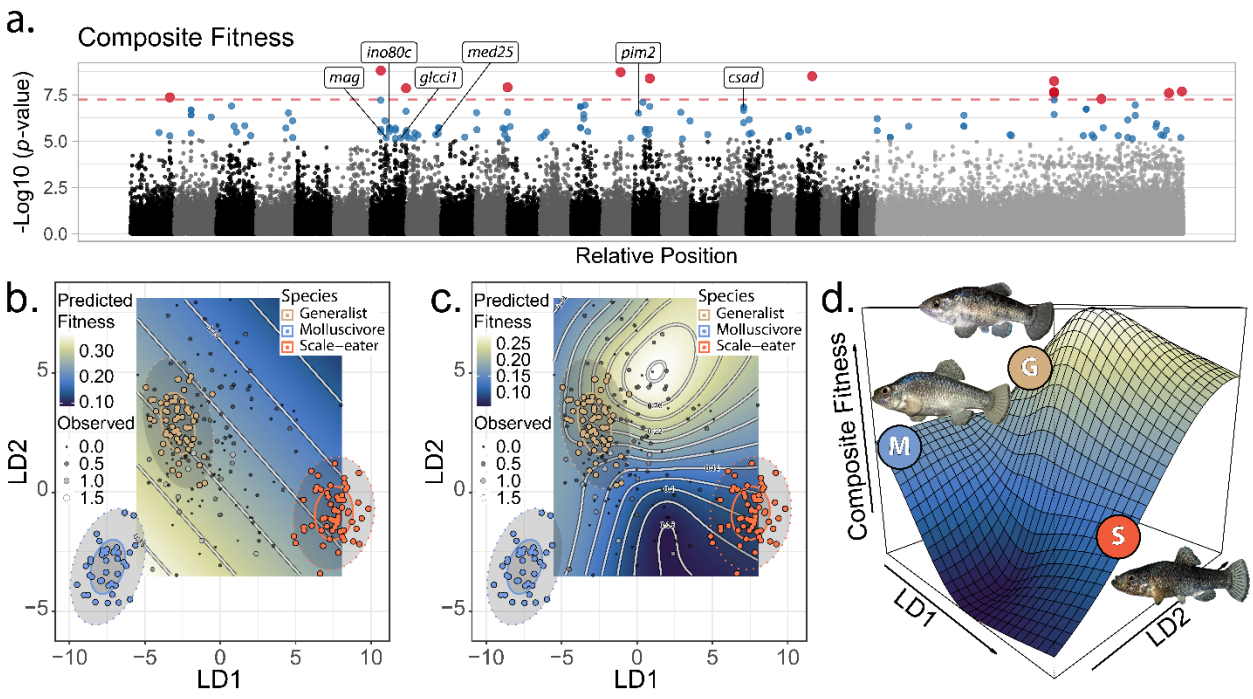


**Figure 2. The genetic basis of fitness variation and improved inference of adaptive landscapes. a)** Per-SNP -log10 *p*-values from a genome-wide association test with GEMMA for composite fitness (survival x growth). Lake and experiment were included as covariates in the linear mixed model. SNPs that were significant at FDR < 0.05 are indicated in blue; red SNPs above dashed red line cross the threshold for Bonferroni significance at α = 0.05. First twenty-four scaffolds are sorted from largest to smallest and remaining scaffolds were pooled. The six genes associated with composite fitness which were both strongly differentiated ($F_{ST}$ > 0.95) and differentially expressed between specialists (69) are annotated. **b-c)** Best-fit adaptive landscape for composite fitness using either morphology alone (**b:** flat surface with only directional selection) or morphology in combination with fitness associated SNPs (**c:** highly nonlinear surface). Best-fit model in C was a GAM including a thin plate spline for both LD axes, fixed effects of experiment and lake, and fixed effects of seven (see supplementary methods) SNPs most strongly associated with fitness shown in red. **c)** Three-dimensional view of **C** with relative positions of the three parental species indicated.

*Genome-wide association mapping of fitness*

From our LD-pruned dataset we used a linear mixed model in GEMMA to identify 132 SNPs in regions that were strongly associated with composite fitness, including 13 which remained significant at the conservative Bonferroni threshold (Fig. 2A, Table S3: See supplement for results for survival and growth alone [Table S4-S5; Figure S5-6]). Gene ontologies for these 132 fitness-associated regions were significantly enriched for synaptic signaling and chemical synaptic transmission (FDR rate < 0.01; Fig. S7; Table S5). Ontologies enriched at an FDR rate

190 < 0.05 were related to signaling and regulation of cell communication. We did not identify any
191 enrichment for ontologies related to craniofacial development which have previously been
192 identified to play a significant role in the adaptive divergence of these fishes (51, 65, 69, 74, 75).
193 This suggests that fitness-associated regions in our field experiments capture other components
194 of fitness in addition to the external phenotypes measured in previous studies. Surprisingly, our
195 fitness associated regions did not overlap with regions showing significant evidence of a hard
196 selective sweep (51). However, we did find six fitness-associated SNPs near genes differentially
197 expressed between specialists in addition to one that was also misexpressed in F1 hybrids (69).
198 This is particularly intriguing because gene misexpression in hybrids, i.e. genes differentially
199 expressed relative to both parents, could indicate the breakdown of genetic regulatory networks
200 in hybrids and intrinsic genetic incompatibilities that may impact their fitness in field enclosures
201 (69, 76).

202 We characterized whether genes in or near fitness-associated regions are implicated in
203 adaptive divergence of the specialists. Five fitness-associated genes have previously been shown
204 to include fixed divergent SNPs between specialists (*csad, glcci1, ino80c, mag, pim2*), and one
205 contained a fixed deletion between specialists (*med25*) (69). *med25* (Mediator Complex Subunit
206 25) is a craniofacial transcription factor associated with cleft palate in humans and zebrafish (77,
207 78). Four of the remaining genes shared across our study and McGirr et al. (69) are associated
208 with growth and/or body size measurements in other fishes. For example, *csad* plays an
209 important role in synthesizing taurine which is a rate-limiting enzyme affecting growth rate in
210 parrotfishes (79), rainbow trout (80), and Japanese flounder (81). Second, *glcci1* is associated
211 with the body depth/length ratio in the large yellow croaker (82). Third, *ino80c* is associated with
212 measures of body size in the Nile tilapia (83). The only gene associated with growth but not

213 composite fitness, *mettl21e*, was also misexpressed in F1 hybrids between scale-eaters and
214 molluscivores at eight days post-fertilization, and thus is a putative genetic incompatibility in this
215 system (69). Although it has not been associated with growth-related or body-size traits in fishes,
216 it is associated with intramuscular fat deposition in cattle (84). Taken together, these findings
217 support the interpretation that our fitness-associated regions are associated with unmeasured
218 traits, particularly physiological growth rates, or craniofacial shape in the case of the deletion in
219 *med25*, that affect fitness in our hybrid field experiments.
220
221 *Fitness-associated SNPs improve inference of the adaptive landscape*
222 We used linear discriminant axes and generalized additive modelling (GAM) to estimate
223 phenotypic fitness landscapes for the sequenced hybrids on a two-dimensional morphospace
224 indicating similarity to each of the three parental populations following previous studies (17, 18).
225 We then tested whether the inclusion of the 13 genomic regions most strongly associated with
226 fitness (red: Fig. 2A) in GAM models improved our inference of the underlying adaptive
227 landscape. Models with fitness-associated SNPs were invariably favored over models with
228 external morphology alone ($\Delta$AICc > 8.6: Tables S8-S9). Morphology-only models predicted a
229 flat linear landscape (Fig. 2B, Fig. S10); whereas including fitness-associated SNPs resulted in
230 inferences of increased curvature and complexity of the fitness surface, despite our limited
231 dataset of 139 hybrids relative to sample sizes in previous studies around 800 hybrids per
232 enclosure.
233 To reduce complexity of the full model estimated from 31 morphological traits including
234 all 13 fitness-associated SNPs, we fit an additional model including only the seven significant
235 fitness-associated SNPs in the full model. This reduced model was the best-fit; the inferred

236 adaptive landscape was complex and characterized by a fitness peak near hybrids resembling
237 generalist phenotypes separated by a small fitness valley from a second region of high fitness for
238 molluscivore hybrid phenotypes. Scale-eater hybrid phenotypes again corresponded to a large
239 fitness valley (Fig. 2B-C: For results pertaining to growth or survival see Supplemental Materials
240 – Fig. S10, Table S10-12). Compared to previous studies, the highest fitness optimum was
241 shifted from molluscivore phenotypes to generalists. This suggests that fitness-associated SNPs
242 increased the fitness of hybrids resembling generalists beyond expectations based on their
243 morphology alone, consistent with the hypothesis that fitness-associated SNPs are associated
244 with unmeasured traits affecting fitness. Indeed, visualization of haplotype frequency on the
245 fitness landscape supported this interpretation: one of the most common haplotypes associated
246 with high fitness was most frequent in hybrids resembling generalists and rare in hybrids
247 resembling specialists (Fig. S11).
248
249 *Trophic novelty is associated with isolation on the genotypic fitness landscape*
250 We reconstructed genotypic fitness networks from 1,498 candidate adaptive alleles previously
251 identified in this system (e.g. Fig. 3). These regions displayed significant evidence of a hard
252 selective sweep using both site frequency spectrum and LD-based methods, SweeD (85) and
253 OmegaPlus (86), and contained fixed or nearly fixed SNPs (Fst > 0.95) differentiating trophic
254 specialists across lakes (51). These fitness networks depict both hybrids and parental species in
255 genotypic space, with nodes representing SNP haplotypes and edges connecting mutational
256 neighbors (Fig. 3B). Genotype space is immense; using SNPs coded as homozygous reference,
257 heterozygote, or homozygous alternate, the number of potential haplotypes is equal to
258 $3^{\#\ SNPs\ in\ network}$. For instance, to construct a reduced network of even 100 SNPs, there would

be a total of $3^{100} = 5.17\ X\ 10^{57}$ possible nodes. Thus, unlike experimental studies of individual proteins in haploid *E. coli* (29, 39) or yeast (40), it is not possible for us to investigate the full breadth of genotypic space.

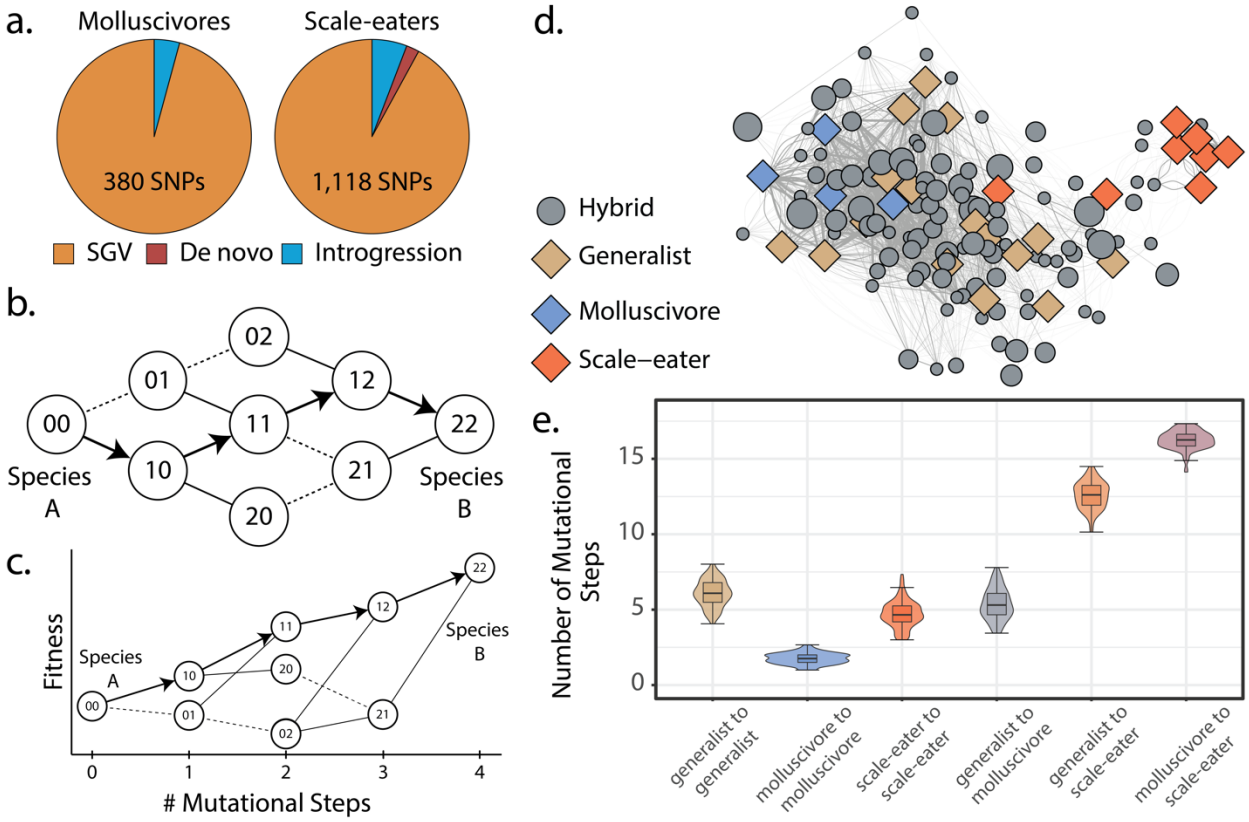


**Figure 3. Genotypic fitness networks connecting San Salvador Island pupfishes. a)** The majority of nearly fixed or fixed variants ($F_{ST} \geq 0.95$) experiencing hard selective sweeps (hereafter 'adaptive alleles') originated as standing genetic variation (SGV: molluscivores = 96%, scale-eaters = 92%), followed by introgression (molluscivores = 4%, scale-eaters = 6%), and lastly *de novo* mutation (scale-eaters = 2%)(51). Pie charts shows adaptive alleles retained in our study for each species. **b)** Diagram illustrating genotypic fitness networks and adaptive walks in a pair of species for two SNPs concatenated into haplotypes. Species A and B are separated by four mutational steps. Dashed lines are inaccessible as they result in a decrease in fitness; this leaves a single possible accessible evolutionary trajectory between species A and B (indicated by bold arrows). Each node is associated with an empirical measure of hybrid fitness. Edges are always drawn as directed, from low to high fitness. **c)** The same network as in B, with fitness plotted on the Y-axis and number of mutational steps from species A to B on the X-axis. Dashed lines are inaccessible (decreasing in fitness), solid lines are accessible (increasing in fitness), and the only accessible path between species A and B is indicated by solid arrows. **d)** Genotypic network constructed using a random sample of ten SNPs, sampled from all SNPs shown in **a**. Each edge between nodes is up to five mutational steps away; edge width is proportional to mutational distance: wider edges connect closer haplotypes. Node size (for hybrids) is scaled proportional to mean composite fitness; larger circles correspond to fitter haplotypes. **e)** Median number of mutational steps within or between species (e.g. Fig. 3C). All pairwise comparisons using Tukey's HSD test (after FDR correction) were significant.

282 Instead, to understand the distribution of parental species and their hybrids in genotypic
283 space, we began by using a random sample of ten SNPs drawn from our set of candidate adaptive
284 alleles in this system. We chose ten SNPs for this first analysis for a larger sample of SNPs to
285 characterize the overall structure of the genotypic fitness network, while not sampling too vast a
286 space; already, the number of possible genotypes exceeds 59,000. Here, we plotted edges
287 between nodes up to five mutational steps away and found that generalists and molluscivores are
288 closer in the genotypic fitness network than either is to scale-eaters (Fig 4A), as expected based
289 on their genetic distance. Most scale-eaters appear quite isolated in genotypic space, separated
290 from the generalist cluster of nodes by 12.6 ± 0.091 (mean ± SE: $P < 0.001$) mutational steps and
291 from molluscivores by 16.3 ± 0.060 steps ($P < 0.001$). In contrast, molluscivores were separated
292 from generalists by 5.37 ± 0.103 steps ($P < 0.001$). Generalists show the greatest intrapopulation
293 distances, separated from each other by 6.08 ± 0.088 steps ($P < 0.001$). In contrast,
294 molluscivores exhibited the smallest intrapopulation distances, separated by 1.75 ± 0.021 steps
295 ($P < 0.001$). Scale-eater intrapopulation distances were intermediate (4.71 ± 0.088 steps: $P <$
296 $0.001$).
297
298 *Adaptive introgression and* de novo *mutations increase accessibility of novel fitness peaks*
299 Evolutionary accessibility reflects the probability that one genotypic trajectory will be favored by
300 natural selection over another, and thus can be related to the predictability of evolution (5, 29,
301 30, 87, 88). Genotypic trajectories with the minimum number of steps between two states that are
302 characterized by monotonically increasing fitness at each step are considered to be the most
303 accessible (5, 29, 30). That is, each mutational step is favored by natural selection and longer

304 paths are less probable (30). This provides two useful metrics of fitness network accessibility: 1)
305 The number of accessible paths and 2) the shortest length of accessible paths.

306 The adaptive radiation of pupfishes on San Salvador island originated within the last
307 10,000 years through a combination of selection on standing genetic variation, adaptive
308 introgression, and *de novo* mutations (51). However, it is unclear how each source of genetic
309 variation aided in the traversal of fitness paths or contributed to the colonization of novel fitness
310 peaks. To address this question, we constructed genotypic fitness networks composed of each of
311 the three main sources of adaptive genetic variation: standing genetic variation, introgression
312 from one of four focal Caribbean generalist populations, or *de novo* mutations unique to San
313 Salvador Island. We also examined combinations of these categories to better reflect the stages
314 of adaptive divergence. We compared sets of 1,000 random 5-SNP genotypic networks drawn
315 from different sources of adaptive variation and identified and scored the lengths of accessible
316 paths (i.e. those monotonically increasing in fitness) from generalist to each specialist. We asked
317 whether source of genetic variation affected 1) the number of accessible paths or 2) the shortest
318 length of accessible paths.

319 We discovered that both scale-eater and molluscivore specialist fitness peaks in
320 genotypic networks constructed from introgressed or *de novo* adaptive mutations were
321 significantly more accessible than networks constructed from standing genetic variation (Fig. 4C,
322 Table S13, S16). Random networks drawn from these sources of adaptive variation contained
323 more accessible fitness paths from generalist to specialists than networks constructed from
324 standing genetic variation, while controlling for differences in overall network size (Figs. S12-
325 S13, Table S13). Specifically, networks constructed from adaptive introgression had 126% more
326 accessible paths than those constructed from standing variation for molluscivores (median: $P <$

0.0001: Fig. 4C), and 39% more for scale-eaters ($P < 0.0001$: Fig. 4C). Likewise, networks constructed from *de novo* mutations had 42% more accessible paths ($P < 0.0001$: Fig. 4C).

Consistent with past experimental studies in *E. coli* (29, 39) and yeast (40), accessible paths were quite rare; the vast majority of genotypic trajectories were inaccessible, i.e. they included one or more mutational steps that decreased in fitness from generalist to specialist. Compared to standing variation, accessible paths were also significantly shorter in introgressed (mean: 9% shorter in molluscivores: $P < 0.0001$, 23% shorter in scale-eaters: $P < 0.0001$) and *de novo* mutation networks (14% shorter in scale-eaters $P < 0.0001$: Fig. 4D. Fig S12, Tables S13, S17). Thus, introgressed and *de novo* adaptive mutations present more possible trajectories and reduce the number of steps needed to traverse between species and access novel trophic specialist fitness peaks (See Supplemental Materials Fig. S14-S15). These results are consistent with a growing body of evidence that *de novo* and introgressed variation may contribute to rapid speciation and evolution towards novel fitness peaks (38, 56, 62, 89–92).

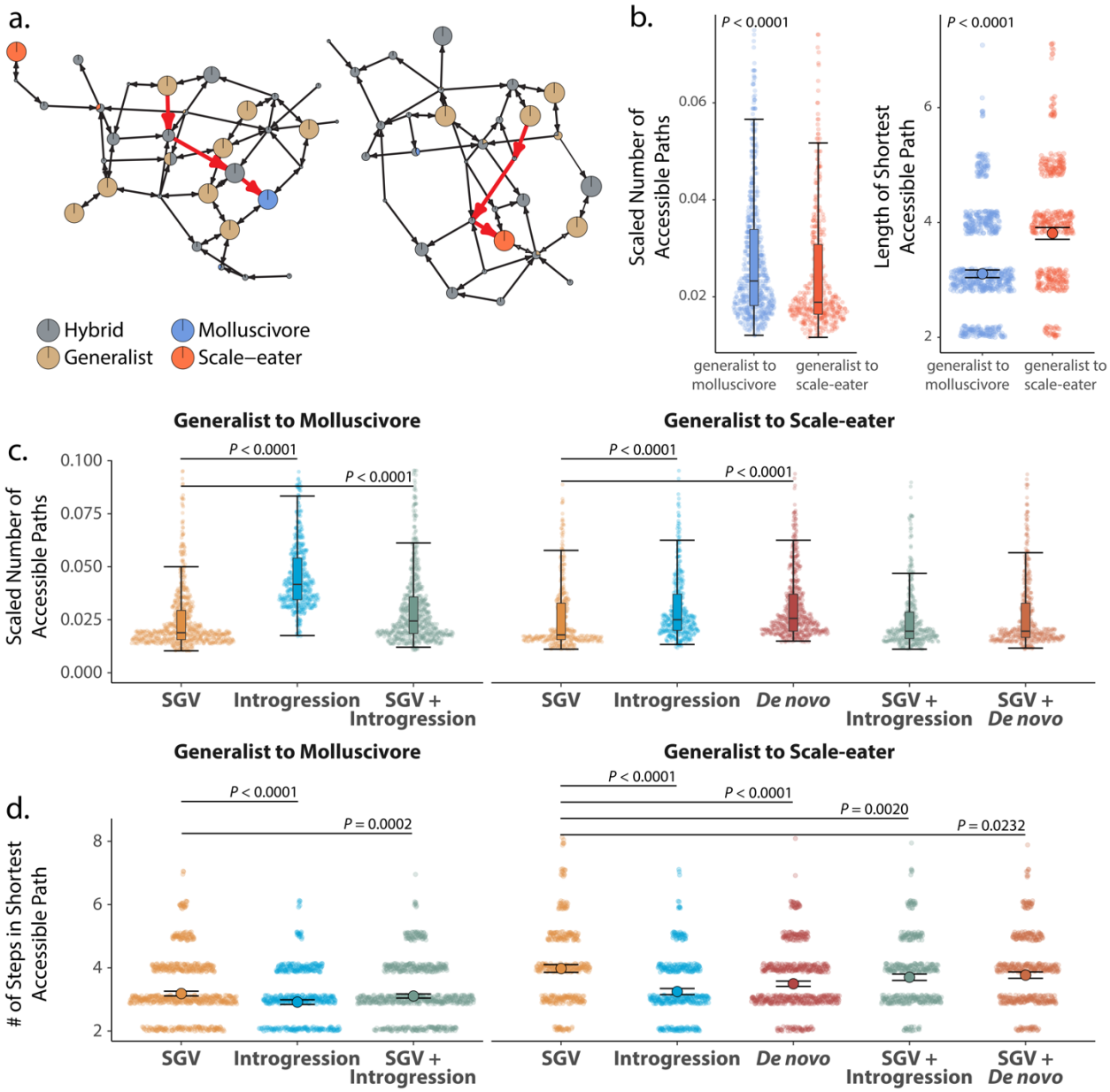


**Figure 4. Adaptive introgression and *de novo* mutations increase access to specialist fitness peaks. a)** Example genotypic fitness networks constructed from five SNPs randomly drawn from introgressed adaptive loci for molluscivores (left) or scale-eaters (right). Edges connect nodes (haplotypes) that are separated by a single mutational step, arrows indicate the direction of mutational steps (directed towards higher fitness or parental haplotypes if not observed in hybrids), and red arrows indicate an example accessible trajectory. **b)** Accessibility of genotypic trajectories separating generalists from specialists as measured using networks constructed from all adaptive loci. Left: Proportion of accessible (i.e. monotonically increasing in fitness) paths per network, scaled by the total size of the network. Right: Number of mutational steps in the shortest accessible path. Because of the discrete nature of these data, means are plotted as large circles, with two standard errors shown. Due to the highly skewed nature of these distributions, pairwise significance among all network sets was determined using a nonparametric Kruskal-Wallis one-way analysis of variance following correction for multiple tests using an estimated False Discovery Rate. **c-d)** The same plots as in **b**, but for fitness landscapes constructed from adaptive loci originating from standing genetic variation (SGV), introgression, *de novo* mutation, or a combination.

355 *Conclusion*

356 Here, we have analyzed the first multi-species genotypic fitness landscape based on hybrid
357 fitness across multiple field experiments. We have shown that adaptive introgression and *de novo*
358 mutation increase the accessibility of novel fitness peaks, thus promoting the evolution of
359 novelty. Adaptation from standing genetic variation may initially be more rapid due to its higher
360 frequency, initial availability, and potentially reduced genetic load within a population (93–95).
361 Novel fitness peaks are not inaccessible from standing genetic variation alone – rather, they are
362 simply *less* accessible and thus we predict that standing genetic variation alone is less likely to
363 have triggered adaptive radiation in this system (93).

364 Once genetic variation arrives from introgression or arises *de novo* in a population,
365 colonization of new adaptive zones may be expedited due to the reduced number of mutational
366 steps in accessible paths. Furthermore, *de novo* mutations that undergo selective sweeps are also
367 predicted to have larger effect sizes (96). These findings are consistent with an interpretation of
368 adaptive radiation unfolding in stages (51, 97), first via standing genetic variation, next
369 introgression from across the Caribbean, and finally *de novo* mutations.

370 Our findings also provide additional support for the isolation of scale-eaters on the fitness
371 landscape and the rare evolution of scale-eating specialists despite comparable environments
372 across the Caribbean with nearly identical levels of adaptive standing genetic variation. That is,
373 adaptive *de novo* mutations may enable the crossing of a large fitness valley by increasing the
374 number of accessible fitness pathways through genotype space. This in turn may then trap scale-
375 eater populations on this peak by reducing the number of accessible fitness pathways back to the
376 generalist peak. In short, by increasing accessibility of adaptive walks to novel trophic specialist

377 niches, *de novo* and introgressed adaptive alleles simultaneously reduce the accessibility of
378 reverting to the generalist niche after the population reaches the new adaptive optimum.
379

380 **Acknowledgements:**
381 We thank Michelle St. John, David Tian, and Jacqueline Galvez for insightful discussion of the
382 results; the Gerace Research Centre and Troy Day for logistical support; the government of the
383 Bahamas for permission to collect, import, and export samples; the Vincent J. Coates Genomics
384 Sequencing Center and Functional Genomics Laboratory at UC Berkeley for performing whole
385 genome library preparation and sequencing (supported by NIH S10 OD018174 Instrumentation
386 Grant), and the University of California, Berkeley and University of North Carolina at Chapel
387 Hill for computational resources. This work was funded by the National Science Foundation
388 DEB CAREER grant #1749764, National Institutes of Health grant 5R01DE027052-02, the
389 University of North Carolina at Chapel Hill, and the University of California, Berkeley to CHM,
390 graduate research funding from the Museum of Vertebrate Zoology to EJR, and an NSF
391 Postdoctoral Research Fellowship in Biology under Grant No. 2109838 to AHP. Genomic data
392 are archived at the National Center for Biotechnology Information BioProject Database
393 (Accessions: PRJNA690558; PRJNA394148, PRJNA391309).
394

395 **Methods:**
396 ***Sampling***
397 Our final dataset is comprised of 139 hybrid samples used in two separate field experiments (17,
398 18) on San Salvador island. Experiments were conducted in two lakes: Little Lake (N = 71) and
399 Crescent Pond (N = 68). Hybrids used in the first field experiment (17) were spawned in the lab
400 between December 2010 and January 2011; juveniles were raised for 2 months, individually

401 tagged by injecting a stainless steel sequential coded wire tag (Northwest Marine Technologies,
402 Inc.) into their left dorsal musculature, and photographed pre-release for morphometric analyses.
403 Experimental field enclosures consisted of high- and low-density treatments; density was varied
404 by the number of tagged juveniles released into each enclosure. Hybrids in the second field
405 experiment (18) were comprised of F4-F5 outbred juveniles resulting from crosses between all
406 three species. Individuals were spawned, raised, and tagged in an equivalent manner and
407 photographed prior to release. Experimental enclosures included high- and low-frequency
408 treatments in which the frequency of rare transgressive hybrid phenotypes was altered between
409 treatments in each lake.

410 All hybrids were measured for 32 external morphological traits (see below). Additionally,
411 we included sequenced parental species of the generalist (N = 17), molluscivores (N = 27) and
412 scale-eaters (N = 25) sampled from these two lakes previously included in Richards et al. (51).
413 Note that we treat samples from Little Lake and Osprey Lake as the same population because
414 these two lakes are connected within one hypersaline lake system and fish from these
415 populations are genetically undifferentiated (50, 51). For morphological analyses, we
416 additionally measured samples of 60 generalists, 38 molluscivores, and 60 scale-eaters raised in
417 the same laboratory common garden environment. A full list of samples is included in the
418 supplement (Table S1).

419

420 ***Sequencing, genotyping and filtering***

421 Raw reads from a combined set of 396 samples (see supplement) were first mapped to the *C.*
422 *brontotheroides* reference genome (genome size = 1.16 Gb; scaffold N50 = 32 Mb) (51) using
423 bwa-mem (v. 0.7.2). Duplicate reads were identified and reads using MarkDuplicates, and BAM

424 indices were subsequently generated using the Picard software package (98). Samples were
425 genotyped following Richards et al., (51) according to GATK best practices (99). Specifically,
426 Single Nucleotide Polymorphisms (SNPs) were called and filtered using hard-filtering criteria in
427 HaplotypeCaller. We used the following criteria in our filtering approach: QD < 2.0; QUAL <
428 20; FS < 60; MQRankSum < -12.5; ReadPosRankSum < -8 (99–101).

429 Following initial genotyping with GATK, we subsequently filtered our data further using
430 VCFtools (102). Specifically, we filtered using the following flags: --maf 0.05; --min-alleles 2; --
431 max-alleles 2; --min-meanDP 7; --max-meanDP 100; --max-missing 0.85. Indels were removed.
432 To reduce non-independence among sites in our final dataset, we conservatively removed sites in
433 strong linkage disequilibrium using plink v1.9 (--indep-pairwise 10['kb'] 50 0.5: (103)). Doing so
434 resulted in the retention of 1,129,771 SNPs across 139 hybrid samples and the 69 samples from
435 Richards et al (51). Unless otherwise specified, these SNPs were used for all downstream
436 analyses.
437

438 ***Hybrid fitness measures***

439 We used three measures of fitness: survival, growth, or a composite measure of the two. Survival
440 was a binary trait indicating whether a fish survived (i.e. a tagged fish was recovered) or not
441 during its exposure period in field enclosures. Growth was a continuous measure, defined as the
442 proportional increase in Standard Length $\left(\frac{Final\ SL - Starting\ SL}{Starting\ SL}\right)$. Lastly, we defined composite
443 fitness as survival * growth, similar to the metric used in (104), and analogous to composite
444 fitness in Hereford (105) who used fecundity as their second fitness measure, rather than growth.
445 Because composite fitness represents the most information rich metric of fitness, we report

446 composite fitness results in the main text; results for growth and survival are included in the
447 supplement.
448
449 ***Population genetic variation***
450 To visualize genetic variation present in hybrids and across lakes (Crescent Pond and Little
451 Lake), we first used a Principal Components Analysis (PCA) of genetic variation using plink
452 v1.90 ((103), Fig. 1), plotting the first two principal component axes using R (version 3.6.3 (R
453 Core team 2020). We then estimated admixture proportions in hybrids using ADMIXTURE
454 v1.3.0 (67). Parental species found on San Salvador Island were substantially differentiated
455 among Crescent Pond and Little Lake (50, 51); thus, independent ADMIXTURE analyses were
456 conducted for each lake. Because we were primarily interested in admixture proportions of
457 hybrids, we set K = 3 in these analyses, corresponding to the three parental species used in
458 hybrid crosses. Using admixture proportions of hybrid individuals, we tested the hypothesis that
459 ancestry predicts hybrid composite fitness in experimental field enclosures by fitting a
460 generalized additive model including either 1) scale-eater ancestry or 2) molluscivore ancestry
461 with fixed effects for experiment and lake. This was repeated for survival and growth separately.
462
463 ***Genome-wide association tests***
464 To identify SNPs that were most strongly associated with fitness (survival, growth, or
465 composite), we implemented the linear mixed model (LMM) approach in GEMMA (v. 0.98.1:
466 (106)). This analysis was repeated using each fitness measure as the response variable. To
467 account for relatedness among samples we estimated the kinship matrix among all 139 hybrid
468 samples, which in turn were used in downstream LMMs. To account for the potentially

469 confounding effect of year/experiment and lake on estimated fitness measures, we included each
470 as covariates in the LMMs. To ensure rare variants were not included in these analyses, we only
471 included sites that had a minor allele frequency greater than 5% across all hybrids. A total of
472 933,520 SNPs were analyzed; 196,251 SNPS were excluded due to allele frequency change
473 following removal of parental species. SNPs strongly associated with fitness were identified as
474 1) a False Discovery Rate (FDR: Benjamini and Hochberg 1995) less than 0.05, or a 2) *P*-value
475 < 0.05 following a Bonferroni correction. We focus primarily on the sites identified by the
476 conservative Bonferroni correction, however.
477
478 ***Gene ontology enrichment***
479 We annotated sites that were significantly associated with fitness using snpEff (107) and the
480 annotated *C. brontotheroides* reference genome (51). That is, we constructed a custom database
481 within snpEff using the functional annotations originally produced by Richards et al. (51), and
482 subsequently extracted information on the annotations and putative functional consequences of
483 each variant.
484 Using genes identified for each SNP that is significantly associated with one of the fitness
485 measures, we performed Gene Ontology (GO) enrichment analyses using ShinyGO v0.61 (108).
486 For genes identified as being intergenic, we included both flanking genes. As in Richards et al.
487 (2021), the gene symbol (abbreviation) database that had the greatest overlap with ours was that
488 of the human database; thus, we tested for enrichment of biological process ontologies curated
489 for human gene functions, based on annotations from Ensembl. Results are reported for
490 biological processes that were significantly enriched with FDR < 0.05. We then compared this

491 list of candidate loci to those identified in past studies of San Salvador Island pupfishes (51, 69,
492 109).
493
494 ***Morphometrics***
495 We measured 31 external morphological traits for all 139 hybrids and 69 parental individuals
496 from Crescent Pond (30 generalists, 19 molluscivores, and 30 scale-eaters) and 85 from Little
497 Lake (30 generalists, 25 molluscivores, and 30 scale-eaters). We digitally landmarked dorsal and
498 lateral photographs (both sides) of each lab-reared hybrid (pre-release) or parent using DLTdv8
499 (110). Measurements include 27 linear characters and three angles. For nearly all individuals,
500 lateral measurements were collected from both lateral photographs and averaged. Morphological
501 variables were size-corrected using the residuals of a log10(trait) – log10(standard length)
502 regression standardized for selection analyses as outlined in the supplement. We used these 31
503 morphological traits to estimate two linear discriminant (LD) axes that best distinguished the
504 generalist, molluscivore, and scale-eater using the LDA function in the mass package in R. We
505 then used the resultant LD model to predict LD-scores for the 139 sequenced hybrids for later
506 use in generalized additive models.
507
508 ***Estimation of adaptive landscapes***
509 We fit generalized additive models (GAMs) using the mgcv package v. 1.8.28 (111) in R to
510 estimate fitness landscapes relating the two discriminant axes (LD1-2) to fitness. All models
511 included a thin-plate spline fitted for the two linear discriminant axes, and we included both lake
512 and experiment in all models as fixed effects. Lake x experiment interaction terms were also
513 included in some models. Models were ranked using the corrected Akaike Information Criterion

514 (AICc) and were considered to be a significantly worse fit if ΔAICc > 4 from the best-fit model
515 (112). The best-fit model from the above approach was in turn used to visualize fitness
516 landscapes, plotting predicted values of fitness measures across LD space in R.
517 Using these results, we tested whether inclusion of SNPs that were strongly associated
518 with fitness (i.e., those that surpassed the 0.05 Bonferroni threshold) improved estimation of
519 fitness landscapes. We first extracted genotypes for the highly significant SNPs identified by
520 GEMMA (13 for composite fitness, four for growth: see section *Fitness-genotype association*
521 *test*), and coded these as either reference, single or double mutants using VCFtools (102). We
522 then used the best-fit models identified above and fit a range of models that included one or all
523 SNPs. Individual fitness-associated SNPs were treated as ordered factors (i.e. transition from
524 homozygous reference to heterozygote to homozygous alternate) and modeled using a factor-
525 smooth in the generalized additive models. Note that factor "smooths" are effectively modeled as
526 step-functions.
527
528 ***Estimation of genotypic fitness networks***
529 We first estimated genotypic networks using sites previously shown to be highly divergent ($F_{ST}$
530 > 0.95) and having undergone hard selective sweeps in specialists. To do so, we identified the
531 SNPs in our unpruned full dataset overlapping with sites inferred to have undergone selective
532 sweeps (51), resulting in 380 SNPs for molluscivores and 1,118 SNPs for scale-eaters. We
533 subsequently constructed genotypic fitness networks in igraph v. 1.2.4.1 (113) following the
534 procedure outlined in the supplement.
535 To visualize the high-dimensional genotypic fitness network, we randomly sampled ten
536 adaptive loci 100 times and plotted haplotypes connected by edges if they were within five

537 mutational steps of one another (Figure 3C). Then we calculated the mean distance between all
538 species pairs (in number of mutational steps). We used pairwise Tukey's HSD tests to test whether
539 inter-species distances differed.
540
541 ***Estimation of evolutionary accessibility***
542 We tested whether the evolutionary accessibility of genotypic fitness trajectories through
543 observed hybrid genotypes from generalist to each specialist species differed based on the source
544 of genetic variation. We restricted our investigation to networks composed of adaptive loci as
545 previously described (Figure 3A: Richards et al. 2021). This included a total of 380 SNPs in the
546 molluscivores, and 1,118 in the scale-eaters. The reduced number of adaptive SNPs sites in our
547 dataset as compared to that of (51) is due in large part to the increased stringency of our filtering.
548 We further partitioned these SNPs by their respective sources: standing genetic variation
549 (molluscivore N = 364; scale-eater N = 1,029), *de novo* mutation (scale-eater N = 24), or
550 introgression (molluscivore N = 16; scale-eater N = 65), again using the assignments from
551 Richards et al. (51). For analyses of trajectories between generalists and molluscivores, we
552 included only SNPs found to be sweeping in molluscivores; likewise, we included only SNPs
553 sweeping in scale-eaters for analysis of trajectories between generalists and scale-eaters.
554 The full procedure for constructing genotypic fitness networks, identifying accessible
555 paths, and quantifying accessibility is outlined in the supplement. Briefly, we randomly
556 generated 1,000 datasets of five SNPs comprised of either 1) standing genetic variation, 2)
557 adaptive introgression, 3) *de novo* mutation, 4) standing genetic variation + adaptive
558 introgression, or 5) standing genetic variation + *de novo* mutation. We additionally repeated this
559 procedure using all three classes of SNPs for scale-eaters to determine whether genotypic

560 trajectories separating generalists to molluscivores are more accessible than those between
561 generalists and scale-eaters. Because different sets of sites are sweeping in each specialist, we
562 conducted these analyses separately for each species. We then constructed genotypic networks,
563 in which nodes are haplotypes of SNPs encoded in 012 format (0 = homozygous reference, 1 =
564 heterozygote, 2 = homozygous alternate), and edges link mutational neighbors. When
565 determining whether a path was accessible or not, we only included paths for which each
566 mutational step (i.e. each intervening haplotype) between generalist to specialist was observed in
567 at least one hybrid sample.

568 For each random network sample and for each measure of fitness we calculated 1) the
569 minimum length of accessible paths between a random generalist and specialist sampled from
570 our sequenced individuals, 2) the number of accessible paths between the same generalist and
571 specialist pair, 3) the number of nodes and 4) the number of edges in the network. Larger
572 networks will necessarily have a greater number of potential paths, including both accessible and
573 inaccessible paths (Fig. S16), and we were interested in the relative proportion of accessible
574 adaptive pathways, not just the raw number. For this reason and because network size differs
575 among permutations, we divided the number of accessible paths in each random network
576 sampled by the number of nodes, thus normalizing the counts and making them comparable
577 across replicates and sources of variation. We assessed whether differences in these measures
578 among the three sources of variation or between the two alternate generalist to specialist
579 trajectories were significant using an ANOVA in R; due to the highly skewed nature of these
580 distributions, post-hoc pairwise significance was assessed using a nonparametric Kruskal-Wallis
581 one way analysis of variance in the agricolae package (114) in R.

**Literature Cited**


1. S. Wright, The roles of mutation, inbreeding, crossbreeding and selection in evolution. *Sixth Int. Congr. Genet.*, 356–366 (1932).
2. S. Gavrilets, Evolution and speciation on holey adaptive landscapes. *Trends Ecol. Evol.* **12**, 307–312 (1997).
3. S. Gavrilets, "High-dimensional fitness landscapes and speciation" in *Evolution—the Extended Synthesis*, M. Pigliucci, G. B. Müller, Eds. (MIT Press, 2010), pp. 51–64.
4. E. Svensson, R. Calsbeek, *The adaptive landscape in evolutionary biology*, E. Svensson, R. Calsbeek, Eds. (Oxford University Press, 2012).
5. I. Fragata, A. Blanckaert, M. A. Dias Louro, D. A. Liberles, C. Bank, Evolution in the light of fitness landscape theory. *Trends Ecol. Evol.* **34**, 69–82 (2019).
6. K. K. Fear, T. Price, The adaptive surface in ecology. *Oikos* **82**, 440–448 (1998).
7. G. G. Simpson, *Tempo and mode in evolution* (Columbia University Press, 1944).
8. S. Kauffman, S. Levin, Towards a general theory of adaptive walks on rugged landscapes. *J. Theor. Biol.* **128**, 11–45 (1987).
9. R. Lande, S. J. Arnold, The measurement of selection on correlated characters. *Evolution* **37**, 1226 (1983).
10. S. J. Arnold, M. E. Pfrender, A. G. Jones, "The adaptive landscape as a conceptual bridge between micro- and macroevolution" in *Microevolution Rate, Pattern, Process*, (Springer, Dordrecht, 2001), pp. 9–32.
11. S. J. Arnold, Performance surfaces and adaptive landscapes. *Integr. Comp. Biol.* **43**, 367–375 (2003).
12. D. Schluter, P. R. Grant, Determinants of morphological patterns in communities of Darwin's finches. *Am. Nat.* **123**, 175–196 (1984).
13. D. Schluter, Estimating the form of natural selection on a quantitative trait. *Evolution* **42**, 849–861 (1988).
14. A. P. Hendry, S. K. Huber, L. F. De León, A. Herrel, J. Podos, Disruptive selection in a bimodal population of Darwin's finches. *Proc. R. Soc. B Biol. Sci.* **276**, 753–759 (2009).
15. M. O. Beausoleil, *et al.*, Temporally varying disruptive selection in the medium ground finch (Geospiza fortis). *Proc. R. Soc. B Biol. Sci.* **286** (2019).
16. C. W. Benkman, Divergent selection drives the adaptive radiation of crossbills. *Evolution* **57**, 1176–1181 (2003).
17. C. H. Martin, P. C. Wainwright, Multiple fitness peaks on the adaptive landscape drive adaptive radiation in the wild. *Science* **339**, 208–211 (2013).
18. C. H. Martin, K. J. Gould, Surprising spatiotemporal stability of a multi-peak fitness landscape revealed by independent field experiments measuring hybrid fitness. *Evol. Lett.*, evl3.195 (2020).
19. S. Gavrilets, *Fitness landscapes and the origin of species* (Princeton University Press, 2004).
20. M. Turelli, N. H. Barton, J. A. Coyne, Theory and speciation. *Trends Ecol. Evol.* **16**, 330–343 (2001).
21. M. R. Servedio, J. W. Boughman, The role of sexual selection in local adaptation and speciation. *Annu. Rev. Ecol. Evol. Syst.* **48**, 85–109 (2017).
22. N. H. Barton, "Founder effect speciation" in *Speciation and Its Consequences*, D. Otte, J. A. Endler, Eds. (Sinauer, 1989), pp. 229–256.
23. U. Dieckmann, M. Doebeli, On the origin of species by sympatric speciation. *Nature* **400**,

354–357 (1999).
24. D. I. Bolnick, Can intraspecific competition drive disruptive selection? An experimental test in natural populations of sticklebacks. *Evolution* **58**, 608–618 (2004).
25. F. J. Weissing, P. Edelaar, G. S. van Doorn, Adaptive speciation theory: A conceptual review. *Behav. Ecol. Sociobiol.* **65**, 461–480 (2011).
26. J. E. Cresswell, C. Galen, Frequency-dependent selection and adaptive surfaces for floral character combinations: the pollination of Polemonium viscosum. *Am. Nat.* **138**, 1342–1353 (1991).
27. S. P. Otto, M. R. Servedio, S. L. Nuismer, Frequency-dependent selection and the evolution of assortative mating. *Genetics* **179**, 2091–2112 (2008).
28. B. C. Haller, A. P. Hendry, Solving the paradox of stasis: Squashed stabilizing selection and the limits of detection. *Evolution* **68**, 483–500 (2014).
29. D. M. Weinreich, N. F. Delaney, M. A. DePristo, D. L. Hartl, Darwinian evolution can follow only very few mutational paths to fitter proteins. *Science* **312**, 111–114 (2006).
30. J. Franke, A. Klözer, J. A. G. M. de Visser, J. Krug, Evolutionary accessibility of mutational pathways. *PLoS Comput. Biol.* **7**, 1002134 (2011).
31. R. A. Fisher, *The genetical theory of natural selection* (Oxford University Press, 1930).
32. H. A. Orr, The genetic theory of adaptation: A brief history. *Nat. Rev. Genet.* **6**, 119–127 (2005).
33. M. Karageorgi, *et al.*, Genome editing retraces the evolution of toxin resistance in the monarch butterfly. *Nature* **574**, 409–412 (2019).
34. M. A. Siddiq, D. W. Loehlin, K. L. Montooth, J. W. Thornton, Experimental test and refutation of a classic case of molecular adaptation in Drosophila melanogaster. *Nat. Ecol. Evol.* **1**, 25 (2017).
35. M. A. Siddiq, J. W. Thornton, Fitness effects but no temperature-mediated balancing selection at the polymorphic Adh gene of Drosophila melanogaster. *Proc. Natl. Acad. Sci. U. S. A.* **116**, 21634–21640 (2019).
36. K. S. Singh, *et al.*, The genetic architecture of a host shift: An adaptive walk protected an aphid and its endosymbiont from plant chemical defenses. *Sci. Adv.* **6**, eaba1070 (2020).
37. F. Peng, *et al.*, Effects of beneficial mutations in pykF gene vary over time and across replicate populations in a long-term experiment with bacteria. *Mol. Biol. Evol.* **35**, 202–210 (2018).
38. Z. D. Blount, C. Z. Borland, R. E. Lenski, Historical contingency and the evolution of a key innovation in an experimental population of Escherichia coli. *Proc. Natl. Acad. Sci. U. S. A.* **105**, 7899–7906 (2008).
39. A. I. Khan, D. M. Dinh, D. Schneider, R. E. Lenski, T. F. Cooper, Negative epistasis between beneficial mutations in an evolving bacterial population. *Science* **332**, 1193–1196 (2011).
40. C. Bank, S. Matuszewski, R. T. Hietpas, J. D. Jensen, On the (un)predictability of a large intragenic fitness landscape. *Proc. Natl. Acad. Sci. U. S. A.* **113**, 14085–14090 (2016).
41. P. Nosil, *et al.*, Ecology shapes epistasis in a genotype–phenotype–fitness map for stick insect colour. *Nat. Ecol. Evol.* **4**, 1673–1684 (2020).
42. C. H. Martin, P. C. Wainwright, A remarkable species flock of Cyprinodon pupfishes endemic to San Salvador Island, Bahamas. *Bull. Peabody Museum Nat. Hist.* **54**, 231–241 (2013).
43. C. H. Martin, Context dependence in complex adaptive landscapes: frequency and trait-

dependent selection surfaces within an adaptive radiation of Caribbean pupfishes. *Evolution* **70**, 1265–1282 (2016).

44. B. J. Turner, D. D. Duvernell, T. M. Bunt, M. G. Barton, Reproductive isolation among endemic pupfishes (Cyprinodon) on San Salvador Island, Bahamas: Microsatellite evidence. *Biol. J. Linn. Soc.* **95**, 566–582 (2008).
45. C. H. Martin, P. C. Wainwright, Trophic novelty is linked to exceptional rates of morphological diversification in two adaptive radiations of cyprinodon pupfish. *Evolution* **65**, 2197–2212 (2011).
46. C. H. Martin, The cryptic origins of evolutionary novelty: 1000-fold faster trophic diversification rates without increased ecological opportunity or hybrid swarm. *Evolution* **70**, 2504–2519 (2016).
47. M. E. St. John, K. E. Dixon, C. H. Martin, Oral shelling within an adaptive radiation of pupfishes: Testing the adaptive function of a novel nasal protrusion and behavioural preference. *J. Fish Biol.* **97**, 163–171 (2020).
48. C. H. Martin, J. A. McGirr, E. J. Richards, M. E. St. John, How to investigate the origins of novelty: Insights gained from genetic, behavioral, and fitness perspectives. *Integr. Org. Biol.* **1** (2019).
49. M. E. St. John, R. Holzman, C. H. Martin, Rapid adaptive evolution of scale-eating kinematics to a novel ecological niche. *J. Exp. Biol.* **223** (2020).
50. C. H. Martin, L. C. Feinstein, Novel trophic niches drive variable progress towards ecological speciation within an adaptive radiation of pupfishes. *Mol. Ecol.* **23**, 1846–1862 (2014).
51. E. J. Richards, *et al.*, A vertebrate adaptive radiation is assembled from an ancient and disjunct spatiotemporal landscape. *Proc. Natl. Acad. Sci.* **118**, e2011811118 (2021).
52. C. H. Martin, P. C. Wainwright, On the measurement of ecological novelty: Scale-eating pupfish are separated by 168 my from other scale-eating fishes. *PLoS One* **8**, e71164 (2013).
53. R. Froese, D. Pauldy, FishBase. *FishBase* (2021).
54. O. Seehausen, others, Genomics and the origin of species. *Nat. Rev. Genet.* **15**, 176–192 (2014).
55. S. H. Martin, C. D. Jiggins, Interpreting the genomic landscape of introgression. *Curr. Opin. Genet. Dev.* **47**, 69–74 (2017).
56. D. A. Marques, J. I. Meier, O. Seehausen, A Combinatorial View on Speciation and Adaptive Radiation. *Trends Ecol. Evol.* **34**, 531–544 (2019).
57. J. W. Poelstra, E. J. Richards, C. H. Martin, Speciation in sympatry with ongoing secondary gene flow and a potential olfactory trigger in a radiation of Cameroon cichlids. *Mol. Ecol.* **27**, 4270–4288 (2018).
58. T. C. Nelson, W. A. Cresko, Ancient genomic variation underlies repeated ecological adaptation in young stickleback populations. *Evol. Lett.* **2**, 9–21 (2018).
59. K. A. Thompson, M. M. Osmond, D. Schluter, Parallel genetic evolution and speciation from standing variation. *Evol. Lett.* **3**, 129–141 (2019).
60. J. B. Pease, D. C. Haak, M. W. Hahn, L. C. Moyle, Phylogenomics reveals three sources of adaptive variation during a rapid radiation. *PLoS Biol.* **14**, e1002379 (2016).
61. E. J. Richards, J. W. Poelstra, C. H. Martin, Don't throw out the sympatric speciation with the crater lake water: fine-scale investigation of introgression provides equivocal support for causal role of secondary gene flow in one of the clearest examples of sympatric

speciation. *Evol. Lett.* **2**, 524–540 (2018).
62. J. I. Meier, *et al.*, Ancient hybridization fuels rapid cichlid fish adaptive radiations. *Nat. Commun.* **8**, 14363 (2017).
63. M. D. McGee, *et al.*, The ecological and genomic basis of explosive adaptive radiation. *Nature* **586**, 75–79 (2020).
64. I. Irisarri, *et al.*, Phylogenomics uncovers early hybridization and adaptive loci shaping the radiation of Lake Tanganyika cichlid fishes. *Nat. Commun.* **9**, 1–12 (2018).
65. E. J. Richards, C. H. Martin, Adaptive introgression from distant Caribbean islands contributed to the diversification of a microendemic adaptive radiation of trophic specialist pupfishes. *PLoS Genet.* **13**, e1006919 (2017).
66. C. H. Martin, K. J. Gould, Surprising spatiotemporal stability of a multi-peak fitness landscape revealed by independent field experiments measuring hybrid fitness. *Evol. Lett.* **4**, 530–544 (2020).
67. D. H. Alexander, J. Novembre, K. Lange, Fast model-based estimation of ancestry in unrelated individuals. *Genome Res.* **19**, 1655–1664 (2009).
68. D. H. Alexander, K. Lange, Enhancements to the ADMIXTURE algorithm for individual ancestry estimation. *BMC Bioinformatics* **12**, 1–6 (2011).
69. J. A. McGirr, C. H. Martin, Ecological divergence in sympatry causes gene misexpression in hybrids. *Mol. Ecol.* **29**, 2707–2721 (2020).
70. M. E. Arnegard, *et al.*, Genetics of ecological divergence during speciation. *Nature* **511**, 307–311 (2014).
71. S. Wang, J. J. Hard, F. Utter, Genetic variation and fitness in salmonids. *Conserv. Genet.* **3**, 321–333 (2002).
72. R. Leimu, P. Mutikainen, J. Koricheva, M. Fischer, How general are positive relationships between plant population size, fitness and genetic variation? *J. Ecol.* **94**, 942–952 (2006).
73. D. Schluter, *et al.*, Fitness maps to a large-effect locus in introduced stickleback populations. *Proc. Natl. Acad. Sci. U. S. A.* **118**, 1914889118 (2021).
74. C. H. Martin, P. A. Erickson, C. T. Miller, The genetic architecture of novel trophic specialists: larger effect sizes are associated with exceptional oral jaw diversification in a pupfish adaptive radiation. *Mol. Ecol.* **26**, 624–638 (2017).
75. J. A. McGirr, C. H. Martin, Parallel evolution of gene expression between trophic specialists despite divergent genotypes and morphologies. *Evol. Lett.* **2**, 62–75 (2018).
76. J. Kulmuni, A. M. Westram, Intrinsic incompatibilities evolving as a by-product of divergent ecological selection: Considering them in empirical studies on divergence with gene flow. *Mol. Ecol.* **26**, 3093–3103 (2017).
77. Y. Nakamura, *et al.*, Wwp2 is essential for palatogenesis mediated by the interaction between Sox9 and mediator subunit 25. *Nat. Commun.* **2**, 1–10 (2011).
78. L. Mork, G. Crump, "Zebrafish craniofacial development: A Window into early patterning" in *Current Topics in Developmental Biology*, Y. Chai, Ed. (Academic Press Inc., 2015), pp. 235–269.
79. S. J. Lim, *et al.*, Taurine is an essential nutrient for juvenile parrot fish Oplegnathus fasciatus. *Aquaculture* **414–415**, 274–279 (2013).
80. T. G. Gaylord, A. M. Teague, F. T. Barrows, Taurine supplementation of all-plant protein diets for rainbow trout (Oncorhynchus mykiss). *J. World Aquac. Soc.* **37**, 509–517 (2006).
81. M. Yokoyama, T. Takeuchi, G. S. Park, J. Nakazoe, Hepatic cysteinesulphinate decarboxylase activity in fish. *Aquac. Res.* **32**, 216–220 (2001).

82. Z. Zhou, *et al.*, Genome-wide association study of growth and body-shape related traits in large yellow croaker (Larimichthys crocea) using ddRAD sequencing. *Mar. Biotechnol.* **21**, 655–670 (2019).
83. G. M. Yoshida, J. M. Yáñez, Multi-trait GWAS using imputed high-density genotypes from whole-genome sequencing identifies genes associated with body traits in Nile tilapia. *BMC Genomics* **22**, 1–13 (2021).
84. L. F. S. Fonseca, *et al.*, Gene expression profiling and identification of hub genes in Nellore cattle with different marbling score levels. *Genomics* **112**, 873–879 (2020).
85. P. Pavlidis, D. Živković, A. Stamatakis, N. Alachiotis, SweeD: Likelihood-based detection of selective sweeps in thousands of genomes. *Mol. Biol. Evol.* **30**, 2224–2234 (2013).
86. N. Alachiotis, A. Stamatakis, P. Pavlidis, OmegaPlus: A scalable tool for rapid detection of selective sweeps in whole-genome datasets. *Bioinformatics* **28**, 2274–2275 (2012).
87. F. J. Poelwijk, D. J. Kiviet, D. M. Weinreich, S. J. Tans, Empirical fitness landscapes reveal accessible evolutionary paths. *Nature* **445**, 383–386 (2007).
88. L. Ferretti, D. Weinreich, F. Tajima, G. Achaz, Evolutionary constraints in fitness landscapes. *Heredity (Edinb).* **121**, 466–481 (2018).
89. T. C. Nelson, *et al.*, Ancient and recent introgression shape the evolutionary history of pollinator adaptation and speciation in a model monkeyflower radiation (Mimulus section Erythranthe). *PLoS Genet.* **17**, e1009095 (2021).
90. H. Svardal, *et al.*, Ancestral hybridization facilitated species diversification in the lake malawi cichlid fish adaptive radiation. *Mol. Biol. Evol.* **37**, 1100–1113 (2020).
91. S. Lamichhaney, *et al.*, Rapid hybrid speciation in Darwin's Finches. *Science* **359**, 224–228 (2018).
92. P. R. Grant, B. R. Grant, Hybridization increases population variation during adaptive radiation. *Proc. Natl. Acad. Sci. U. S. A.* **116**, 23216–23224 (2019).
93. R. D. H. Barrett, D. Schluter, Adaptation from standing genetic variation. *Trends Ecol. Evol.* **23**, 38–44 (2008).
94. J. Hermisson, P. S. Pennings, Soft sweeps and beyond: understanding the patterns and probabilities of selection footprints under rapid adaptation. *Methods Ecol. Evol.* **8**, 700–716 (2017).
95. P. W. Hedrick, Adaptive introgression in animals: examples and comparison to new mutation and standing variation as sources of adaptive variation. *Mol. Ecol.* **22**, 4606–4618 (2013).
96. S. Matuszewski, J. Hermisson, M. Kopp, Catch me if you can: Adaptation from standing genetic variation to a moving phenotypic optimum. *Genetics* **200**, 1255–1274 (2015).
97. J. T. Streelman, P. D. Danley, The stages of vertebrate evolutionary radiation. *Trends Ecol. Evol.* **18**, 126–131 (2003).
98. Broad Institute, Picard Toolkit (2018).
99. M. A. Depristo, *et al.*, A framework for variation discovery and genotyping using next-generation DNA sequencing data. *Nat. Genet.* **43**, 491–501 (2011).
100. R. Poplin, *et al.*, Scaling accurate genetic variant discovery to tens of thousands of samples. *bioRxiv*, 201178 (2017).
101. C. D. Marsden, *et al.*, Diversity, differentiation, and linkage disequilibrium: Prospects for association mapping in the malaria vector anopheles arabiensis. *G3 Genes, Genomes, Genet.* **4**, 121–131 (2014).

102. P. Danecek, *et al.*, The variant call format and VCFtools. *Bioinformatics* **27**, 2156–2158 (2011).
103. S. Purcell, *et al.*, PLINK: A tool set for whole-genome association and population-based linkage analyses. *Am. J. Hum. Genet.* **81**, 559–575 (2007).
104. C. T. DiVittorio, *et al.*, Natural selection maintains species despite frequent hybridization in the desert shrub Encelia. *Proc. Natl. Acad. Sci. U. S. A.* **117**, 33373–33383 (2021).
105. J. Hereford, A quantitative survey of local adaptation and fitness trade-offs. *Am. Nat.* **173**, 579–588 (2009).
106. X. Zhou, M. Stephens, Genome-wide efficient mixed-model analysis for association studies. *Nat. Genet.* **44**, 821–824 (2012).
107. P. Cingolani, *et al.*, Using Drosophila melanogaster as a model for genotoxic chemical mutational studies with a new program, SnpSift. *Front. Genet.* **3** (2012).
108. S. X. Ge, D. Jung, D. Jung, R. Yao, ShinyGO: A graphical gene-set enrichment tool for animals and plants. *Bioinformatics* **36**, 2628–2629 (2020).
109. J. A. McGirr, C. H. Martin, Few fixed variants between trophic specialist pupfish species reveal candidate cis-regulatory alleles underlying rapid craniofacial divergence. *Mol. Biol. Evol.* **38**, 405–423 (2021).
110. T. L. Hedrick, Software techniques for two- and three-dimensional kinematic measurements of biological and biomimetic systems. *Bioinspiration and Biomimetics* **3**, 034001 (2008).
111. S. N. Wood, Fast stable restricted maximum likelihood and marginal likelihood estimation of semiparametric generalized linear models. *J. R. Stat. Soc. Ser. B (Statistical Methodol.* **73**, 3–36 (2011).
112. K. P. Burnham, D. R. Anderson, *Model Selection and Multimodel Inference* (Springer New York, 2002).
113. G. Csardi, T. Nepusz, The igraph software package for complex network research. *InterJournal Complex Syst.* **1695**, 1–9 (2006).
114. F. de Mendiburu, agricolae: Statistical procedures for agricultural research (2020).
115. T. Guillerme, dispRity: A modular R package for measuring disparity. *Methods Ecol. Evol.* **9**, 1755–1763 (2018).
116. B. J. Knaus, N. J. Grünwald, VCFR: a package to manipulate and visualize variant call format data in R. *Mol. Ecol. Resour.* **17**, 44–53 (2017).
117. S. Der Yang, T. S. Lin, F. G. Liu, C. H. Liou, Influence of dietary phosphorus levels on growth, metabolic response and body composition of juvenile silver perch (Bidyanus bidyanus). *Aquaculture* **253**, 592–601 (2006).
118. J. M. Costa, *et al.*, Inadequate dietary phosphorus levels cause skeletal anomalies and alter osteocalcin gene expression in Zebrafish. *Int. J. Mol. Sci.* **19**, 364 (2018).
119. H. Yu, *et al.*, Effects of stocking density and dietary phosphorus levels on the growth performance, antioxidant capacity, and nitrogen and phosphorus emissions of juvenile blunt snout bream (Megalobrama amblycephala). *Aquac. Nutr.* **27**, 581–591 (2021).

## Supplementary Methods

### *Sampling of hybrid individuals*

Samples of hybrid *Cyprinodon* pupfish included herein were first collected following two separate fitness experiments, conducted on San Salvador Island in 2011 (17) and 2016 (18) respectively. Experiments were carried out in two lakes: Little Lake (LL), and Crescent Pond (CP). Following their initial collection at the conclusion of their respective experiments (see (17) and (18) for protocols), samples were stored in ethanol. In late 2018, 149 hybrid samples were selected for use in this experiment. Of these, 27 are from the experiment conducted in 2011 (14 from LL, 13 from CP), and the remaining 122 are from the 2016 experiment (58 from LL, 64 from CP). Due to reduced sample size for some species within Little Lake, we include fish obtained from Osprey Lake for downstream analyses comparing hybrids to Little Lake, as the two comprise a single, interconnected body of water.

### *Genomic Library Prep*

DNA was extracted from the muscle tissue of hybrids using DNeasy Blood and Tissue kits (Qiagen, Inc.); these extractions were then quantified using a Qubit 3.0 fluorometer (Thermo Scientific, Inc). Genomic libraries were prepared by the Vincent J. Coates Genomic Sequencing Center (QB3) on the automated Apollo 324 system (WaterGen Biosystems, Inc.). Samples were fragmented using a Covaris sonicator, and barcoded with Illumina indices. Samples were quality checked using a Fragment Analyzer (Advanced Analyical Technologies, Inc.). All samples were sequenced to approximately 10x raw coverage on an Illumina NovaSeq.

### *Genotyping and filtering*

Because we are interested in genomic variants found not only within our hybrid samples but across San Salvador island and the Caribbean, we conducted genotyping including all 247 samples from Richards et al. (51). These samples include members of the three species (*C. variegatus*, *C. brontotheroides*, *C. desquamator*) found on San Salvador Island, as well as individuals of *C. variegatus* found throughout the Caribbean, and numerous outgroups (*C. laciniatus*, *C. higuey*, *C. dearborni*, *Megupsilon aporus*, and *Cualac tesselatus*). We then excluded *M. aporus* and *C. tesselatus* along with 18 additional samples for which necessary data for downstream analyses were missing (e.g. quality photographs for the collection of morphological data). This approach led to the retention of a total of 4,206,786 total SNPs and 139 hybrid individuals.

### *Morphometrics*

Because the morphological measurements used in the 2013 and 2016 experiments differ slightly, we remeasured all sequenced hybrid individuals and up to 30 individuals of each parent species for the 30 morphological characters described in Martin & Gould (18), as well as for standard length (SL).

For each photograph, unit-scale was obtained by additionally landmarking points on a regular grid included in each photograph using DLTdv8a (110). Landmark data (x-y coordinates in units of pixels) were subsequently uploaded into R and converted to millimeters (in the case of linear measurements) or degrees (for angular measurements) using a custom script.

We then assessed, for each trait, the need for size-correction. That is, we sought to avoid an outsized role of body size in downstream interpretation. Thus, if a trait was colinear with SL, we regressed the two (treating SL as the predictor) and took the residuals. In each case, both SL

and the response were Log-10 transformed. Subsequently, residuals were scaled such that their distribution had a mean of 0, and a standard deviation of 1. Traits that did not need size correction were also Log-transformed and unit-scaled.

We used these morphological measurements to estimate two linear discriminant (LD) axes that distinguish the generalist, molluscivore, and scale-eater using the LDA function in R. That is, we used morphological data from the 165 parental fish to estimate LD scores for each individual. Doing so, we were able to correctly assign individual fish to their corresponding species with 99.4% accuracy (Fig. S8-S9: Table S7). Attempting to predict species assignment by lake did not improve this prediction accuracy (instead reducing prediction accuracy to 98.7%); consequently, we proceeded with the LD axes estimated without accounting for lake.

We additionally asked whether 1) specialists were more morphologically constrained than generalists and 2) if hybrids were less constrained than the three parental species. To do so, we calculated morphological disparity per group using the dispRity.per.group function implemented in the R package dispRity v1.3.3 (115). Specifically, this function calculates the median distance between each row (sample) and the centroid of the matrix per group. By bootstrapping the data 100 times, we tested the hypothesis that each of the three parental species differed significantly in their morphological disparity, first using an ANOVA, followed by a post-hoc pairwise t-test to assess pairwise significance in R. We corrected for multiple tests using an FDR correction.

To test whether genetic distance predicts morphological distance, we calculated two distance matrices. First, we calculated pairwise Euclidean distances between all hybrids using all morphological variables. Then, we calculated pairwise genetic distances between all hybrids using the final set of SNPs described above with the genet.dist function implemented in vcfR (116). We then fit a simple linear model, regressing genetic distance on morphological distance.

***Estimation of Adaptive Landscapes***

We sought to characterize the extent to which the three measures of fitness are predicted by morphology alone and to, in turn, visualize fitness landscapes for our sequenced hybrids. To do so, we fitted six generalized additive models (GAMs) using the mgcv package v. 1.8.28 (111) in R. All models included a thin-plate spline fitted for the two linear discriminant axes. Because we have strong *a priori* knowledge that fitness outcomes will be contingent to some extent on experiment year and on the lake in which hybrids were placed, we include experiment and lake in all fitted models, modeled either as fixed effects, or as an interaction term between the two. Additionally, we fitted models that included individual splines for each linear discriminant axis, either with or without experiment or lake as a factor smooth. The full list of models and their respective fits are included in the supplement (Supplementary Tables S8-S10).

For composite fitness, we excluded three SNPs that were within close proximity (i.e. < 1000bp) to a SNP that was more significantly associated. Because of the reduced number of significantly associated SNPs identified for growth (four) as compared to composite fitness (ten), we were able to fit and compare all combinations of significantly associated SNPs for the former. The best-fit model for composite fitness was also the most complex, including all fitness associated SNPs. Thus, to reduce model complexity, we fit one additional model, excluding any of the three SNP (fixed effect) that was not significant in the full model. The full range of models and their associated fits are reported in Tables S11-S12. As before, predicted fitness values across LD space were extracted from the best-fit model and plotted using R.

***Genotypic Fitness Networks***

Recent work has shown that the adaptive radiation of the pupfish of San Salvador island involved selection on standing genetic variation, adaptive introgression, and *de novo* mutation (51). Furthermore, the specialists on San Salvador Island received approximately twice as much adaptive introgression as did generalists on neighboring islands. These findings imply that each source of genetic variation may exert a unique influence on the fitness landscape, in turn facilitating the radiation. We sought to explore this possibility and so estimated genotypic fitness networks using sites previously shown to have undergone hard selective sweeps in specialists. To do so, we identified the SNPs in our un-thinned dataset overlapping with sites inferred to have undergone selective sweeps (51) to produce two datasets (one for each specialist). We then constructed networks using the following procedure:

1) Target SNPs were extracted from the vcf file of all sequenced hybrids and parental species from Crescent Pond and Little Lake in 0/1/2 format using VCFtools. That is, individuals genotyped as homozygote reference were coded as 0, heterozygotes as 1, and homozygote alternatives as 2. Note again that the reference genome used was that of the molluscivore, *C. brontotheroides*.
2) These SNPs were subsequently loaded into R, and concatenated into haplotypes, such that each sequenced individual has a haplotype. These per-sample haplotypes were subsequently associated with metadata, namely the observed binary survival, growth, assignment as hybrid or one of the three parental species, and lake of origin.
3) Each haplotype was subsequently collapsed and summarized, such that mean survival, growth, and composite fitness are retained for each unique haplotype. Additionally, the number of hybrids, generalists, molluscivores and scale-eaters that have the haplotype were recorded.
4) The distance, in number of mutational steps was then calculated for each pairwise combination of haplotypes. For example, the distance between haplotype 000 and 001 is a single mutational step, whereas haplotypes 000 and 002 are two steps away.
5) Lastly, we constructed networks using the R package igraph v. 1.2.4.1 (113). Specifically, nodes represent haplotypes, and edges are drawn between haplotypes that are mutational neighbors (i.e. are a single mutational step away). Nodes present in hybrids were colored and sized proportional to their respective mean fitness. Nodes present only in parental species were colored according to the species in which that haplotype is unique to.

***Estimation of evolutionary accessibility***

The large number of SNPs in our dataset above raises numerous challenges in the visualization and summarization of fitness networks. Perhaps most significant, is that as the number of sites assessed increases, the sequence space increases vastly; the number of potential haplotypes is defined by 3 to the power of the number of SNPs, and the number of potential edges is defined by the number of haplotypes choose 2. Consequently, networks constructed from a larger number of focal SNPs are comprised of haplotypes that are separated on average by more mutational steps than those constructed from fewer SNPs. Because we can only interpret the fitness consequences of evolutionary trajectories for which we have data along each mutational step, we restricted analysis to haplotypes that are mutational neighbors (i.e., separated by a single mutational step).

To do so, we developed a permutation approach to construct fitness networks from SNPs that were sourced from the three sources of genetic variation defined above as well as their combinations (i.e. standing genetic variation + adaptive introgression or de novo mutation). Specifically, from each set we sampled five SNPs up to 1000 times. Then, from each permutation, we constructed fitness networks using the five steps defined above; these networks served as the subsequent assessment of evolutionary accessibility of genotypic trajectories separating the generalists from either specialist. Edges were only drawn such that the network is directed; that is, edges were drawn from low to high fitness nodes.

We constructed networks using both parental species and hybrids. For each trajectory under consideration (generalist → molluscivore & generalist → scale-eater), we first identified all generalist to specialist trajectories that are connected by accessible (monotonically increasing) paths. From these connected generalist-specialist node pairs, we randomly sampled a single pair. We then identified the number and length of accessible paths separating the generalist node from the specialist node and recorded these values using the "all_simple_paths" function in igraph and excluded any paths that traversed through haplotypes not found in any hybrid (i.e., exclusive to parental species) and thus had no information on fitness.

## Supplementary Results

### *Genomic associations recovered for composite fitness and growth, not survival*

Whereas we identified 132 SNPs that were associated with composite fitness, only 58 were associated with growth and none were associated with survival. Of the SNPs associated with growth, only four remained significant using the conservative Bonferroni threshold. Across all significant sites (either via FDR or Bonferroni correction) a total of 11 were shared across analyses. The only gene proximate to a growth associated SNP was *csad.* Lastly, we found a single gene shared between our study and the 125 ecological DMIs (putatitve genetic incompatibilities that are differentially expressed among specialists and misexpressed in F1 hybrids) presented in McGirr & Martin (69). This gene, associated with growth (but not composite fitness) in our study, is *mettl21e*.

When considering SNPs found to be associated with growth, we did not identify any gene ontologies that were significantly enriched at a False Discovery Rate < 0.01. However, looking at those enriched at an FDR < 0.05, we do observe a number of ontologies related to biosynthetic processes, and regulation of metabolic processes (Fig. S6). Specifically, the greatest (and most significant) enrichment was for that of phosphorus and phosphate containing compound metabolic processes and their regulation. Phosphorous deficiencies have previously been associated with poor growth in silver perch (*Bidyanus bidyanus*: (117)) and skeletal deformaties (including vertebral compression and craniofacial deformaties) in zebrafish (*Danio rerio*: (118)). Similarly, blunt snout bream (*Megalobrama amblycephala*) exhibited greater growth rates with increasing phosphorous levels in their diets (119). In short, enrichment of growth-associated SNPs for ontologies pertaining to phosphorous metabolism is consistent with the substantial literature documenting that phosphorous availability and metabolism is a determinant of growth in fishes.

### *Morphological variation within sampled hybrids*

As in the previous two experiments, there is a relative paucity of hybrids exhibiting the morphologies that characterize either specialist. Rather, most hybrids fall near the generalists, with a number exhibiting transgressive morphologies (Fig. S9A). As expected, both specialists

exhibit reduced morphological disparity as compared to generalists, and hybrids show the greatest (Fig. S9B). That is, the specialists appear more morphologically constrained than generalists, falling on average closer to the group centroid. Interestingly molluscivores exhibit the least disparity, even less so than scale-eaters.

***Fitness-associated SNPs improve estimation of the adaptive landscape***

Using morphology alone, the best fit generalized additive model for survival, growth, and composite fitness were simpler than the model for composite fitness using both morphology and fitness-associated SNPs (Tables S8-10). For survival and composite fitness (Figure S10A & S10B), this model included a thin-plate spline for LD1 & LD2, with experiment and lake included as fixed effects. The resultant landscape was also similar for these two analyses, supporting an interpretation of directional selection, favoring molluscivores. For growth, the best-fit model had the thin-plate spline for LD1 & LD2, but included an interaction term between experiment and lake (Table S9). In contrast to the previous two models, the landscape predicted using growth as our proxy of fitness supported an interpretation of directional selection in favor or hybrids most similar to generalists, and to a lesser extent, scale-eaters.

Notably, model selection using AICc invariably supported the inclusion of fitness associated SNPs for growth and composite fitness (Tables S11-S12). For growth, the best-fit model including genotypes was an improvement of 22.99 AICc over the model including morphology alone, whereas for composite fitness, the improvement was 94.527 AICc. Interestingly, the best-fit models and growth including associated SNPs was similar to that of the landscape without fitness-associated SNPs, but largely supported an interpretation of directional selection in favor of scale-eaters, and to a lesser extent generalists.

***Evolutionary accessibility is influenced by the source of genetic variation***

As with composite fitness, we find that fitness landscapes including either adaptive introgression or *de novo* mutation are always smaller (i.e. fewer nodes and edges in the network) than networks constructed from standing genetic variation (SGV) alone (Fig. S13; Table S13-S15). In fact, for networks constructed using growth as our fitness proxy, the influence appears even stronger. These results hold even when rarefying our standing genetic variation SNPs to 65, the number of introgressed variants in scale-eaters and the second largest set of variants (data not shown).

Similar to composite fitness, we find that fitness landscapes estimated using both survival (but see generalist to scale-eater) and growth including adaptive introgression have both proportionally more accessible paths between generalists and specialists that are shorter (Fig. S14-S15, Table S13, S16-S17). However, there are several exceptions both for fitness landscapes constructed using survival as our proxy of fitness and looking at genotypic trajectories separating generalists from scale-eaters. First, we found that fitness landscapes constructed using adaptive introgression alone actually had relatively fewer accessible paths than those constructed using standing variation (Fig. S14A, Tables S16), however as with other analyses, these accessible paths were significantly shorter (Fig. S14B, Table S16). Second, we did not observe significant differences between any other group in the relative number of accessible paths (Fig. S14A, Table S16). Lastly, we did not find that accessible paths in networks constructed from a combination of standing genetic variation and adaptive introgression were significantly shorter than those from standing genetic variation along (Fig. S14, Table S17). One potential explanation for these contrasting findings for accessible paths between generalists and scale-eaters is that because the

measure of fitness used to obtain these results, survival, is a binary, the fitness landscape essentially converges on that of a holey adaptive landscape (2, 3, 19). Thus, adaptation between generalists and scale eaters, which are particularly isolated on these fitness landscapes, may occur through predominantly neutral evolution, erasing some of the signal detected for other measures of fitness.

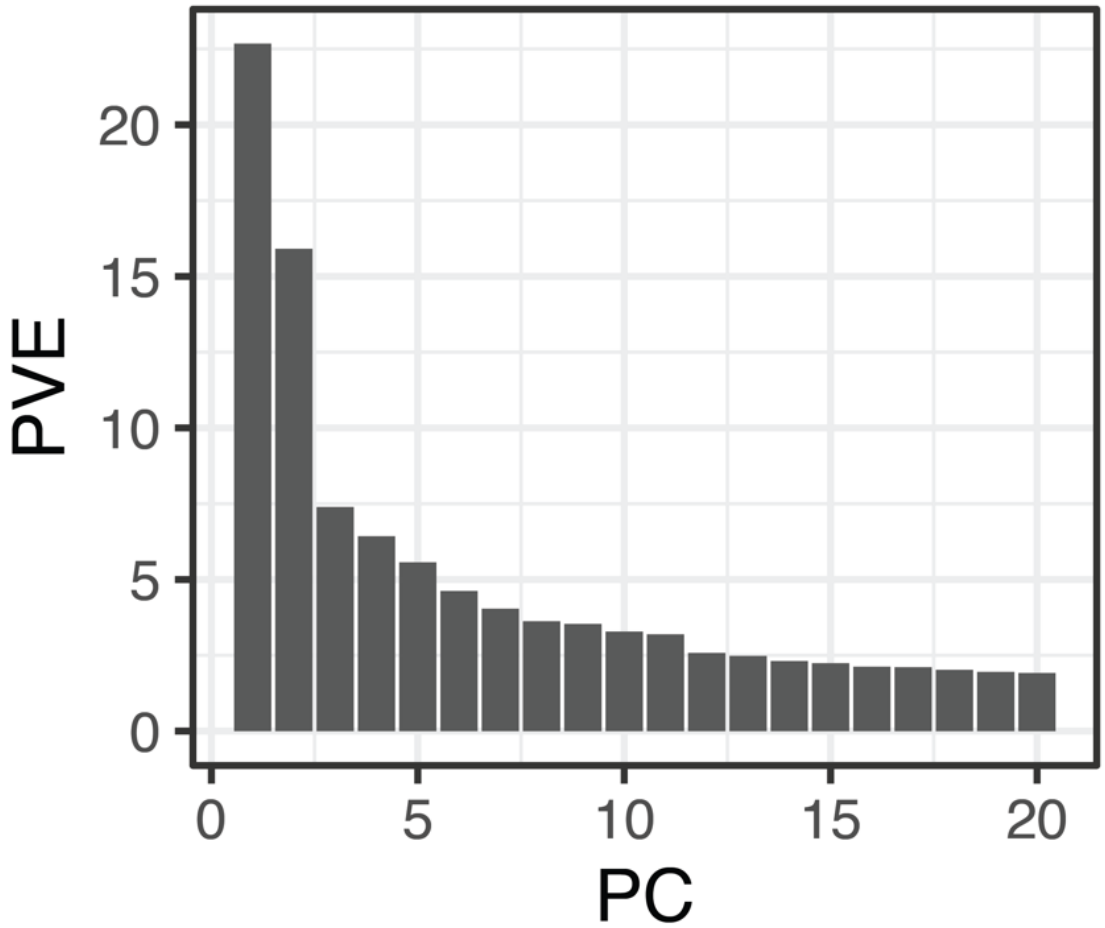


**Figure S1. Proportion (%) genetic variance explained by the first 20 Principal Components obtained using all SNPs and individuals from Crescent Pond, Little Lake, and Osprey Lake, as well as experimental hybrids**. The first two principal component axes are plotted in Figure 1.

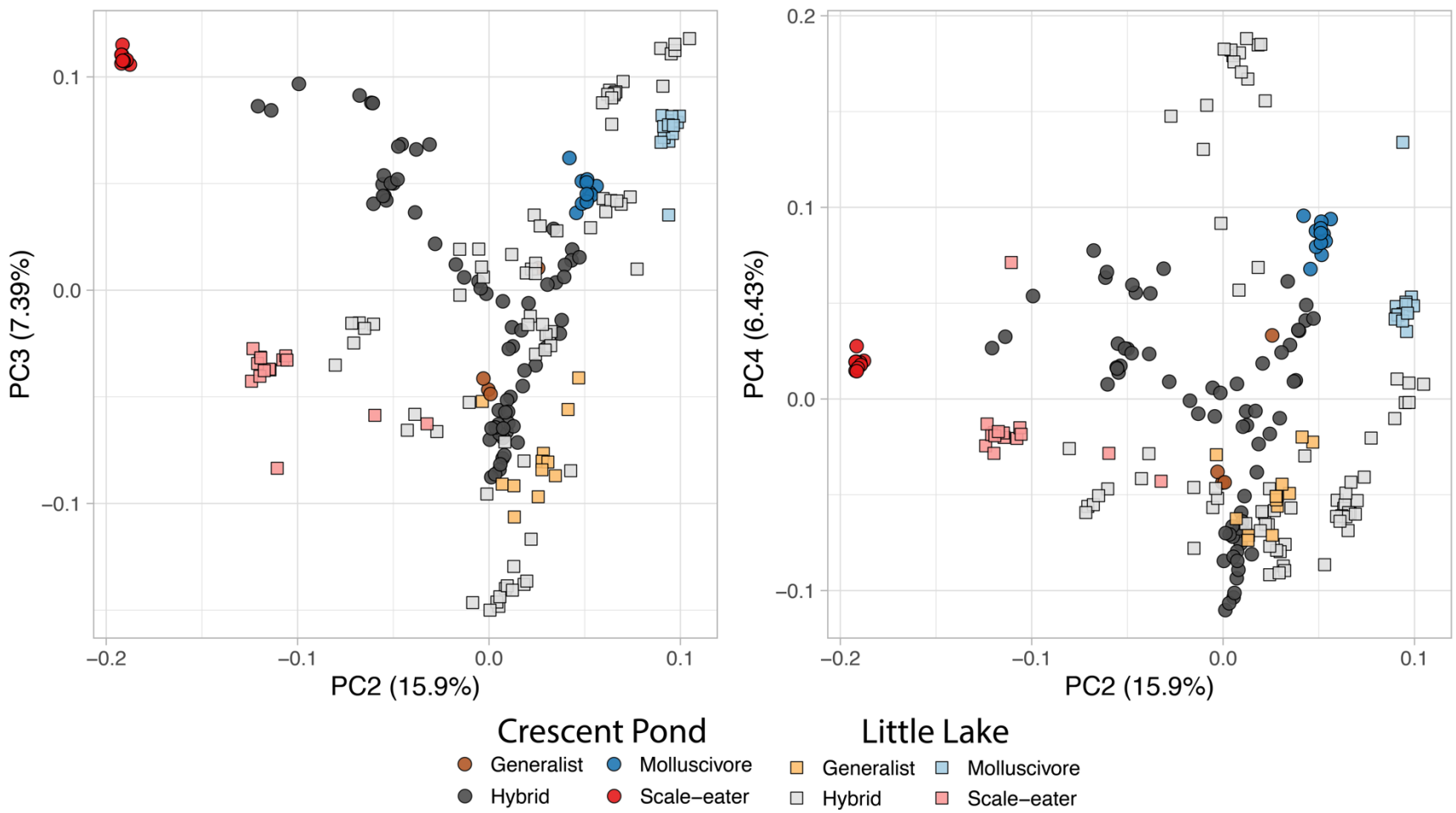


**Figure S2. Principal components two, three, and four.**

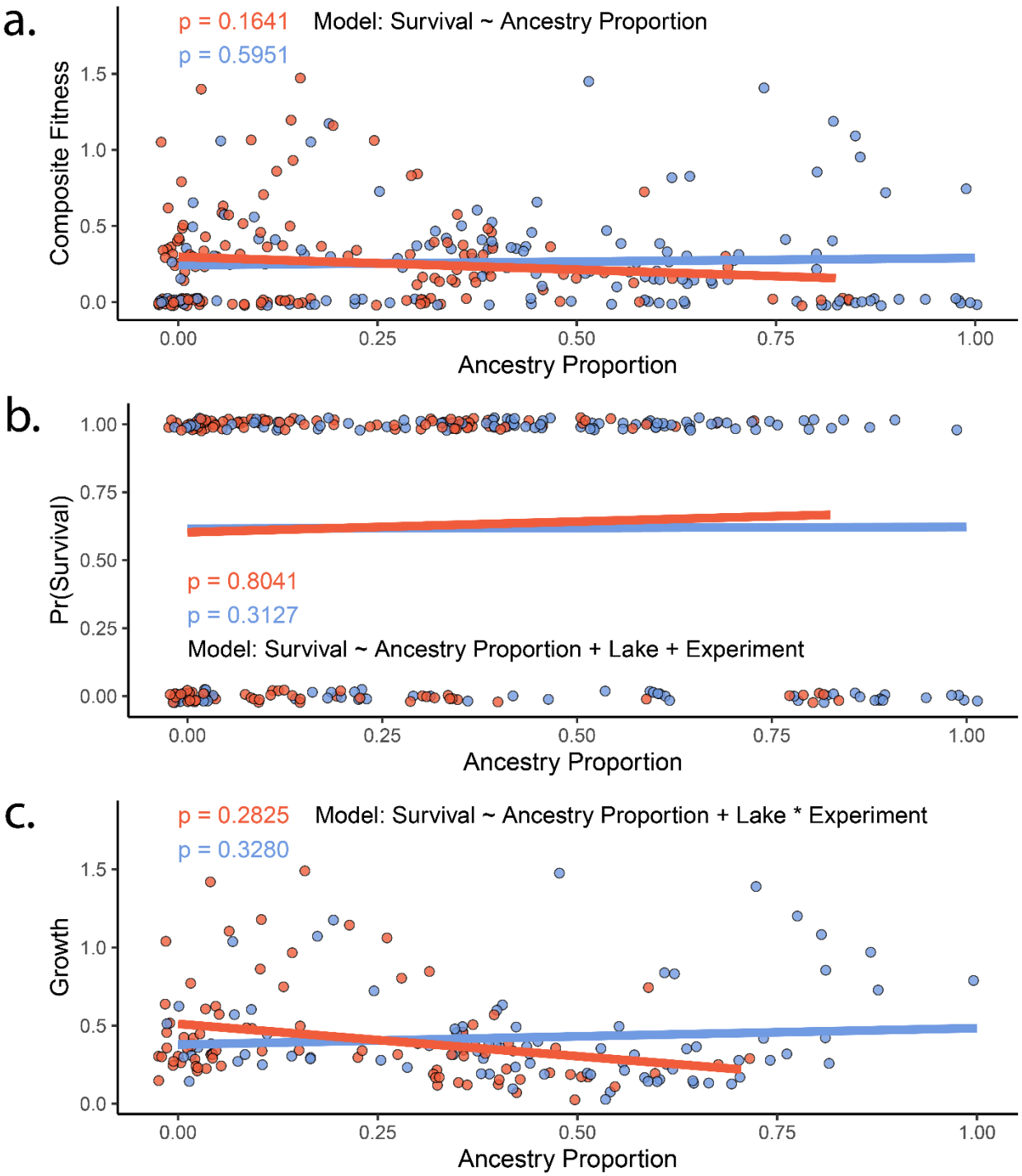


**Figure S3. The proportion of specialist ancestry in hybrids did not predict in experimental hybrids using either A) composite fitness, B) survival or C) growth.** Results of a generalized in which survival (modeled as a binomial) is predicted by ancestry proportion, including lake and experiment as fixed effects. Points represent individual hybrids, with each individual represented by two points, one indicating their respective scale-eater (salmon, and molluscivore (blue) ancestry proportions. *P*-values correspond to the effect of each type of ancestry (scale-eater – red, molluscivore – blue) on survival probability. Lines are predicted values and are colored according to species.

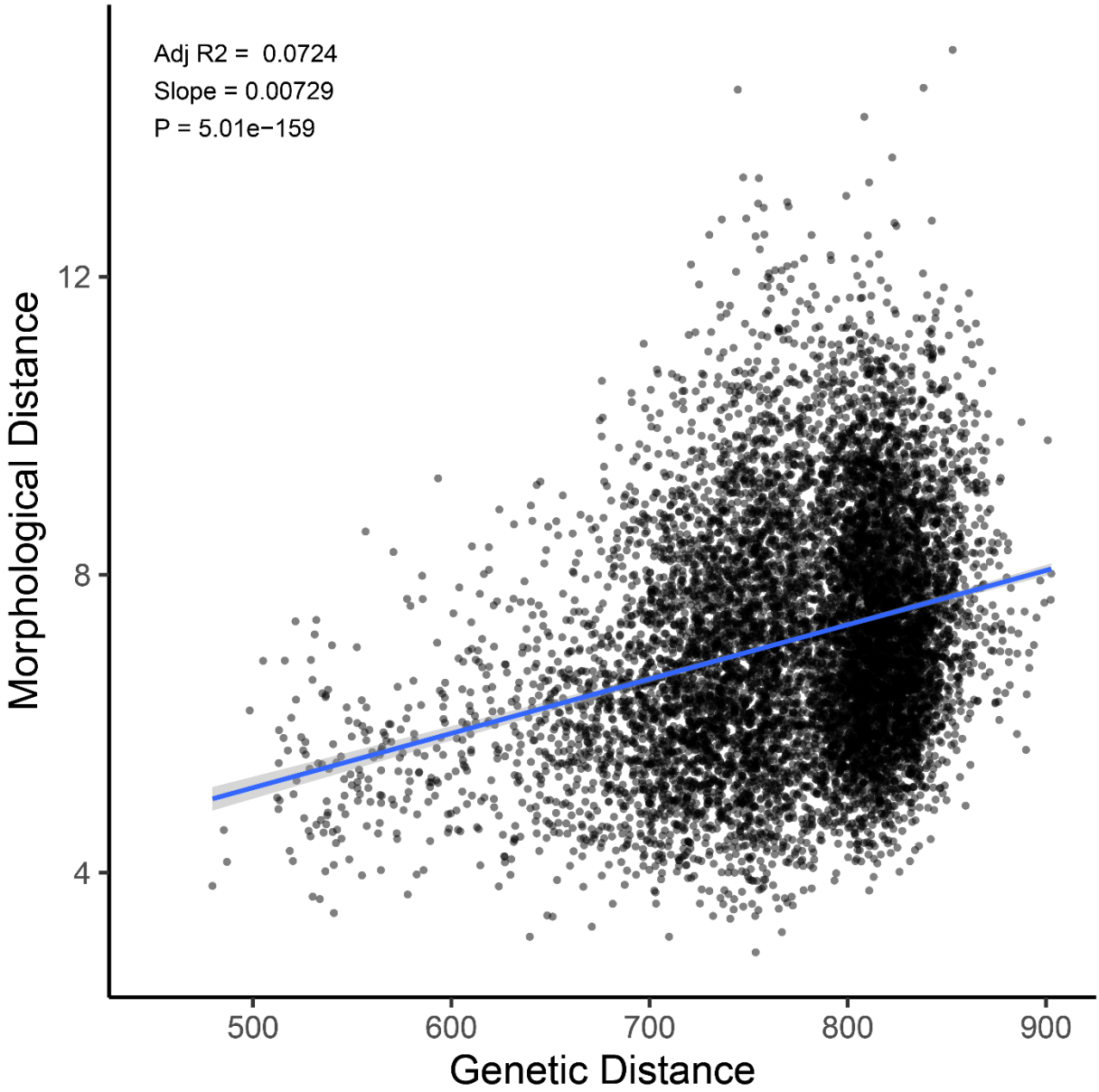


**Figure S4. Genetic distance predicts morphological distance among sampled hybrids.**

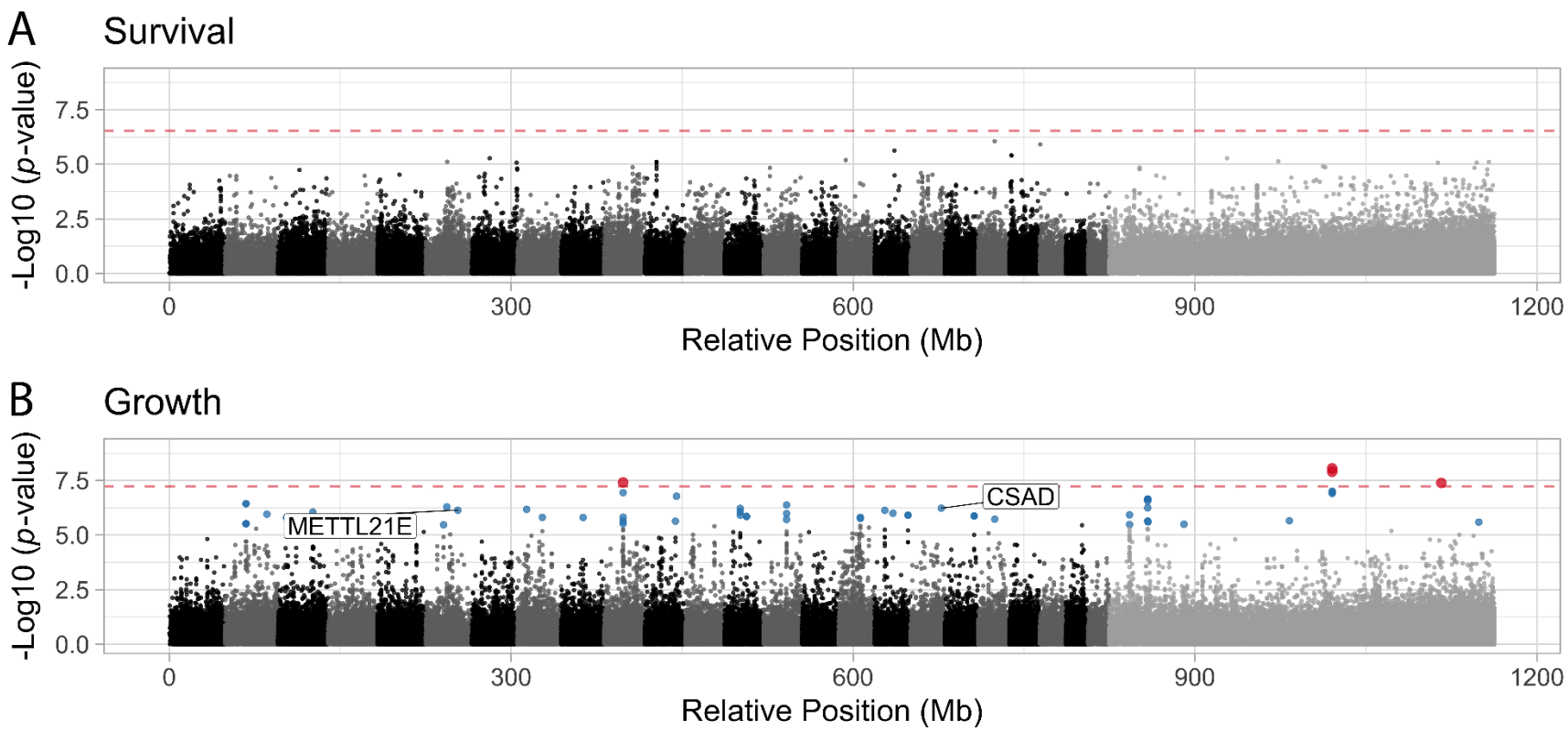


**Figure S5. Manhattan plots illustrating the strength of association between individual SNPs and either Survival (A) or Growth (B) as inferred by GEMMA.** Significant associations are highlighted in blue (FDR < 0.05) or red (Bonferroni correction P < 0.05). The dashed red line indicates the threshold for significance following Bonferroni p-value adjustment. METTL21E and CSAD are both highly differentiated ($F_{ST}$ > 0.95) among specialists, differentially expressed. METTL21E is also misexpressed in F1 hybrids, meaning it exhibits gene expression that is higher or lower than observed in both parental species (69), indicating it is involved in intrinsic incompatibilies.

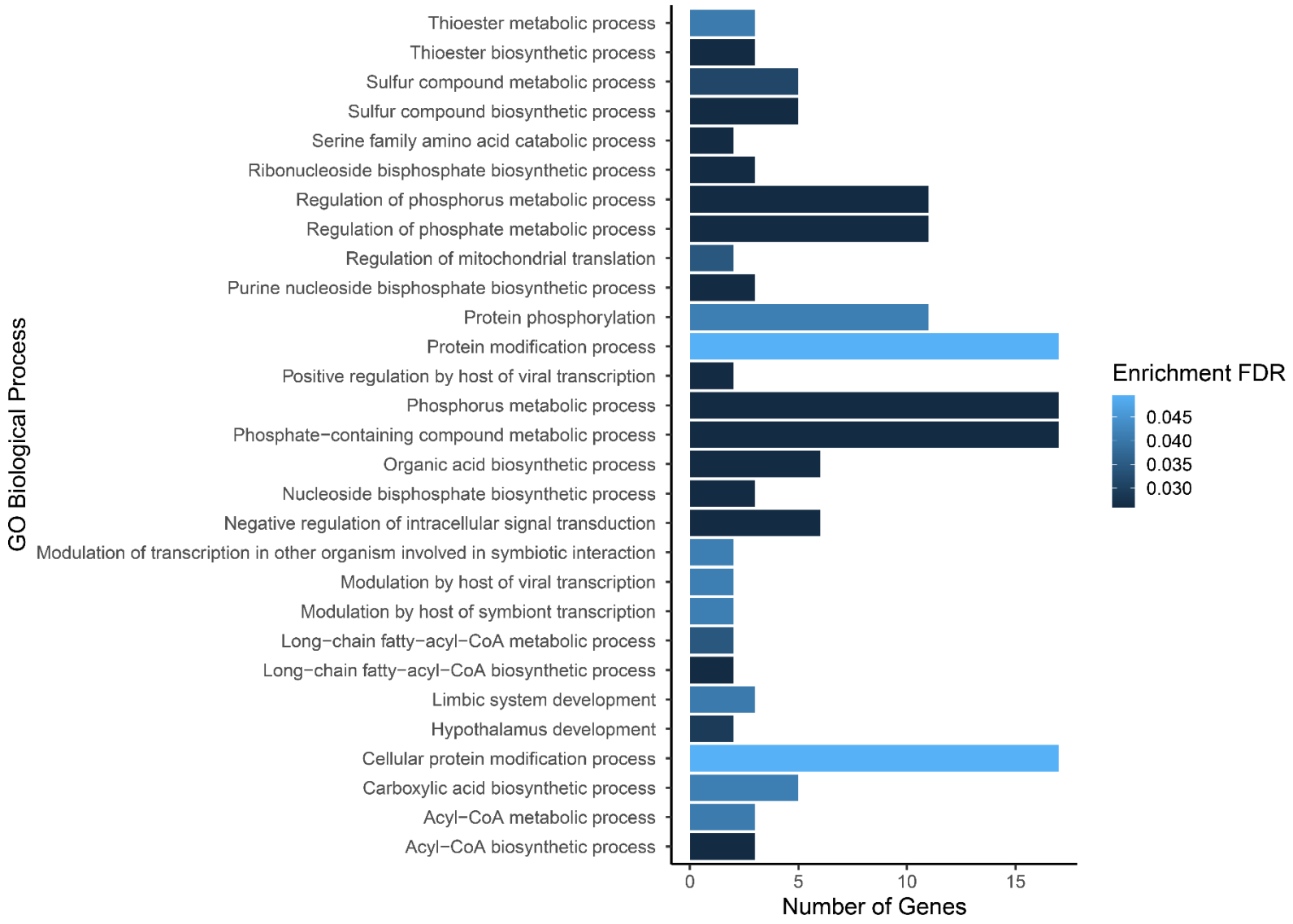


**Figure S6. Gene ontology enrichment for SNPs found to be associated with growth.** Darker colors indicate ontologies that are more significantly enriched following FDR correction. Length of bar is proportional to the number of genes assigned to an ontology.

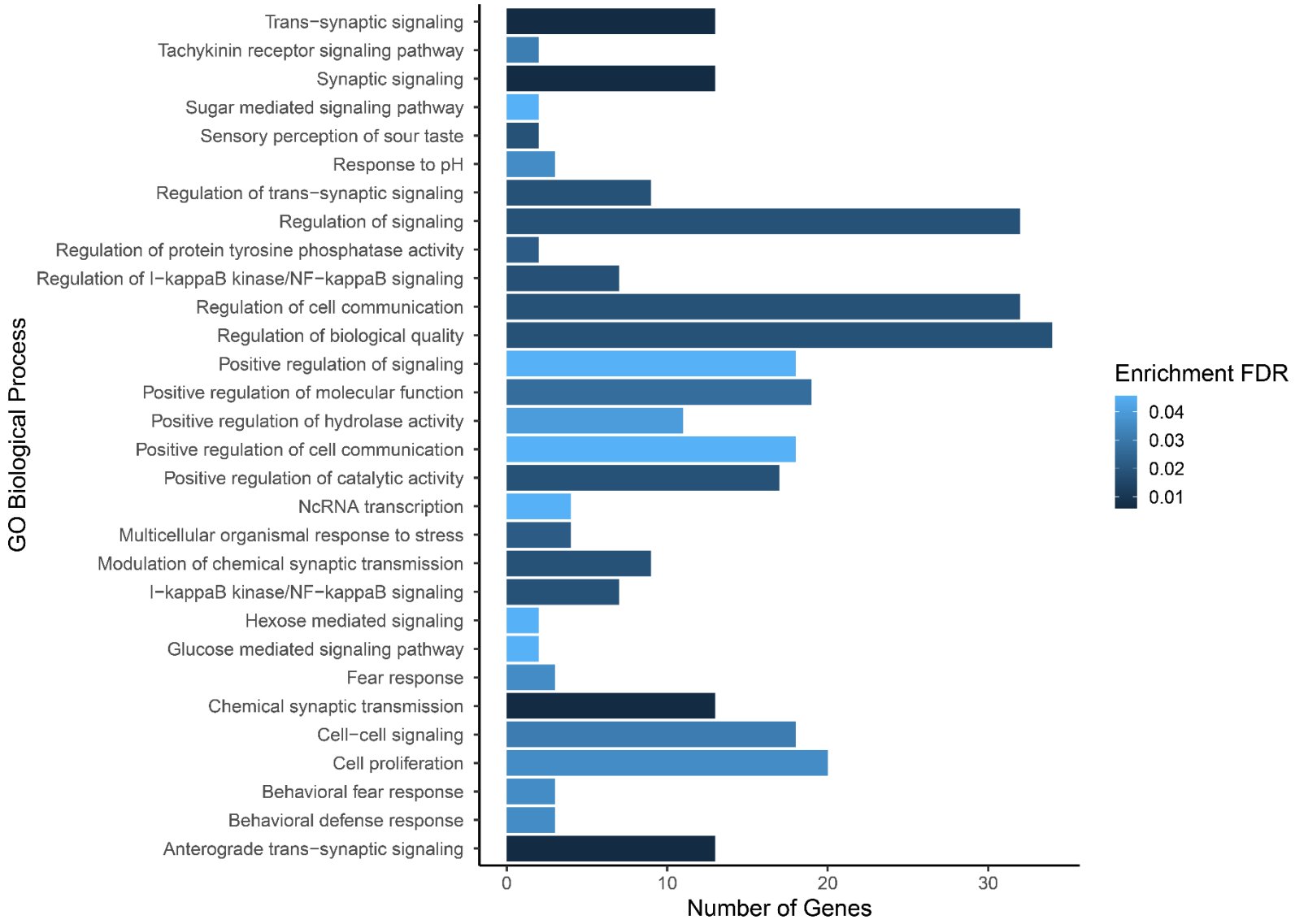


**Figure S7. Gene ontology enrichment for SNPs found to be associated with composite fitness.** Darker colors indicate ontologies that are more significantly enriched following FDR correction. Length of bar is proportional to the number of genes assigned to an ontology,

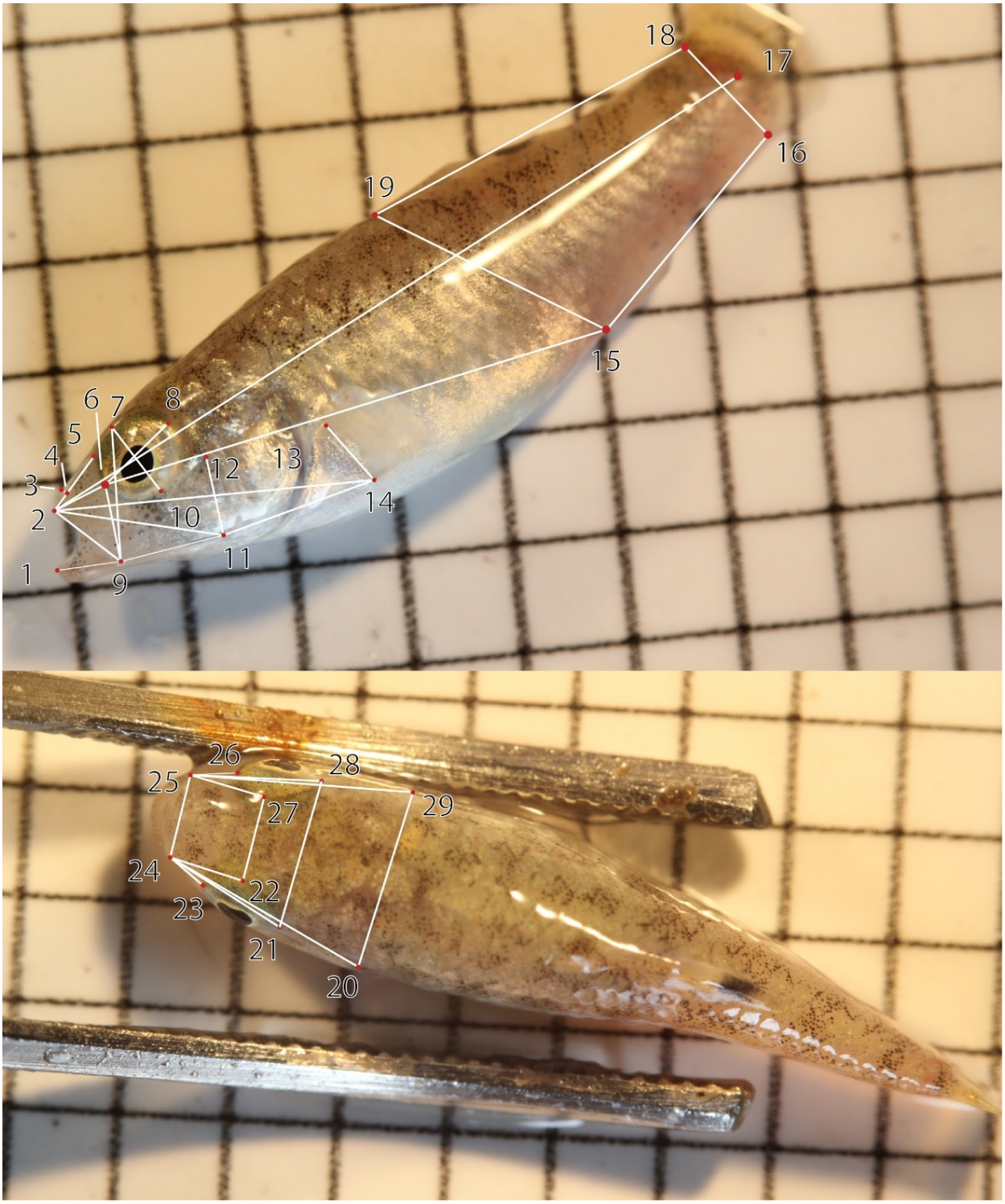


**Figure S8. The 29 landmarks used to digitally measure thirty traits plus standard length using DLTDV8a** (110)**.** The corresponding traits are shown in Table S7.

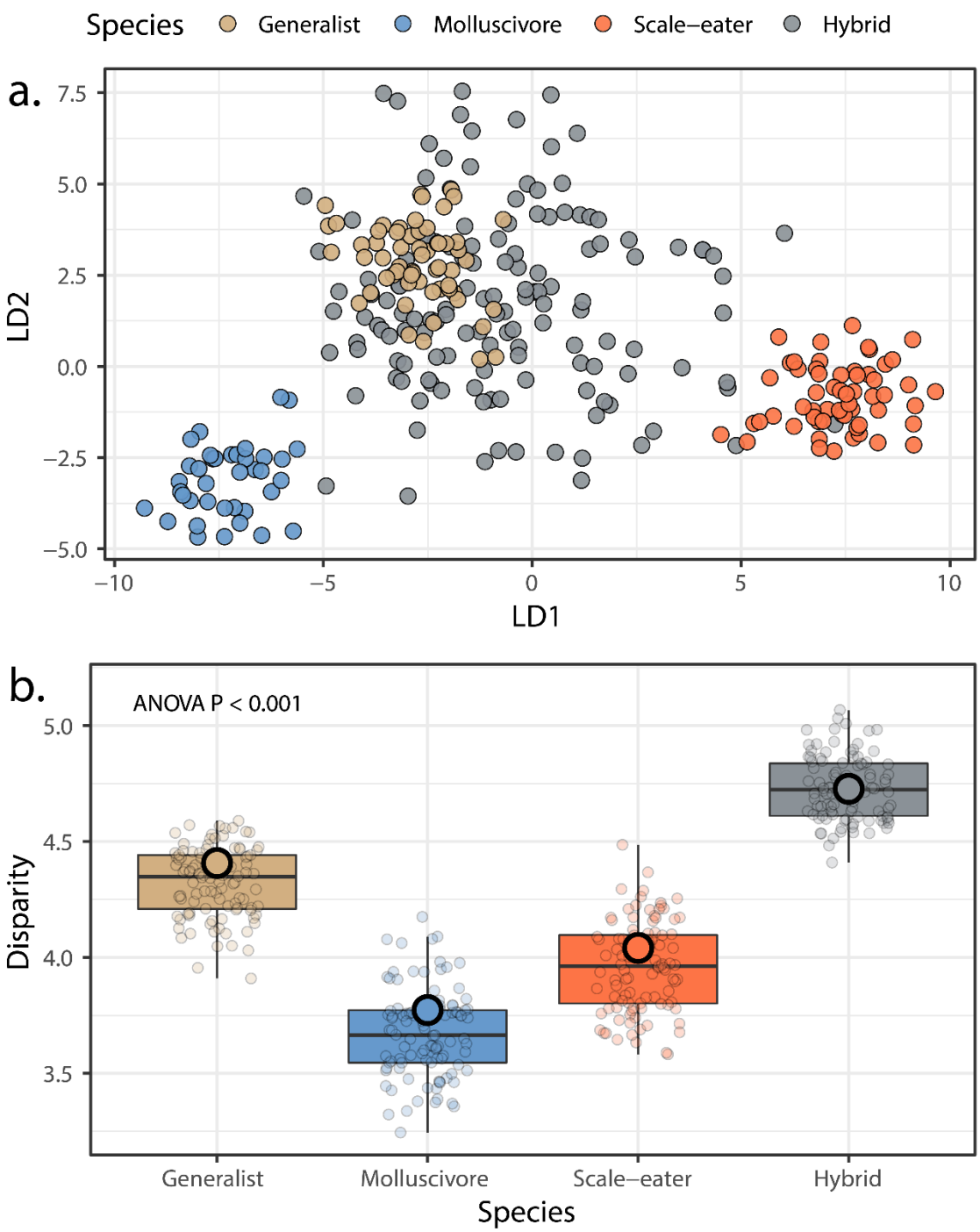


**Figure S9. Morphological variation in the three San Salvador Island pupfish species and their experimentally produced hybrids. A.** Linear discriminant (LD) morphospace. Parent species and hybrids are plotted using the two LD axes that together serve to distinguish species with 99.4% accuracy. **B.** Within-group disparity calculated as the median distance between each individual and the groups centroid. Small, semitransparent points are the result of 100 bootstrap replicates, and are summarized by box plots, which in turn show the median and interquartile ranges of these bootstrap replicates. Large, opaque points are the observed disparities using the full dataset per group. All pairwise comparisons using t-tests following correction for the false discovery rate were significant ($P < 0.001$).

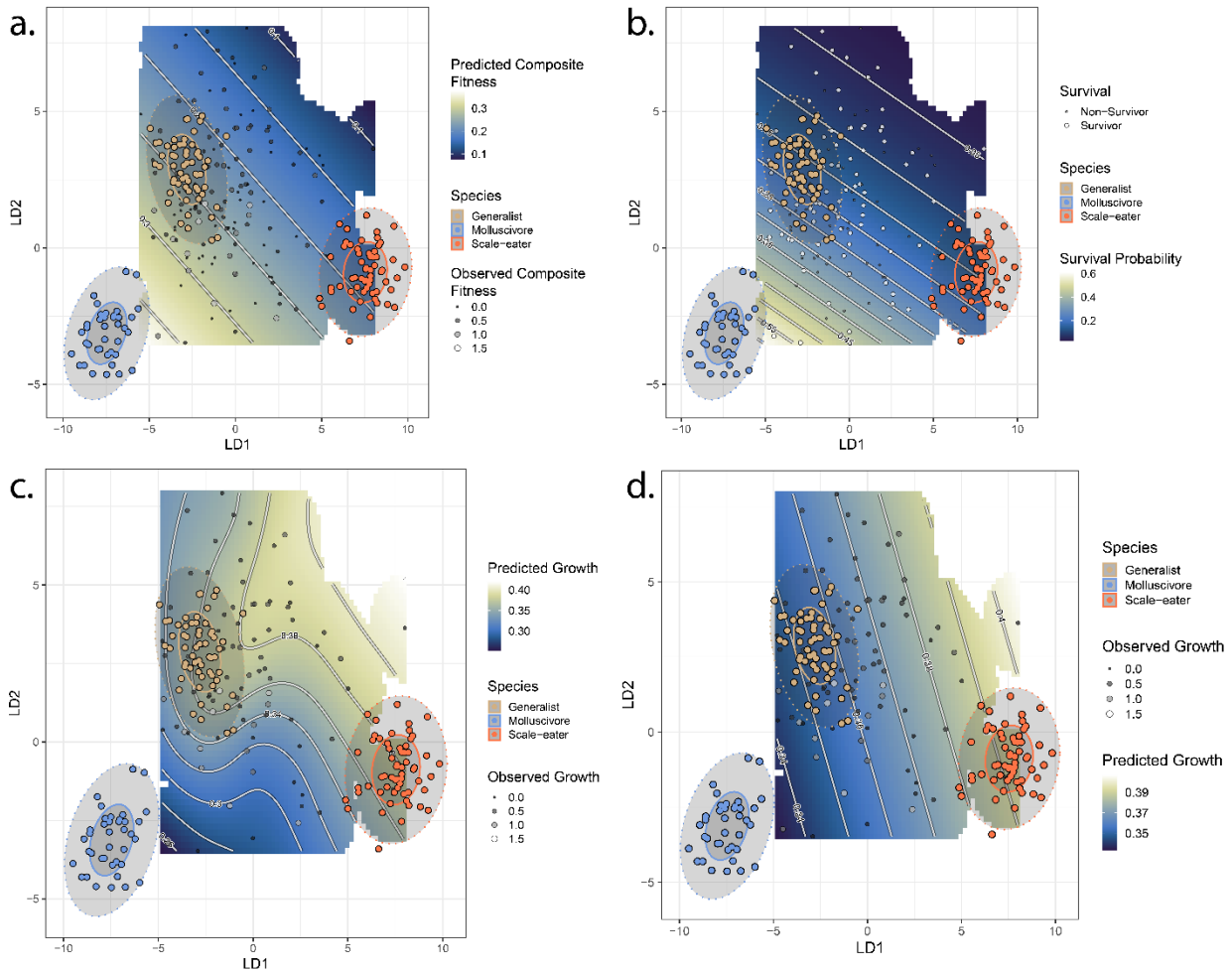


**Figure S10. Best-fit fitness landscapes for composite fitness without fitness associated SNPs (A) survival (B), growth without associated SNPs (C) and growth including associated SNPs (D).** Colored points indicate locations of parent species in LD morphospace, and ellipses indicate their 50% (solid) and 95% (dotted) confidence intervals. Grey points indicate location of hybrid individuals, with size proportional to their fitness measure. Cooler colors on the adaptive landscape indicate lower predicted fitness.

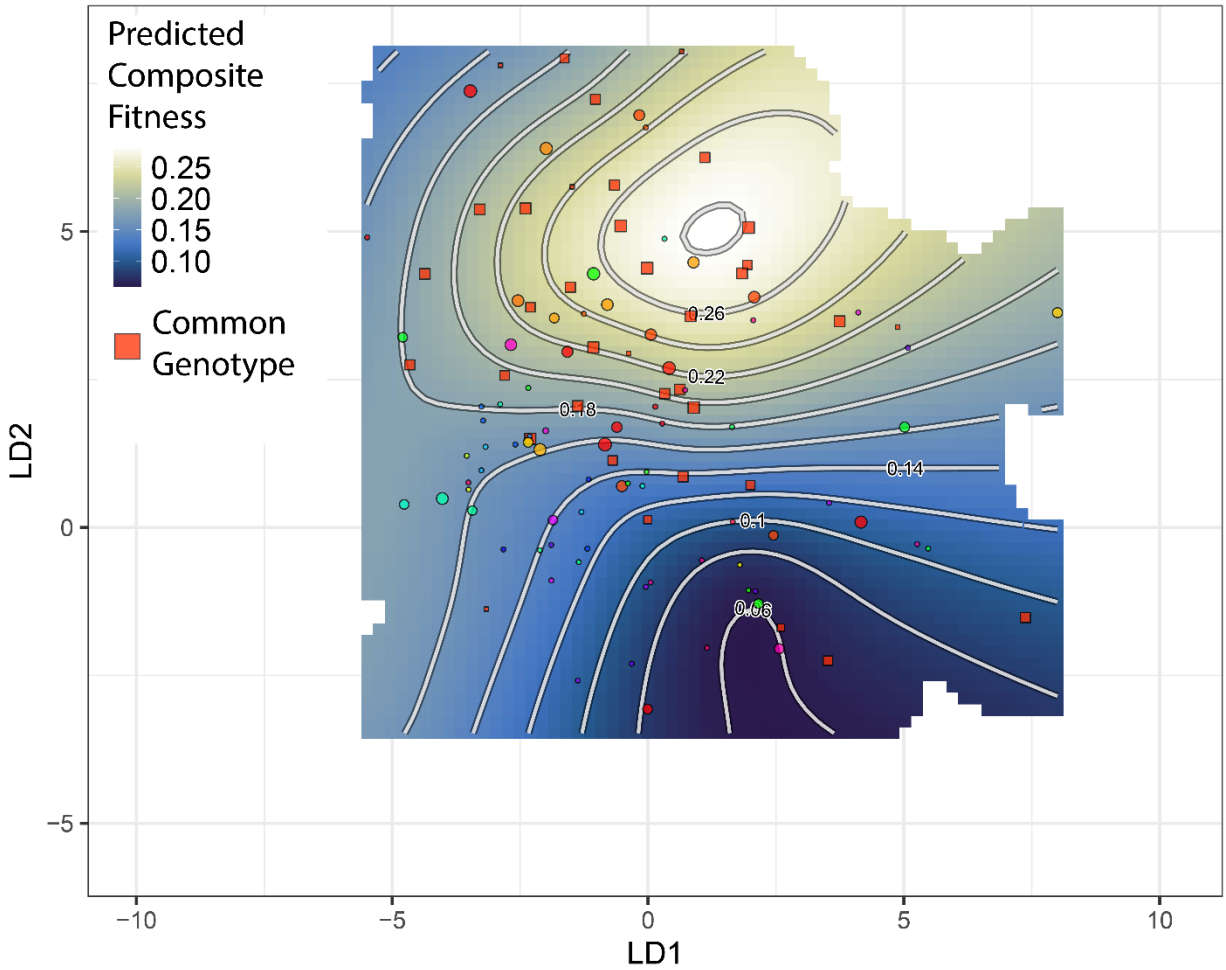


**Figure S11. The topography of the composite fitness adaptive landscape is influenced by the distribution of a common SNP haplotype.** Shown is the same landscape as in Figure 2, but the plotted points are unique SNP haplotypes for the thirteen most strongly fitness-associated SNPs. One haplotype is particularly frequent among hybrids; individuals with this haplotype are closer in morphospace to generalists and drive the emergence of a local fitness optimum for generalists. All other haplotypes (points) are plotted with a distinct color per haplotype.

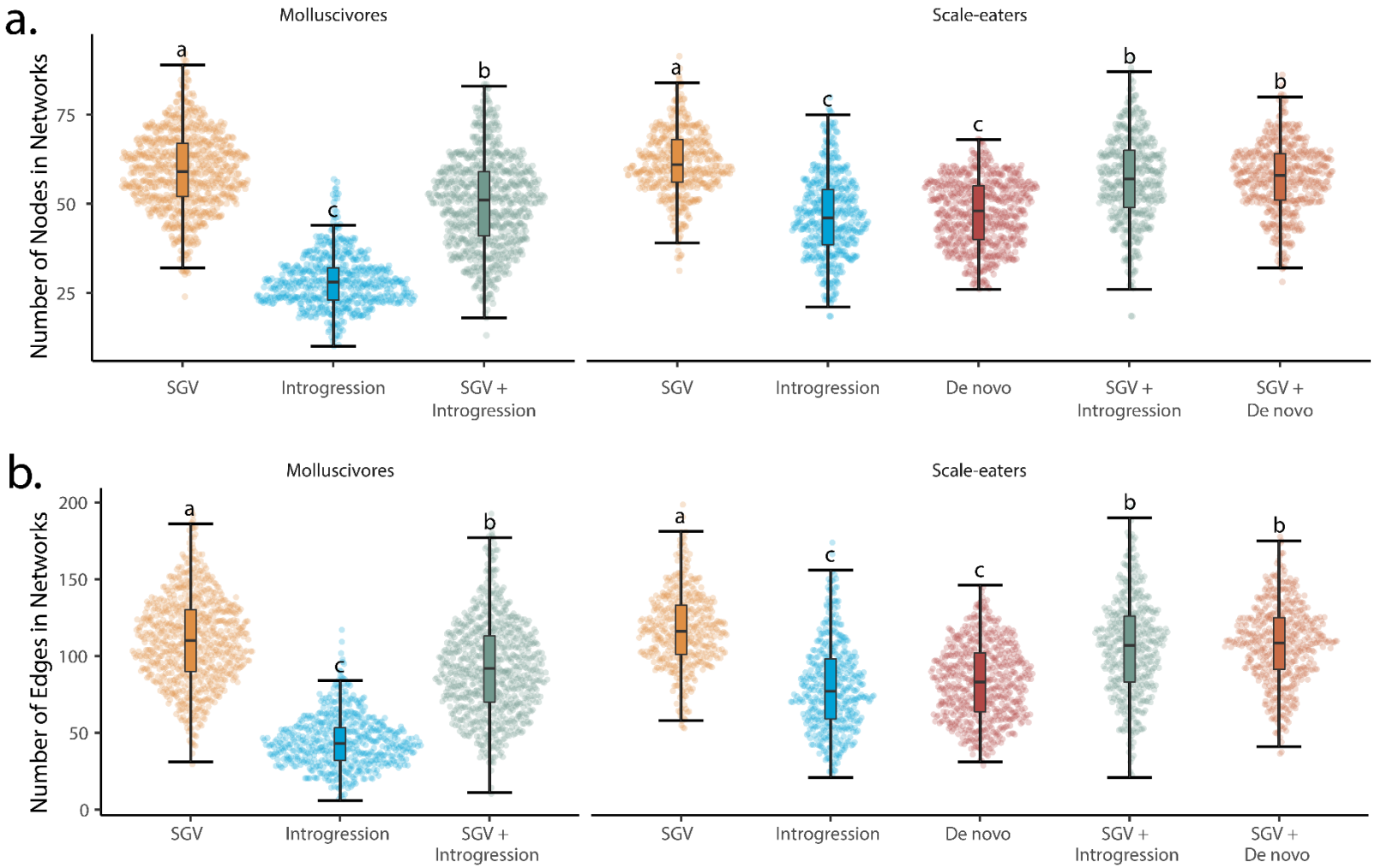


**Figure S12. Genotypic fitness networks (using composite fitness or survival) are smaller both with respect to number of nodes (A) and number of edges (B) when SNPs sourced from introgression or *de novo* mutation are included than networks constructed from standing genetic variation (SGV) alone.** Compact letter display reports pairwise significance according to a nonparametric Kruskal-Wallis one-way analysis of variance following correction for multiple tests using an estimated False Discovery Rate. Letters are ordered (i.e. **a** to **c**) in decreasing values of the median. These results are constant whether survival or composite fitness are used because they comprise the same set of samples (both survivors and non-survivors)

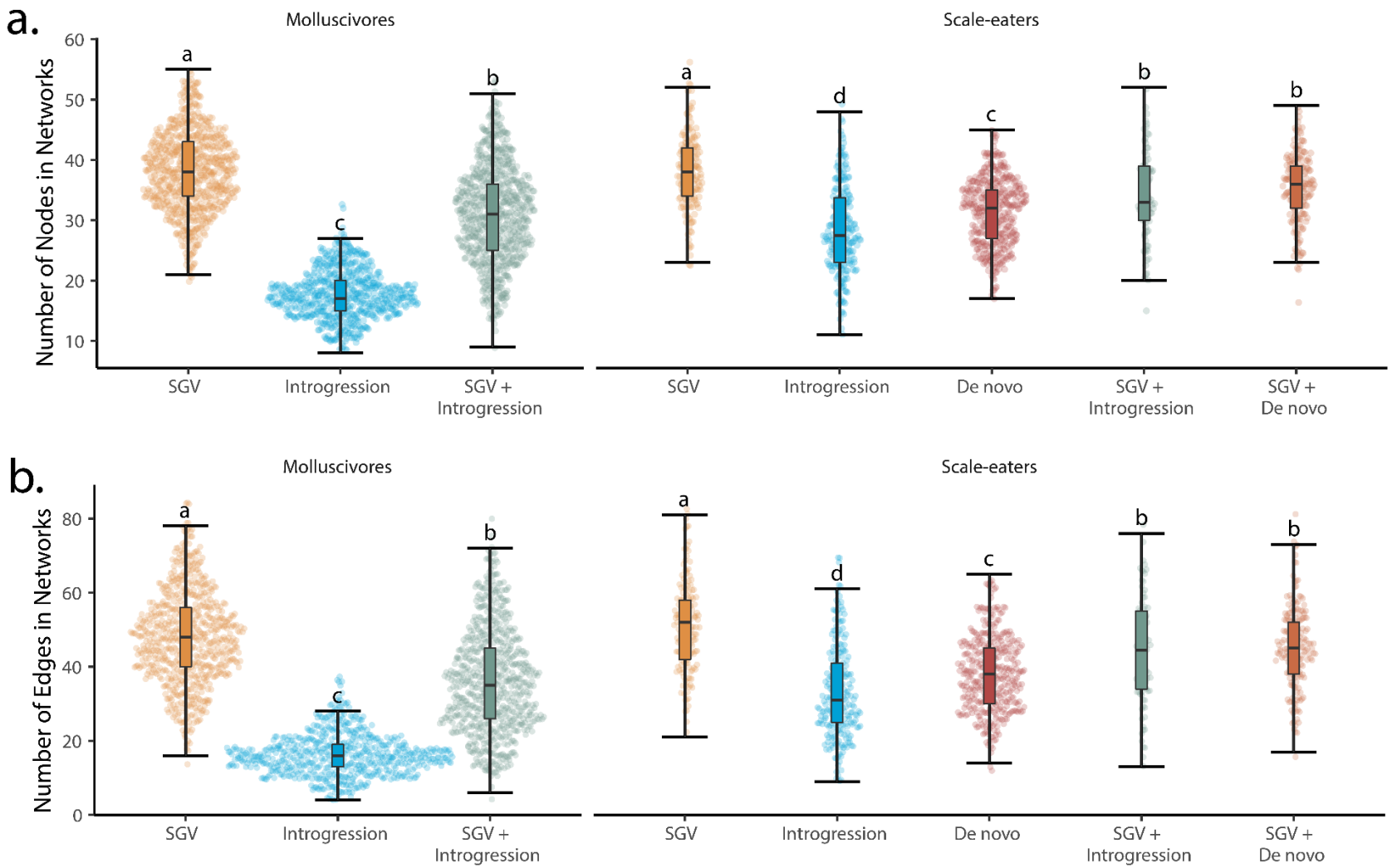


**Figure S13. Genotypic fitness networks (using growth) are smaller both with respect to number of nodes (A) and number of edges (B) when SNPs sourced from introgression or *de novo* mutation are included than networks constructed from standing genetic variation (SGV) alone.** Compact letter display reports pairwise significance according to a nonparametric Kruskal-Wallis one-way analysis of variance following correction for multiple tests using an estimated False Discovery Rate. Letters are ordered (i.e. **a** to **c**) in decreasing values of the median. These results include only survivors and thus differ from those shown in Figure S12.

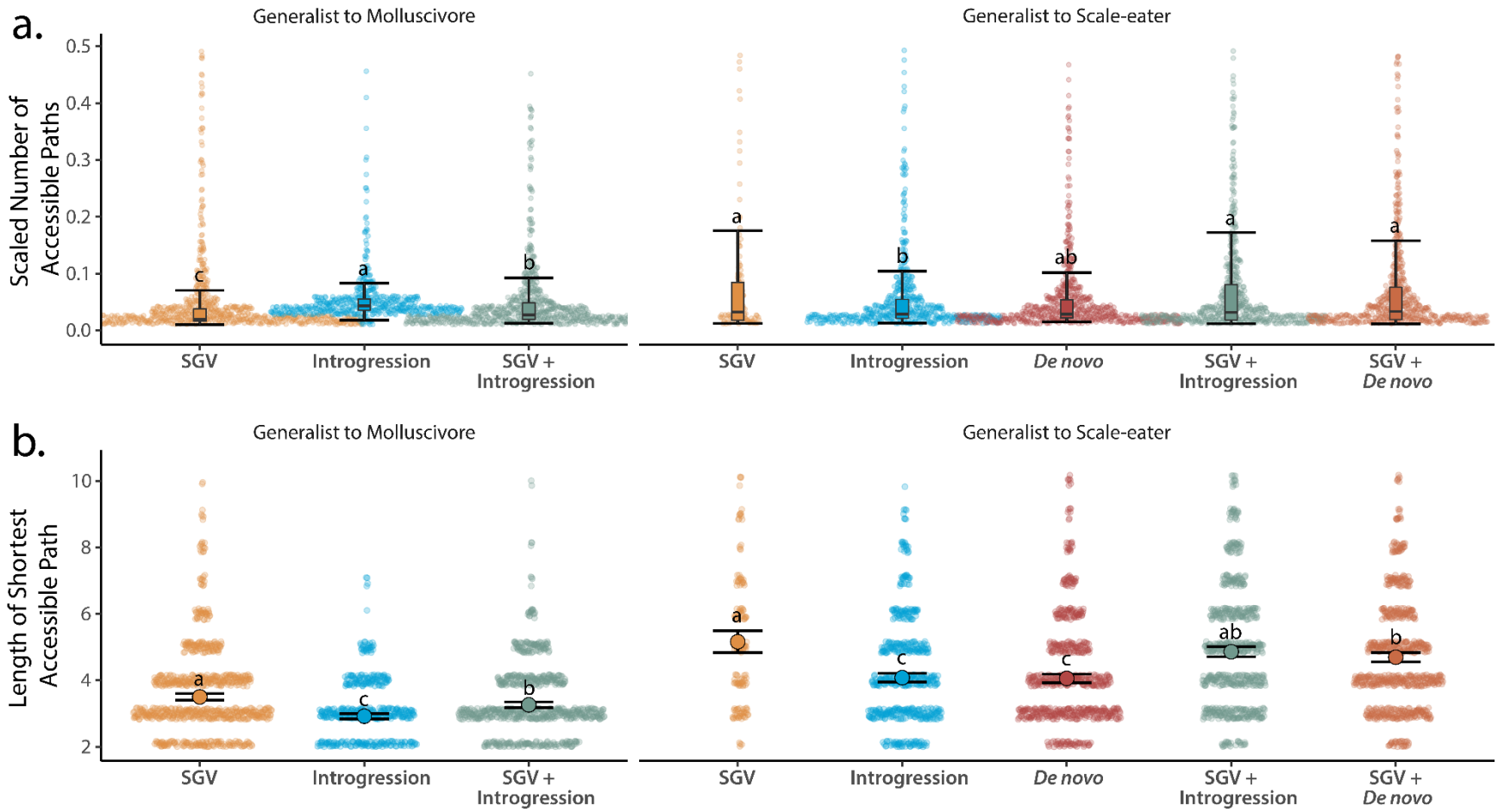


**Figure S14. Accessibility of between-species genotypic trajectories in survival fitness landscapes constructed from SNPs exhibiting signatures of divergent selection (Richards et al. 2021) that are sourced from either standing genetic variation (SGV), introgression, *de novo* mutation, or a combination. A)** The number of accessible (i.e. monotonically increasing in fitness) paths per network, scaled by the size of the network. Compact letter display reports pairwise significance according to a nonparametric Kruskal-Wallis one-way analysis of variance following correction for multiple tests using an estimated False Discovery Rate. **B)** Number of mutational steps in the shortest accessible path.

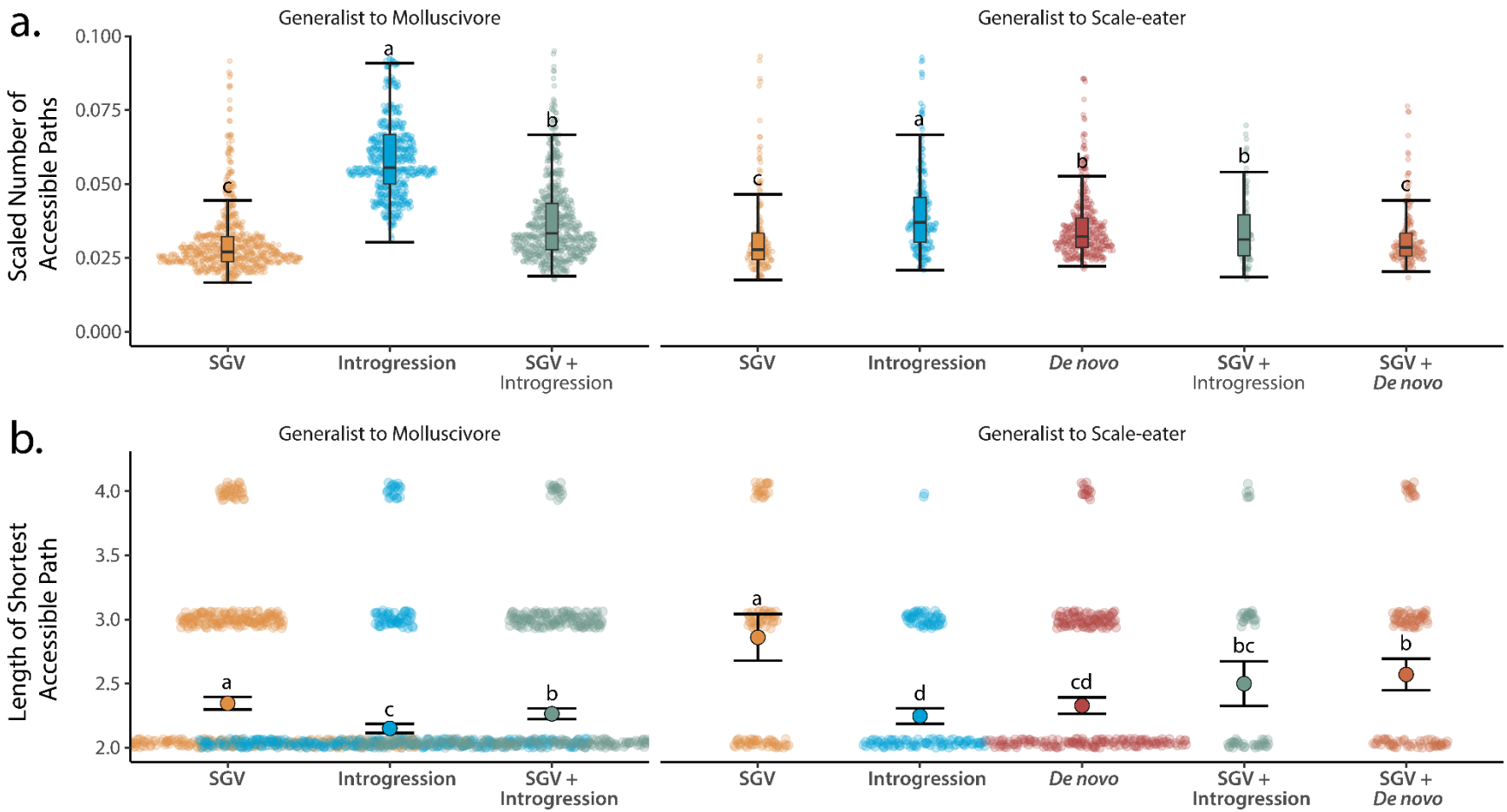


**Figure S15. Accessibility of between-species genotypic trajectories in growth fitness landscapes constructed from SNPs exhibiting signatures of divergent selection (Richards et al. 2021) that are sourced from either standing genetic variation (SGV), introgression, *de novo* mutation, or a combination. A)** The number of accessible (i.e. monotonically increasing in fitness) paths per network, scaled by the size of the network. Compact letter display reports pairwise significance according to a nonparametric Kruskal-Wallis one-way analysis of variance following correction for multiple tests using an estimated False Discovery Rate. **B)** Number of mutational steps in the shortest accessible path.

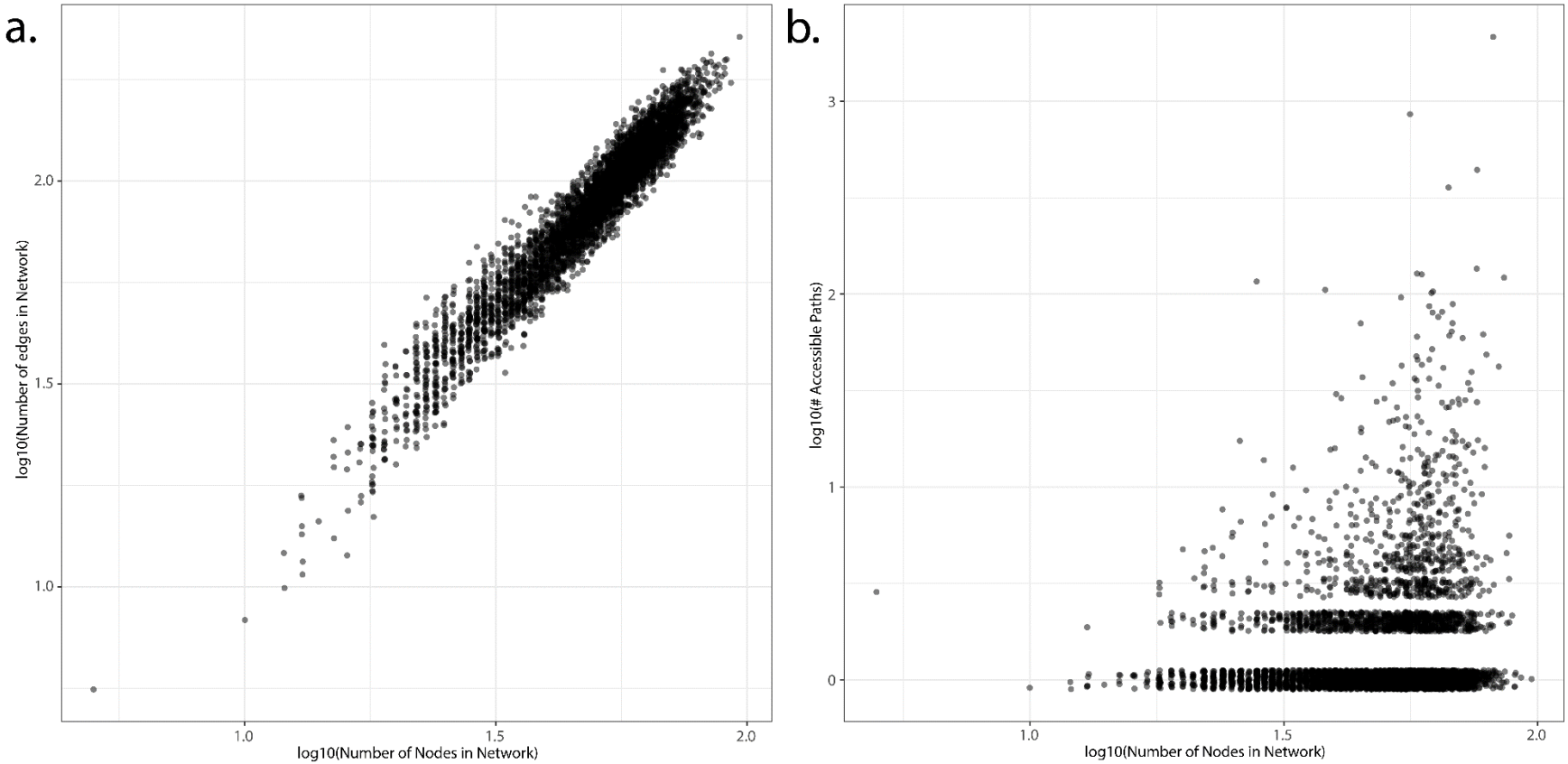


**Figure S16. The number of edges and thus potential number of paths (A) and accessible paths (B) increases as network size (number of nodes) increases.**

**Table S1. Samples of hybrids and parental studies used either in genomic or morphological analyses, along with associated metadata.**

| ID | Sequenced | Morphology | Survivorship | Experiment | Lake | Species |
|---|---|---|---|---|---|---|
| CP04E02 | This study | Yes | Non-Survivor | Martin & Gould 2020 | Crescent Pond | Hybrid |
| CP07F05 | This study | Yes | Non-Survivor | Martin & Gould 2020 | Crescent Pond | Hybrid |
| CP08H06 | This study | Yes | Non-Survivor | Martin & Gould 2020 | Crescent Pond | Hybrid |
| CP09C02 | This study | Yes | Non-Survivor | Martin & Gould 2020 | Crescent Pond | Hybrid |
| CP09D01 | This study | Yes | Non-Survivor | Martin & Gould 2020 | Crescent Pond | Hybrid |
| CP09F10 | This study | Yes | Non-Survivor | Martin & Gould 2020 | Crescent Pond | Hybrid |
| CP10B05 | This study | Yes | Non-Survivor | Martin & Gould 2020 | Crescent Pond | Hybrid |
| CP11C10 | This study | Yes | Non-Survivor | Martin & Gould 2020 | Crescent Pond | Hybrid |
| CP13E03 | This study | Yes | Non-Survivor | Martin & Gould 2020 | Crescent Pond | Hybrid |
| CP13F01 | This study | Yes | Non-Survivor | Martin & Gould 2020 | Crescent Pond | Hybrid |
| LL01F03 | This study | Yes | Non-Survivor | Martin & Gould 2020 | Little Lake | Hybrid |
| LL01F05 | This study | Yes | Non-Survivor | Martin & Gould 2020 | Little Lake | Hybrid |
| LL01G05 | This study | Yes | Non-Survivor | Martin & Gould 2020 | Little Lake | Hybrid |
| LL02A08 | This study | Yes | Non-Survivor | Martin & Gould 2020 | Little Lake | Hybrid |
| LL02D09 | This study | Yes | Non-Survivor | Martin & Gould 2020 | Little Lake | Hybrid |
| LL02D11 | This study | Yes | Non-Survivor | Martin & Gould 2020 | Little Lake | Hybrid |
| LL02E04 | This study | Yes | Non-Survivor | Martin & Gould 2020 | Little Lake | Hybrid |
| LL02E07 | This study | Yes | Non-Survivor | Martin & Gould 2020 | Little Lake | Hybrid |
| LL02E09 | This study | Yes | Non-Survivor | Martin & Gould 2020 | Little Lake | Hybrid |
| LL04E03 | This study | Yes | Non-Survivor | Martin & Gould 2020 | Little Lake | Hybrid |
| LL04E09 | This study | Yes | Non-Survivor | Martin & Gould 2020 | Little Lake | Hybrid |
| LL04F02 | This study | Yes | Non-Survivor | Martin & Gould 2020 | Little Lake | Hybrid |
| LL04F07 | This study | Yes | Non-Survivor | Martin & Gould 2020 | Little Lake | Hybrid |
| LL05A01 | This study | Yes | Non-Survivor | Martin & Gould 2020 | Little Lake | Hybrid |
| LL05C06 | This study | Yes | Non-Survivor | Martin & Gould 2020 | Little Lake | Hybrid |
| LL05C09 | This study | Yes | Non-Survivor | Martin & Gould 2020 | Little Lake | Hybrid |
| LL05C10 | This study | Yes | Non-Survivor | Martin & Gould 2020 | Little Lake | Hybrid |
| LL05D10 | This study | Yes | Non-Survivor | Martin & Gould 2020 | Little Lake | Hybrid |
| LL05E06 | This study | Yes | Non-Survivor | Martin & Gould 2020 | Little Lake | Hybrid |
| LL05E08 | This study | Yes | Non-Survivor | Martin & Gould 2020 | Little Lake | Hybrid |
| LL05H10 | This study | Yes | Non-Survivor | Martin & Gould 2020 | Little Lake | Hybrid |
| LL06A10 | This study | Yes | Non-Survivor | Martin & Gould 2020 | Little Lake | Hybrid |
| LL06B03 | This study | Yes | Non-Survivor | Martin & Gould 2020 | Little Lake | Hybrid |
| LL06C10 | This study | Yes | Non-Survivor | Martin & Gould 2020 | Little Lake | Hybrid |
| LL06D12 | This study | Yes | Non-Survivor | Martin & Gould 2020 | Little Lake | Hybrid |
| LL06E10 | This study | Yes | Non-Survivor | Martin & Gould 2020 | Little Lake | Hybrid |
| LL06F08 | This study | Yes | Non-Survivor | Martin & Gould 2020 | Little Lake | Hybrid |
| LL08B09 | This study | Yes | Non-Survivor | Martin & Gould 2020 | Little Lake | Hybrid |
| LL08B11 | This study | Yes | Non-Survivor | Martin & Gould 2020 | Little Lake | Hybrid |
| LL08G07 | This study | Yes | Non-Survivor | Martin & Gould 2020 | Little Lake | Hybrid |
| LL08G10 | This study | Yes | Non-Survivor | Martin & Gould 2020 | Little Lake | Hybrid |
| LL08H01 | This study | Yes | Non-Survivor | Martin & Gould 2020 | Little Lake | Hybrid |
| LL09A09 | This study | Yes | Non-Survivor | Martin & Gould 2020 | Little Lake | Hybrid |
| LL09A10 | This study | Yes | Non-Survivor | Martin & Gould 2020 | Little Lake | Hybrid |
| LL09B05 | This study | Yes | Non-Survivor | Martin & Gould 2020 | Little Lake | Hybrid |
| LL09C03 | This study | Yes | Non-Survivor | Martin & Gould 2020 | Little Lake | Hybrid |
| LL09D01 | This study | Yes | Non-Survivor | Martin & Gould 2020 | Little Lake | Hybrid |
| LL09D10 | This study | Yes | Non-Survivor | Martin & Gould 2020 | Little Lake | Hybrid |
| LL09E01 | This study | Yes | Non-Survivor | Martin & Gould 2020 | Little Lake | Hybrid |
| LL09F03 | This study | Yes | Non-Survivor | Martin & Gould 2020 | Little Lake | Hybrid |
| LL09H07 | This study | Yes | Non-Survivor | Martin & Gould 2020 | Little Lake | Hybrid |
| LL09H10 | This study | Yes | Non-Survivor | Martin & Gould 2020 | Little Lake | Hybrid |
| LL10A08 | This study | Yes | Non-Survivor | Martin & Gould 2020 | Little Lake | Hybrid |

| | | | | | | |
|---|---|---|---|---|---|---|
| CP02D01 | This study | Yes | Survivor | Martin & Gould 2020 | Crescent Pond | Hybrid |
| CP02E09 | This study | Yes | Survivor | Martin & Gould 2020 | Crescent Pond | Hybrid |
| CP03D02 | This study | Yes | Survivor | Martin & Gould 2020 | Crescent Pond | Hybrid |
| CP03G03 | This study | Yes | Survivor | Martin & Gould 2020 | Crescent Pond | Hybrid |
| CP03G07 | This study | Yes | Survivor | Martin & Gould 2020 | Crescent Pond | Hybrid |
| CP05B08 | This study | Yes | Survivor | Martin & Gould 2020 | Crescent Pond | Hybrid |
| CP05E02 | This study | Yes | Survivor | Martin & Gould 2020 | Crescent Pond | Hybrid |
| CP05G12 | This study | Yes | Survivor | Martin & Gould 2020 | Crescent Pond | Hybrid |
| CP05H10 | This study | Yes | Survivor | Martin & Gould 2020 | Crescent Pond | Hybrid |
| CP06E09 | This study | Yes | Survivor | Martin & Gould 2020 | Crescent Pond | Hybrid |
| CP06G01 | This study | Yes | Survivor | Martin & Gould 2020 | Crescent Pond | Hybrid |
| CP06H09 | This study | Yes | Survivor | Martin & Gould 2020 | Crescent Pond | Hybrid |
| CP07E08 | This study | Yes | Survivor | Martin & Gould 2020 | Crescent Pond | Hybrid |
| CP07H01 | This study | Yes | Survivor | Martin & Gould 2020 | Crescent Pond | Hybrid |
| CP07H11 | This study | Yes | Survivor | Martin & Gould 2020 | Crescent Pond | Hybrid |
| CP08F07 | This study | Yes | Survivor | Martin & Gould 2020 | Crescent Pond | Hybrid |
| CP08G08 | This study | Yes | Survivor | Martin & Gould 2020 | Crescent Pond | Hybrid |
| CP09D02 | This study | Yes | Survivor | Martin & Gould 2020 | Crescent Pond | Hybrid |
| CP10A03 | This study | Yes | Survivor | Martin & Gould 2020 | Crescent Pond | Hybrid |
| CP10C04 | This study | Yes | Survivor | Martin & Gould 2020 | Crescent Pond | Hybrid |
| CP10C07 | This study | Yes | Survivor | Martin & Gould 2020 | Crescent Pond | Hybrid |
| CP10C12 | This study | Yes | Survivor | Martin & Gould 2020 | Crescent Pond | Hybrid |
| CP10F12 | This study | Yes | Survivor | Martin & Gould 2020 | Crescent Pond | Hybrid |
| CP10H01 | This study | Yes | Survivor | Martin & Gould 2020 | Crescent Pond | Hybrid |
| CP11B03 | This study | Yes | Survivor | Martin & Gould 2020 | Crescent Pond | Hybrid |
| CP11C08 | This study | Yes | Survivor | Martin & Gould 2020 | Crescent Pond | Hybrid |
| CP11D04 | This study | Yes | Survivor | Martin & Gould 2020 | Crescent Pond | Hybrid |
| CP11G06 | This study | Yes | Survivor | Martin & Gould 2020 | Crescent Pond | Hybrid |
| CP11G12 | This study | Yes | Survivor | Martin & Gould 2020 | Crescent Pond | Hybrid |
| CP12E05 | This study | Yes | Survivor | Martin & Gould 2020 | Crescent Pond | Hybrid |
| CP12E07 | This study | Yes | Survivor | Martin & Gould 2020 | Crescent Pond | Hybrid |
| CP12H04 | This study | Yes | Survivor | Martin & Gould 2020 | Crescent Pond | Hybrid |
| CP13B02 | This study | Yes | Survivor | Martin & Gould 2020 | Crescent Pond | Hybrid |
| CP13B08 | This study | Yes | Survivor | Martin & Gould 2020 | Crescent Pond | Hybrid |
| CP14C04 | This study | Yes | Survivor | Martin & Gould 2020 | Crescent Pond | Hybrid |
| CP15A10 | This study | Yes | Survivor | Martin & Gould 2020 | Crescent Pond | Hybrid |
| CP15B08 | This study | Yes | Survivor | Martin & Gould 2020 | Crescent Pond | Hybrid |
| CP15E01 | This study | Yes | Survivor | Martin & Gould 2020 | Crescent Pond | Hybrid |
| CP15E03 | This study | Yes | Survivor | Martin & Gould 2020 | Crescent Pond | Hybrid |
| CP17A01 | This study | Yes | Survivor | Martin & Gould 2020 | Crescent Pond | Hybrid |
| CP18B11 | This study | Yes | Survivor | Martin & Gould 2020 | Crescent Pond | Hybrid |
| CP19B02 | This study | Yes | Survivor | Martin & Gould 2020 | Crescent Pond | Hybrid |
| CP19C02 | This study | Yes | Survivor | Martin & Gould 2020 | Crescent Pond | Hybrid |
| CP19C07 | This study | Yes | Survivor | Martin & Gould 2020 | Crescent Pond | Hybrid |
| CP19F01 | This study | Yes | Survivor | Martin & Gould 2020 | Crescent Pond | Hybrid |
| CP19G03 | This study | Yes | Survivor | Martin & Gould 2020 | Crescent Pond | Hybrid |
| CPH01 | This study | Yes | Survivor | Martin & Wainwright 2013 | Crescent Pond | Hybrid |
| CPH02 | This study | Yes | Survivor | Martin & Wainwright 2013 | Crescent Pond | Hybrid |
| CPH03 | This study | Yes | Survivor | Martin & Wainwright 2013 | Crescent Pond | Hybrid |
| CPH04 | This study | Yes | Survivor | Martin & Wainwright 2013 | Crescent Pond | Hybrid |
| CPH05 | This study | Yes | Survivor | Martin & Wainwright 2013 | Crescent Pond | Hybrid |
| CPH07 | This study | Yes | Survivor | Martin & Wainwright 2013 | Crescent Pond | Hybrid |
| CPH08 | This study | Yes | Survivor | Martin & Wainwright 2013 | Crescent Pond | Hybrid |
| CPH09 | This study | Yes | Survivor | Martin & Wainwright 2013 | Crescent Pond | Hybrid |
| CPH10 | This study | Yes | Survivor | Martin & Wainwright 2013 | Crescent Pond | Hybrid |
| CPH100 | This study | Yes | Survivor | Martin & Wainwright 2013 | Crescent Pond | Hybrid |
| CPH11 | This study | Yes | Survivor | Martin & Wainwright 2013 | Crescent Pond | Hybrid |

| | | | | | | |
|---|---|---|---|---|---|---|
| CPH123 | This study | Yes | Survivor | Martin & Wainwright 2013 | Crescent Pond | Hybrid |
| LL01H04 | This study | Yes | Survivor | Martin & Gould 2020 | Little Lake | Hybrid |
| LL02G09 | This study | Yes | Survivor | Martin & Gould 2020 | Little Lake | Hybrid |
| LL06B06 | This study | Yes | Survivor | Martin & Gould 2020 | Little Lake | Hybrid |
| LL06E04 | This study | Yes | Survivor | Martin & Gould 2020 | Little Lake | Hybrid |
| LL07E12 | This study | Yes | Survivor | Martin & Gould 2020 | Little Lake | Hybrid |
| LL07G04 | This study | Yes | Survivor | Martin & Gould 2020 | Little Lake | Hybrid |
| LL08A09 | This study | Yes | Survivor | Martin & Gould 2020 | Little Lake | Hybrid |
| LL08B04 | This study | Yes | Survivor | Martin & Gould 2020 | Little Lake | Hybrid |
| LL08D05 | This study | Yes | Survivor | Martin & Gould 2020 | Little Lake | Hybrid |
| LL10F08 | This study | Yes | Survivor | Martin & Gould 2020 | Little Lake | Hybrid |
| LL12B04 | This study | Yes | Survivor | Martin & Gould 2020 | Little Lake | Hybrid |
| LL13B06 | This study | Yes | Survivor | Martin & Gould 2020 | Little Lake | Hybrid |
| LL13D04 | This study | Yes | Survivor | Martin & Gould 2020 | Little Lake | Hybrid |
| LL17H03 | This study | Yes | Survivor | Martin & Gould 2020 | Little Lake | Hybrid |
| LL106 | This study | Yes | Survivor | Martin & Wainwright 2013 | Little Lake | Hybrid |
| LL114 | This study | Yes | Survivor | Martin & Wainwright 2013 | Little Lake | Hybrid |
| LL124 | This study | Yes | Survivor | Martin & Wainwright 2013 | Little Lake | Hybrid |
| LL129 | This study | Yes | Survivor | Martin & Wainwright 2013 | Little Lake | Hybrid |
| LL175 | This study | Yes | Survivor | Martin & Wainwright 2013 | Little Lake | Hybrid |
| LL23 | This study | Yes | Survivor | Martin & Wainwright 2013 | Little Lake | Hybrid |
| LL247 | This study | Yes | Survivor | Martin & Wainwright 2013 | Little Lake | Hybrid |
| LL251 | This study | Yes | Survivor | Martin & Wainwright 2013 | Little Lake | Hybrid |
| LL271 | This study | Yes | Survivor | Martin & Wainwright 2013 | Little Lake | Hybrid |
| LLH12 | This study | Yes | Survivor | Martin & Wainwright 2013 | Little Lake | Hybrid |
| LLH34 | This study | Yes | Survivor | Martin & Wainwright 2013 | Little Lake | Hybrid |
| LLH41 | This study | Yes | Survivor | Martin & Wainwright 2013 | Little Lake | Hybrid |
| LLH51 | This study | Yes | Survivor | Martin & Wainwright 2013 | Little Lake | Hybrid |
| LLH94 | This study | Yes | Survivor | Martin & Wainwright 2013 | Little Lake | Hybrid |
| CRPA1 | Richards et al. 2021 | No | NA | NA | Crescent Pond | Generalist |
| CRPA1000 | Richards et al. 2021 | No | NA | NA | Crescent Pond | Generalist |
| CRPA1001 | Richards et al. 2021 | No | NA | NA | Crescent Pond | Generalist |
| CRPA1003 | Richards et al. 2021 | No | NA | NA | Crescent Pond | Generalist |
| CRPA3 | Richards et al. 2021 | No | NA | NA | Crescent Pond | Generalist |
| LILA1 | Richards et al. 2021 | No | NA | NA | Little Lake | Generalist |
| OSPA1 | Richards et al. 2021 | No | NA | NA | Osprey Pond (Little Lake) | Generalist |
| OSPA1000 | Richards et al. 2021 | No | NA | NA | Osprey Pond (Little Lake) | Generalist |
| OSPA1001 | Richards et al. 2021 | No | NA | NA | Osprey Pond (Little Lake) | Generalist |
| OSPA11 | Richards et al. 2021 | No | NA | NA | Osprey Pond (Little Lake) | Generalist |
| OSPA12 | Richards et al. 2021 | No | NA | NA | Osprey Pond (Little Lake) | Generalist |
| OSPA13 | Richards et al. 2021 | No | NA | NA | Osprey Pond (Little Lake) | Generalist |
| OSPA4 | Richards et al. 2021 | No | NA | NA | Osprey Pond (Little Lake) | Generalist |
| OSPA5 | Richards et al. 2021 | No | NA | NA | Osprey Pond (Little Lake) | Generalist |
| OSPA6 | Richards et al. 2021 | No | NA | NA | Osprey Pond (Little Lake) | Generalist |
| OSPA8 | Richards et al. 2021 | No | NA | NA | Osprey Pond (Little Lake) | Generalist |
| OSPA9 | Richards et al. 2021 | No | NA | NA | Osprey Pond (Little Lake) | Generalist |
| CRPM1 | Richards et al. 2021 | No | NA | NA | Crescent Pond | Molluscivore |
| CRPM10 | Richards et al. 2021 | No | NA | NA | Crescent Pond | Molluscivore |
| CRPM1000 | Richards et al. 2021 | No | NA | NA | Crescent Pond | Molluscivore |
| CRPM1001 | Richards et al. 2021 | No | NA | NA | Crescent Pond | Molluscivore |
| CRPM11 | Richards et al. 2021 | No | NA | NA | Crescent Pond | Molluscivore |
| CRPM2 | Richards et al. 2021 | No | NA | NA | Crescent Pond | Molluscivore |
| CRPM3 | Richards et al. 2021 | No | NA | NA | Crescent Pond | Molluscivore |
| CRPM5 | Richards et al. 2021 | No | NA | NA | Crescent Pond | Molluscivore |
| CRPM6 | Richards et al. 2021 | No | NA | NA | Crescent Pond | Molluscivore |
| CRPM7 | Richards et al. 2021 | No | NA | NA | Crescent Pond | Molluscivore |
| CRPM8 | Richards et al. 2021 | No | NA | NA | Crescent Pond | Molluscivore |

| | | | | | | |
|---|---|---|---|---|---|---|
| CRPM9 | Richards et al. 2021 | No | NA | NA | Crescent Pond | Molluscivore |
| LILM-QTL | Richards et al. 2021 | No | NA | NA | Little Lake | Molluscivore |
| LILM3 | Richards et al. 2021 | No | NA | NA | Little Lake | Molluscivore |
| LILM4 | Richards et al. 2021 | No | NA | NA | Little Lake | Molluscivore |
| LILM5 | Richards et al. 2021 | No | NA | NA | Little Lake | Molluscivore |
| OSPM1 | Richards et al. 2021 | No | NA | NA | Osprey Pond (Little Lake) | Molluscivore |
| OSPM1000 | Richards et al. 2021 | No | NA | NA | Osprey Pond (Little Lake) | Molluscivore |
| OSPM1001 | Richards et al. 2021 | No | NA | NA | Osprey Pond (Little Lake) | Molluscivore |
| OSPM11 | Richards et al. 2021 | No | NA | NA | Osprey Pond (Little Lake) | Molluscivore |
| OSPM2 | Richards et al. 2021 | No | NA | NA | Osprey Pond (Little Lake) | Molluscivore |
| OSPM3 | Richards et al. 2021 | No | NA | NA | Osprey Pond (Little Lake) | Molluscivore |
| OSPM4 | Richards et al. 2021 | No | NA | NA | Osprey Pond (Little Lake) | Molluscivore |
| OSPM5 | Richards et al. 2021 | No | NA | NA | Osprey Pond (Little Lake) | Molluscivore |
| OSPM7 | Richards et al. 2021 | No | NA | NA | Osprey Pond (Little Lake) | Molluscivore |
| OSPM8 | Richards et al. 2021 | No | NA | NA | Osprey Pond (Little Lake) | Molluscivore |
| OSPM9 | Richards et al. 2021 | No | NA | NA | Osprey Pond (Little Lake) | Molluscivore |
| CRPP-QTL | Richards et al. 2021 | No | NA | NA | Crescent Pond | Scale-eater |
| CRPP1000 | Richards et al. 2021 | No | NA | NA | Crescent Pond | Scale-eater |
| CRPP1001 | Richards et al. 2021 | No | NA | NA | Crescent Pond | Scale-eater |
| CRPP2 | Richards et al. 2021 | No | NA | NA | Crescent Pond | Scale-eater |
| CRPP3 | Richards et al. 2021 | No | NA | NA | Crescent Pond | Scale-eater |
| CRPP4 | Richards et al. 2021 | No | NA | NA | Crescent Pond | Scale-eater |
| CRPP5 | Richards et al. 2021 | No | NA | NA | Crescent Pond | Scale-eater |
| CRPP7 | Richards et al. 2021 | No | NA | NA | Crescent Pond | Scale-eater |
| CRPP8 | Richards et al. 2021 | No | NA | NA | Crescent Pond | Scale-eater |
| CRPP9 | Richards et al. 2021 | No | NA | NA | Crescent Pond | Scale-eater |
| LILP-QTL | Richards et al. 2021 | No | NA | NA | Little Lake | Scale-eater |
| LILP3 | Richards et al. 2021 | No | NA | NA | Little Lake | Scale-eater |
| LILP4 | Richards et al. 2021 | No | NA | NA | Little Lake | Scale-eater |
| LILP5 | Richards et al. 2021 | No | NA | NA | Little Lake | Scale-eater |
| OSPP1 | Richards et al. 2021 | No | NA | NA | Osprey Pond (Little Lake) | Scale-eater |
| OSPP10 | Richards et al. 2021 | No | NA | NA | Osprey Pond (Little Lake) | Scale-eater |
| OSPP1000 | Richards et al. 2021 | No | NA | NA | Osprey Pond (Little Lake) | Scale-eater |
| OSPP1001 | Richards et al. 2021 | No | NA | NA | Osprey Pond (Little Lake) | Scale-eater |
| OSPP11 | Richards et al. 2021 | No | NA | NA | Osprey Pond (Little Lake) | Scale-eater |
| OSPP2 | Richards et al. 2021 | No | NA | NA | Osprey Pond (Little Lake) | Scale-eater |
| OSPP3 | Richards et al. 2021 | No | NA | NA | Osprey Pond (Little Lake) | Scale-eater |
| OSPP4 | Richards et al. 2021 | No | NA | NA | Osprey Pond (Little Lake) | Scale-eater |
| OSPP5 | Richards et al. 2021 | No | NA | NA | Osprey Pond (Little Lake) | Scale-eater |
| OSPP7 | Richards et al. 2021 | No | NA | NA | Osprey Pond (Little Lake) | Scale-eater |
| OSPP9 | Richards et al. 2021 | No | NA | NA | Osprey Pond (Little Lake) | Scale-eater |
| CPA01 | NA | Yes | Parental | NA | Crescent Pond | Generalist |
| CPA03 | NA | Yes | Parental | NA | Crescent Pond | Generalist |
| CPA05 | NA | Yes | Parental | NA | Crescent Pond | Generalist |
| CPA07 | NA | Yes | Parental | NA | Crescent Pond | Generalist |
| CPA09 | NA | Yes | Parental | NA | Crescent Pond | Generalist |
| CPA11 | NA | Yes | Parental | NA | Crescent Pond | Generalist |
| CPA13 | NA | Yes | Parental | NA | Crescent Pond | Generalist |
| CPA15 | NA | Yes | Parental | NA | Crescent Pond | Generalist |
| CPA17 | NA | Yes | Parental | NA | Crescent Pond | Generalist |
| CPA19 | NA | Yes | Parental | NA | Crescent Pond | Generalist |
| CPA21 | NA | Yes | Parental | NA | Crescent Pond | Generalist |
| CPA23 | NA | Yes | Parental | NA | Crescent Pond | Generalist |
| CPA25 | NA | Yes | Parental | NA | Crescent Pond | Generalist |
| CPA27 | NA | Yes | Parental | NA | Crescent Pond | Generalist |
| CPA29 | NA | Yes | Parental | NA | Crescent Pond | Generalist |
| CPA31 | NA | Yes | Parental | NA | Crescent Pond | Generalist |

| | | | | | | |
|---|---|---|---|---|---|---|
| CPA33 | NA | Yes | Parental | NA | Crescent Pond | Generalist |
| CPA35 | NA | Yes | Parental | NA | Crescent Pond | Generalist |
| CPA37 | NA | Yes | Parental | NA | Crescent Pond | Generalist |
| CPA39 | NA | Yes | Parental | NA | Crescent Pond | Generalist |
| CPA41 | NA | Yes | Parental | NA | Crescent Pond | Generalist |
| CPA43 | NA | Yes | Parental | NA | Crescent Pond | Generalist |
| CPA45 | NA | Yes | Parental | NA | Crescent Pond | Generalist |
| CPA47 | NA | Yes | Parental | NA | Crescent Pond | Generalist |
| CPA49 | NA | Yes | Parental | NA | Crescent Pond | Generalist |
| CPA51 | NA | Yes | Parental | NA | Crescent Pond | Generalist |
| CPA53 | NA | Yes | Parental | NA | Crescent Pond | Generalist |
| CPA55 | NA | Yes | Parental | NA | Crescent Pond | Generalist |
| CPA57 | NA | Yes | Parental | NA | Crescent Pond | Generalist |
| CPA59 | NA | Yes | Parental | NA | Crescent Pond | Generalist |
| LLA20 | NA | Yes | Parental | NA | Little Lake | Generalist |
| LLA21 | NA | Yes | Parental | NA | Little Lake | Generalist |
| LLA22 | NA | Yes | Parental | NA | Little Lake | Generalist |
| LLA23 | NA | Yes | Parental | NA | Little Lake | Generalist |
| LLA24 | NA | Yes | Parental | NA | Little Lake | Generalist |
| LLA25 | NA | Yes | Parental | NA | Little Lake | Generalist |
| LLA26 | NA | Yes | Parental | NA | Little Lake | Generalist |
| LLA27 | NA | Yes | Parental | NA | Little Lake | Generalist |
| LLA28 | NA | Yes | Parental | NA | Little Lake | Generalist |
| LLA29 | NA | Yes | Parental | NA | Little Lake | Generalist |
| LLA30 | NA | Yes | Parental | NA | Little Lake | Generalist |
| LLA31 | NA | Yes | Parental | NA | Little Lake | Generalist |
| LLA32 | NA | Yes | Parental | NA | Little Lake | Generalist |
| LLA33 | NA | Yes | Parental | NA | Little Lake | Generalist |
| LLA34 | NA | Yes | Parental | NA | Little Lake | Generalist |
| LLA35 | NA | Yes | Parental | NA | Little Lake | Generalist |
| LLA36 | NA | Yes | Parental | NA | Little Lake | Generalist |
| LLA37 | NA | Yes | Parental | NA | Little Lake | Generalist |
| LLA38 | NA | Yes | Parental | NA | Little Lake | Generalist |
| LLA39 | NA | Yes | Parental | NA | Little Lake | Generalist |
| LLA40 | NA | Yes | Parental | NA | Little Lake | Generalist |
| LLA41 | NA | Yes | Parental | NA | Little Lake | Generalist |
| LLA42 | NA | Yes | Parental | NA | Little Lake | Generalist |
| LLA43 | NA | Yes | Parental | NA | Little Lake | Generalist |
| LLA44 | NA | Yes | Parental | NA | Little Lake | Generalist |
| LLA45 | NA | Yes | Parental | NA | Little Lake | Generalist |
| LLA46 | NA | Yes | Parental | NA | Little Lake | Generalist |
| LLA47 | NA | Yes | Parental | NA | Little Lake | Generalist |
| LLA48 | NA | Yes | Parental | NA | Little Lake | Generalist |
| LLA49 | NA | Yes | Parental | NA | Little Lake | Generalist |
| CPM01 | NA | Yes | Parental | NA | Crescent Pond | Molluscivore |
| CPM02 | NA | Yes | Parental | NA | Crescent Pond | Molluscivore |
| CPM03 | NA | Yes | Parental | NA | Crescent Pond | Molluscivore |
| CPM04 | NA | Yes | Parental | NA | Crescent Pond | Molluscivore |
| CPM05 | NA | Yes | Parental | NA | Crescent Pond | Molluscivore |
| CPM06 | NA | Yes | Parental | NA | Crescent Pond | Molluscivore |
| CPM07 | NA | Yes | Parental | NA | Crescent Pond | Molluscivore |
| CPM08 | NA | Yes | Parental | NA | Crescent Pond | Molluscivore |
| CPM09 | NA | Yes | Parental | NA | Crescent Pond | Molluscivore |
| CPM10 | NA | Yes | Parental | NA | Crescent Pond | Molluscivore |
| CPM11 | NA | Yes | Parental | NA | Crescent Pond | Molluscivore |
| CPM12 | NA | Yes | Parental | NA | Crescent Pond | Molluscivore |
| CPM13 | NA | Yes | Parental | NA | Crescent Pond | Molluscivore |

| | | | | | | |
|---|---|---|---|---|---|---|
| CPM14 | NA | Yes | Parental | NA | Crescent Pond | Molluscivore |
| CPM15 | NA | Yes | Parental | NA | Crescent Pond | Molluscivore |
| CPM16 | NA | Yes | Parental | NA | Crescent Pond | Molluscivore |
| CPM17 | NA | Yes | Parental | NA | Crescent Pond | Molluscivore |
| CPM18 | NA | Yes | Parental | NA | Crescent Pond | Molluscivore |
| CPM19 | NA | Yes | Parental | NA | Crescent Pond | Molluscivore |
| CPM20 | NA | Yes | Parental | NA | Crescent Pond | Molluscivore |
| LLM01 | NA | Yes | Parental | NA | Little Lake | Molluscivore |
| LLM02 | NA | Yes | Parental | NA | Little Lake | Molluscivore |
| LLM03 | NA | Yes | Parental | NA | Little Lake | Molluscivore |
| LLM04 | NA | Yes | Parental | NA | Little Lake | Molluscivore |
| LLM05 | NA | Yes | Parental | NA | Little Lake | Molluscivore |
| LLM06 | NA | Yes | Parental | NA | Little Lake | Molluscivore |
| LLM07 | NA | Yes | Parental | NA | Little Lake | Molluscivore |
| LLM08 | NA | Yes | Parental | NA | Little Lake | Molluscivore |
| LLM09 | NA | Yes | Parental | NA | Little Lake | Molluscivore |
| LLM10 | NA | Yes | Parental | NA | Little Lake | Molluscivore |
| LLM11 | NA | Yes | Parental | NA | Little Lake | Molluscivore |
| LLM12 | NA | Yes | Parental | NA | Little Lake | Molluscivore |
| LLM13 | NA | Yes | Parental | NA | Little Lake | Molluscivore |
| LLM14 | NA | Yes | Parental | NA | Little Lake | Molluscivore |
| LLM15 | NA | Yes | Parental | NA | Little Lake | Molluscivore |
| LLM16 | NA | Yes | Parental | NA | Little Lake | Molluscivore |
| LLM17 | NA | Yes | Parental | NA | Little Lake | Molluscivore |
| LLM18 | NA | Yes | Parental | NA | Little Lake | Molluscivore |
| CPP01 | NA | Yes | Parental | NA | Crescent Pond | Scale-eater |
| CPP02 | NA | Yes | Parental | NA | Crescent Pond | Scale-eater |
| CPP03 | NA | Yes | Parental | NA | Crescent Pond | Scale-eater |
| CPP04 | NA | Yes | Parental | NA | Crescent Pond | Scale-eater |
| CPP05 | NA | Yes | Parental | NA | Crescent Pond | Scale-eater |
| CPP06 | NA | Yes | Parental | NA | Crescent Pond | Scale-eater |
| CPP07 | NA | Yes | Parental | NA | Crescent Pond | Scale-eater |
| CPP08 | NA | Yes | Parental | NA | Crescent Pond | Scale-eater |
| CPP09 | NA | Yes | Parental | NA | Crescent Pond | Scale-eater |
| CPP10 | NA | Yes | Parental | NA | Crescent Pond | Scale-eater |
| CPP11 | NA | Yes | Parental | NA | Crescent Pond | Scale-eater |
| CPP12 | NA | Yes | Parental | NA | Crescent Pond | Scale-eater |
| CPP13 | NA | Yes | Parental | NA | Crescent Pond | Scale-eater |
| CPP14 | NA | Yes | Parental | NA | Crescent Pond | Scale-eater |
| CPP15 | NA | Yes | Parental | NA | Crescent Pond | Scale-eater |
| CPP16 | NA | Yes | Parental | NA | Crescent Pond | Scale-eater |
| CPP17 | NA | Yes | Parental | NA | Crescent Pond | Scale-eater |
| CPP18 | NA | Yes | Parental | NA | Crescent Pond | Scale-eater |
| CPP19 | NA | Yes | Parental | NA | Crescent Pond | Scale-eater |
| CPP20 | NA | Yes | Parental | NA | Crescent Pond | Scale-eater |
| CPP21 | NA | Yes | Parental | NA | Crescent Pond | Scale-eater |
| CPP22 | NA | Yes | Parental | NA | Crescent Pond | Scale-eater |
| CPP23 | NA | Yes | Parental | NA | Crescent Pond | Scale-eater |
| CPP24 | NA | Yes | Parental | NA | Crescent Pond | Scale-eater |
| CPP25 | NA | Yes | Parental | NA | Crescent Pond | Scale-eater |
| CPP26 | NA | Yes | Parental | NA | Crescent Pond | Scale-eater |
| CPP27 | NA | Yes | Parental | NA | Crescent Pond | Scale-eater |
| CPP28 | NA | Yes | Parental | NA | Crescent Pond | Scale-eater |
| CPP29 | NA | Yes | Parental | NA | Crescent Pond | Scale-eater |
| CPP30 | NA | Yes | Parental | NA | Crescent Pond | Scale-eater |
| LLP01 | NA | Yes | Parental | NA | Little Lake | Scale-eater |
| LLP02 | NA | Yes | Parental | NA | Little Lake | Scale-eater |

| | | | | | | |
|---|---|---|---|---|---|---|
| LLP03 | NA | Yes | Parental | NA | Little Lake | Scale-eater |
| LLP04 | NA | Yes | Parental | NA | Little Lake | Scale-eater |
| LLP05 | NA | Yes | Parental | NA | Little Lake | Scale-eater |
| LLP06 | NA | Yes | Parental | NA | Little Lake | Scale-eater |
| LLP07 | NA | Yes | Parental | NA | Little Lake | Scale-eater |
| LLP08 | NA | Yes | Parental | NA | Little Lake | Scale-eater |
| LLP09 | NA | Yes | Parental | NA | Little Lake | Scale-eater |
| LLP10 | NA | Yes | Parental | NA | Little Lake | Scale-eater |
| LLP11 | NA | Yes | Parental | NA | Little Lake | Scale-eater |
| LLP12 | NA | Yes | Parental | NA | Little Lake | Scale-eater |
| LLP13 | NA | Yes | Parental | NA | Little Lake | Scale-eater |
| LLP14 | NA | Yes | Parental | NA | Little Lake | Scale-eater |
| LLP15 | NA | Yes | Parental | NA | Little Lake | Scale-eater |
| LLP16 | NA | Yes | Parental | NA | Little Lake | Scale-eater |
| LLP17 | NA | Yes | Parental | NA | Little Lake | Scale-eater |
| LLP18 | NA | Yes | Parental | NA | Little Lake | Scale-eater |
| LLP19 | NA | Yes | Parental | NA | Little Lake | Scale-eater |
| LLP20 | NA | Yes | Parental | NA | Little Lake | Scale-eater |
| LLP21 | NA | Yes | Parental | NA | Little Lake | Scale-eater |
| LLP22 | NA | Yes | Parental | NA | Little Lake | Scale-eater |
| LLP23 | NA | Yes | Parental | NA | Little Lake | Scale-eater |
| LLP24 | NA | Yes | Parental | NA | Little Lake | Scale-eater |
| LLP25 | NA | Yes | Parental | NA | Little Lake | Scale-eater |
| LLP26 | NA | Yes | Parental | NA | Little Lake | Scale-eater |
| LLP27 | NA | Yes | Parental | NA | Little Lake | Scale-eater |
| LLP28 | NA | Yes | Parental | NA | Little Lake | Scale-eater |
| LLP29 | NA | Yes | Parental | NA | Little Lake | Scale-eater |
| LLP30 | NA | Yes | Parental | NA | Little Lake | Scale-eater |

**Table S2. Models tested to assess the extent to which specialist ancestry are genome-wide variation (PC1/PC2) predicts measures of fitness and their respective fits.** Best-fit models are bolded

| Fitness Measure | Species | Model | AIC | Ancestry/PC *P*-value |
|---|---|---|---|---|
| Composite Fitness | Molluscivore | **Composite ~ AncestryProp** | **77.69** | **0.5951** |
| | | Composite ~ AncestryProp + Lake | 78.19 | 0.4048 |
| | | Composite ~ AncestryProp + Experiment | 78.28 | 0.4435 |
| | | Composite ~ AncestryProp + Lake + Experiment | 78.67 | 0.2845 |
| | | Composite ~ AncestryProp + Lake * Experiment | 80.62 | 0.2797 |
| | Scale-eater | **Composite ~ AncestryProp** | **76.01** | **0.1641** |
| | | Composite ~ AncestryProp + Lake | 77.41 | 0.2283 |
| | | Composite ~ AncestryProp + Experiment | 77.78 | 0.3000 |
| | | Composite ~ AncestryProp + Lake + Experiment | 79.12 | 0.4013 |
| | | Composite ~ AncestryProp + Lake * Experiment | 81.12 | 0.4079 |
| | PC1 | **Composite ~ PC1** | **76.32** | **0.2017** |
| | | Composite ~ PC1 + Lake | 77.04 | 0.1778 |
| | | Composite ~ PC1 + Experiment | 77.43 | 0.2341 |
| | | Composite ~ PC1 + Lake + Experiment | 78.64 | 0.2786 |
| | | Composite ~ PC1 + Lake * Experiment | 80.39 | 0.2389 |
| | PC2 | **Composite ~ PC2** | **76.32** | **0.2740** |
| | | Composite ~ PC2 + Lake | 76.32 | 0.1124 |
| | | Composite ~ PC2 + Experiment | 78.15 | 0.3985 |
| | | Composite ~ PC2 + Lake + Experiment | 77.99 | 0.1793 |
| | | Composite ~ PC2 + Lake * Experiment | 79.96 | 0.1797 |
| Growth | Molluscivore | Growth ~ AncestryProp | 42.52 | 0.4231 |
| | | Growth ~ AncestryProp + Lake | 29.24 | 0.3383 |
| | | Growth ~ AncestryProp + Experiment | 13.91 | 0.0041 |
| | | Growth ~ AncestryProp + Lake + Experiment | -23.57 | 0.3932 |
| | | **Growth ~ AncestryProp + Lake * Experiment** | **-88.32** | **0.3280** |
| | Scale-eater | Growth ~ AncestryProp | 36.71 | 0.0122 |
| | | Growth ~ AncestryProp + Lake | 12.25 | 0.0000 |
| | | Growth ~ AncestryProp + Experiment | 21.98 | 0.4870 |
| | | Growth ~ AncestryProp + Lake + Experiment | -22.80 | 0.9950 |
| | | **Growth ~ AncestryProp + Lake * Experiment** | **-88.53** | **0.2825** |
| | PC1 | Growth ~ PC1 | 30.97 | 0.0006 |
| | | Growth ~ PC1 + Lake | 29.37 | 0.3723 |
| | | Growth ~ PC1 + Experiment | -32.37 | 0.0000 |
| | | Growth ~ PC1 + Lake + Experiment | -30.92 | 0.0055 |
| | | **Growth ~ PC1 + Lake * Experiment** | **-87.40** | **0.7638** |
| | PC2 | Growth ~ PC2 | 23.61 | 0.0002 |
| | | Growth ~ PC2 + Lake | 23.61 | 0.0119 |
| | | Growth ~ PC2 + Experiment | 14.04 | 0.0044 |
| | | Growth ~ PC2 + Lake + Experiment | -23.65 | 0.3677 |
| | | **Growth ~ PC2 + Lake * Experiment** | **-87.49** | **0.6724** |
| Survival | Molluscivore | Survival ~ AncestryProp | 188.78 | 0.9643 |
| | | Survival ~ AncestryProp + Lake | 155.11 | 0.0936 |
| | | Survival ~ AncestryProp + Experiment | 161.41 | 0.3709 |
| | | **Survival ~ AncestryProp + Lake + Experiment** | **123.06** | **0.3127** |
| | | Survival ~ AncestryProp + Lake * Experiment | 125.06 | 0.3127 |
| | Scale-eater | Survival ~ AncestryProp | 188.61 | 0.6756 |
| | | Survival ~ AncestryProp + Lake | 154.93 | 0.0852 |
| | | Survival ~ AncestryProp + Experiment | 158.99 | 0.0828 |
| | | **Survival ~ AncestryProp + Lake + Experiment** | **124.04** | **0.8041** |
| | | Survival ~ AncestryProp + Lake * Experiment | 126.04 | 0.8041 |
| | PC1 | **Survival ~ PC1** | **156.24** | **0.0000** |
| | | Survival ~ PC1 + Lake | 157.87 | 0.6943 |
| | | Survival ~ PC1 + Experiment | 121.52 | 0.0000 |
| | | Survival ~ PC1 + Lake + Experiment | 123.51 | 0.4386 |
| | | Survival ~ PC1 + Lake * Experiment | 125.51 | 0.4386 |
| | PC2 | **Survival ~ PC2** | **157.96** | **0.0268** |
| | | Survival ~ PC2 + Lake | 157.96 | 0.7988 |
| | | Survival ~ PC2 + Experiment | 160.72 | 0.2248 |
| | | Survival ~ PC2 + Lake + Experiment | 123.39 | 0.4047 |
| | | Survival ~ PC2 + Lake * Experiment | 125.39 | 0.4047 |

1181 **Table S3. SNPs found to be strongly associated with composite fitness using SnpEff** (107)**.** SNPs that were identified as being strongly associated with both growth and composite fitness are
1182 italicized, and those that remain significant after a Bonferroni correction are bolded.

| Scaffold | Position | Significance | REF | ALT | Variant Type | Gene Identifier | Gene Card |
|---|---|---|---|---|---|---|---|
| HiC_scaffold_1 | 32071263 | FDR | A | C | intergenic | CBRO_00000660-CBRO_00000661 | Znf250-Ptgdr2 |
| **HiC_scaffold_1** | **43866598** | **Bonferroni** | **G** | **A** | **intergenic** | **CBRO_00000910-CBRO_00000911** | **PPM1K-OVCH2** |
| HiC_scaffold_1 | 43867614 | FDR | C | T | intergenic | CBRO_00000910-CBRO_00000911 | PPM1K-OVCH2 |
| HiC_scaffold_3 | 2658774 | FDR | T | A | intergenic | CBRO_00017856-CBRO_00017857 | KMT2E-Magi2 |
| HiC_scaffold_3 | 2658775 | FDR | T | C | intergenic | CBRO_00017856-CBRO_00017857 | KMT2E-Magi2 |
| HiC_scaffold_3 | 2658793 | FDR | C | A | intergenic | CBRO_00017856-CBRO_00017857 | KMT2E-Magi2 |
| HiC_scaffold_4 | 18899496 | FDR | T | C | intergenic | CBRO_00012427-CBRO_00012428 | UNKNOWN-edc4 |
| HiC_scaffold_5 | 18306419 | FDR | C | G | upstream; intergenic | CBRO_00001232; CBRO_00001231-CBRO_00001232 | xlrs1; PPEF2-xlrs1 |
| HiC_scaffold_5 | 18306428 | FDR | A | T | upstream; intergenic | CBRO_00001232; CBRO_00001231-CBRO_00001232 | xlrs1; PPEF2-xlrs1 |
| HiC_scaffold_5 | 18307019 | FDR | G | T | intronic | CBRO_00001232 | xlrs1 |
| HiC_scaffold_5 | 18307030 | FDR | G | A | intronic | CBRO_00001232 | xlrs1 |
| HiC_scaffold_5 | 18311696 | FDR | C | T | intronic | CBRO_00001232 | xlrs1 |
| HiC_scaffold_5 | 40475116 | FDR | T | A | intergenic | CBRO_00001627-CBRO_00001628 | SLC25A44-UBE2Q2 |
| HiC_scaffold_7 | 10290141 | FDR | T | C | downstream; intergenic | CBRO_00009717; CBRO_00009716-CBRO_00009717 | Nfkbie; SLC35B2-Nfkbie |
| HiC_scaffold_7 | 10290142 | FDR | G | C | downstream; intergenic | CBRO_00009717; CBRO_00009716-CBRO_00009717 | Nfkbie; SLC35B2-Nfkbie |
| HiC_scaffold_7 | 10290165 | FDR | A | G | downstream; intergenic | CBRO_00009717; CBRO_00009716-CBRO_00009717 | Nfkbie; SLC35B2-Nfkbie |
| HiC_scaffold_7 | 10290166 | FDR | T | C | downstream; intergenic | CBRO_00009717; CBRO_00009716-CBRO_00009717 | Nfkbie; SLC35B2-Nfkbie |
| HiC_scaffold_7 | 10290168 | FDR | T | C | downstream; intergenic | CBRO_00009717; CBRO_00009716-CBRO_00009717 | Nfkbie; SLC35B2-Nfkbie |
| HiC_scaffold_7 | 13815058 | FDR | A | G | synonymous; downstream | CBRO_00009805; CBRO_00009804 | Aloxe3; UNKNOWN |
| HiC_scaffold_7 | 13815326 | FDR | C | T | intronic | CBRO_00009805 | Aloxe3 |
| HiC_scaffold_7 | 15349830 | FDR | C | A | intergenic | CBRO_00009834-CBRO_00009835 | Adcy8-efr3b |
| HiC_scaffold_7 | 18378061 | FDR | T | A | intergenic | CBRO_00009902-CBRO_00009903 | Fam84a-DDX1 |

| | | | | | | | |
|---|---|---|---|---|---|---|---|
| **HiC_scaffold_8** | **20263964** | **Bonferroni** | **G** | **A** | **upstream; intergenic** | **CBRO_00010647; CBRO_00010647-CBRO_00010648** | **Srcin1; Srcin1-Srcin1** |
| HiC_scaffold_8 | 31539262 | FDR | G | A | upstream; intergenic | CBRO_00010835; CBRO_00010834-CBRO_00010835 | Gjd3; Gjd3-Gjd3 |
| HiC_scaffold_11 | 3106766 | FDR | T | A | intronic | CBRO_00013361 | prkdc |
| HiC_scaffold_11 | 3138733 | FDR | G | A | intergenic | CBRO_00013361-CBRO_00013362 | prkdc-arhgap29 |
| HiC_scaffold_11 | 5658921 | FDR | A | G | intronic | CBRO_00013404 | KAZN |
| HiC_scaffold_14 | 17556007 | FDR | C | T | intergenic | CBRO_00014134-CBRO_00014135 | UNKNOWN-Abr |
| HiC_scaffold_14 | 17556026 | FDR | C | A | intergenic | CBRO_00014134-CBRO_00014135 | UNKNOWN-Abr |
| HiC_scaffold_16 | 32837191 | FDR | T | C | intronic | CBRO_00003226 | KIF1B |
| HiC_scaffold_16 | 35727503 | FDR | G | C | intergenic | CBRO_00003289-CBRO_00003290 | Pip5k1c-Polr2e |
| HiC_scaffold_16 | 40215889 | FDR | G | A | intergenic | CBRO_00003383-CBRO_00003384 | chst10-UNKNOWN |
| HiC_scaffold_16 | 40300592 | FDR | C | A | intergenic | CBRO_00003384-CBRO_00003385 | UNKNOWN-Carmil3 |
| HiC_scaffold_18 | 26969972 | FDR | T | G | intronic | CBRO_00013239 | CSAD |
| HiC_scaffold_18 | 26970123 | FDR | C | T | synonymous | CBRO_00013239 | CSAD |
| HiC_scaffold_18 | 26970601 | FDR | T | A | intronic | CBRO_00013239 | CSAD |
| HiC_scaffold_18 | 26978410 | FDR | G | A | intronic | CBRO_00013240 | Znf740 |
| HiC_scaffold_20 | 332642 | FDR | G | A | missense | CBRO_00016084 | GTF3C4 |
| HiC_scaffold_20 | 332689 | FDR | A | G | missense | CBRO_00016084 | GTF3C4 |
| HiC_scaffold_20 | 14820437 | FDR | A | T | intronic | CBRO_00016304 | MALT1 |
| HiC_scaffold_20 | 14820448 | FDR | T | C | intronic | CBRO_00016304 | MALT1 |
| HiC_scaffold_24 | 1469530 | FDR | G | T | intergenic | CBRO_00014375-CBRO_00014376 | UNKNOWN-UNKNOWN |
| HiC_scaffold_24 | 3223583 | FDR | T | A | intergenic | CBRO_00014421-CBRO_00014422 | Gal3st3-RIN2 |
| HiC_scaffold_24 | 11618442 | FDR | T | G | intronic | CBRO_00014601 | ABCA4 |
| **HiC_scaffold_24** | **15964553** | **Bonferroni** | **C** | **T** | **intergenic** | **CBRO_00014635-CBRO_00014636** | **Lrfn2-SNX15** |
| HiC_scaffold_27 | 1898180 | FDR | G | A | downstream; intergenic | CBRO_00005887; CBRO_00005886-CBRO_00005887 | UNKNOWN; hoxb13a-UNKNOWN |
| HiC_scaffold_27 | 8137335 | FDR | G | T | intronic | CBRO_00005998 | SMARCA4 |
| HiC_scaffold_27 | 9065056 | FDR | C | A | intergenic | CBRO_00006026-CBRO_00006027 | ANKFN1-ccdc134 |
| HiC_scaffold_27 | 12370585 | FDR | C | T | intergenic | CBRO_00006131-CBRO_00006132 | SHISA9-Desi1 |
| HiC_scaffold_27 | 32078665 | FDR | C | G | intergenic | CBRO_00006685-CBRO_00006686 | med25-Lrrc4b |

| | | | | | | | |
|---|---|---|---|---|---|---|---|
| HiC_scaffold_27 | 34904388 | FDR | A | C | intergenic | CBRO_00006756-CBRO_00006757 | Grin2c-nog3 |
| HiC_scaffold_27 | 35431570 | FDR | G | C | intergenic | CBRO_00006756-CBRO_00006757 | Grin2c-nog3 |
| HiC_scaffold_27 | 35431578 | FDR | C | T | intergenic | CBRO_00006756-CBRO_00006757 | Grin2c-nog3 |
| HiC_scaffold_27 | 35431585 | FDR | A | G | intergenic | CBRO_00006756-CBRO_00006757 | Grin2c-nog3 |
| HiC_scaffold_34 | 16654675 | FDR | G | C | intergenic | CBRO_00001997-CBRO_00001998 | MDFIC2-foxp1b |
| HiC_scaffold_34 | 19393244 | FDR | A | T | upstream; intergenic | CBRO_00002027; CBRO_00002027-CBRO_00002028 | SUOX; SUOX-SUOX |
| HiC_scaffold_34 | 22010499 | FDR | C | T | intronic | CBRO_00002117 | GNAI2 |
| HiC_scaffold_34 | 31220916 | FDR | T | A | upstream; intergenic | CBRO_00002389; CBRO_00002388-CBRO_00002389 | CTTNBP2NL; Kcnd3-CTTNBP2NL |
| HiC_scaffold_34 | 37769304 | FDR | A | C | intergenic | CBRO_00002519-CBRO_00002520 | ASIC2-asic1 |
| HiC_scaffold_37 | 5963405 | FDR | T | C | intergenic | CBRO_00011020-CBRO_00011021 | C14orf93-pim2 |
| HiC_scaffold_37 | 11017168 | FDR | G | A | intergenic | CBRO_00011155-CBRO_00011156 | GALNT12-elp2 |
| HiC_scaffold_37 | 13822135 | FDR | A | G | upstream; intergenic | CBRO_00011221; CBRO_00011220-CBRO_00011221 | SATB1; KCNH8-SATB1 |
| HiC_scaffold_37 | 13823678 | FDR | G | A | upstream; intergenic | CBRO_00011221; CBRO_00011220-CBRO_00011221 | SATB1; KCNH8-SATB1 |
| HiC_scaffold_37 | 13832007 | FDR | T | A | missense | CBRO_00011221 | SATB1 |
| HiC_scaffold_37 | 16920863 | FDR | T | C | intergenic | CBRO_00011259-CBRO_00011260 | CSMD1-UNKNOWN |
| **HiC_scaffold_37** | **18591438** | **Bonferroni** | **G** | **A** | **intergenic** | **CBRO_00011301-CBRO_00011302** | **cck-trim71** |
| HiC_scaffold_37 | 18591463 | FDR | C | T | intergenic | CBRO_00011301-CBRO_00011302 | cck-trim71 |
| HiC_scaffold_37 | 18596716 | FDR | A | T | intergenic | CBRO_00011301-CBRO_00011302 | cck-trim71 |
| HiC_scaffold_40 | 5885291 | FDR | G | T | downstream; intergenic | CBRO_00016614; CBRO_00016613-CBRO_00016614 | C14orf93 homolog; HTR2A-C14orf93 homolog |
| HiC_scaffold_43 | 2568535 | FDR | A | G | intergenic | CBRO_00008246-CBRO_00008247 | UNKNOWN-Gpr68 |
| HiC_scaffold_44 | 25886134 | FDR | A | C | intergenic | CBRO_00007276-CBRO_00007277 | RAPGEF2-QDPR |
| HiC_scaffold_45 | 885834 | FDR | A | C | upstream; intergenic | CBRO_00018766; CBRO_00018766-CBRO_00018767 | Mog; Mog-EPHB4 |
| HiC_scaffold_45 | 2213441 | FDR | G | T | intronic | CBRO_00018814 | Nlrp12 |
| HiC_scaffold_46 | 856248 | FDR | A | G | intergenic | CBRO_00007439-CBRO_00007440 | UNKNOWN-NLRP12 |
| HiC_scaffold_46 | 1232350 | FDR | G | A | intronic | CBRO_00007448 | NEB |
| HiC_scaffold_46 | 30183758 | FDR | C | G | intergenic | CBRO_00008059-CBRO_00008060 | TFRC-Rgs11 |

| | | | | | | | |
|---|---|---|---|---|---|---|---|
| HiC_scaffold_46 | 32048848 | FDR | A | C | intronic | CBRO_00008105 | Hsd17b7 |
| HiC_scaffold_46 | 32050109 | FDR | G | T | synonymous | CBRO_00008105 | Hsd17b7 |
| **HiC_scaffold_46** | **35151009** | **Bonferroni** | **T** | **C** | **downstream; intergenic** | **CBRO_00008165; CBRO_00008165-CBRO_00008166** | **Klf9; Klf9-Tsen15** |
| HiC_scaffold_46 | 35163681 | FDR | T | C | downstream; downstream; intergenic | CBRO_00008166; CBRO_00008167; CBRO_00008166-CBRO_00008167 | Tsen15; UNKNOWN; Tsen15-UNKNOWN |
| HiC_scaffold_46 | 35164267 | FDR | A | G | downstream; downstream; intergenic | CBRO_00008166; CBRO_00008167; CBRO_00008166-CBRO_00008167 | Tsen15; UNKNOWN; Tsen15-UNKNOWN |
| HiC_scaffold_47 | 787141 | FDR | T | G | upstream; intergenic | CBRO_00008838; CBRO_00008837-CBRO_00008838 | Nlrc3; NLRC3-Nlrc3 |
| HiC_scaffold_47 | 4300295 | FDR | G | A | downstream; intergenic | CBRO_00008933; CBRO_00008933-CBRO_00008934 | NEK6; NEK6-Psmb7 |
| HiC_scaffold_47 | 6767766 | FDR | T | C | intergenic | CBRO_00008991-CBRO_00008992 | TACR1-Grk5 |
| HiC_scaffold_52 | 20791197 | FDR | T | A | upstream; intronic | CBRO_00011892; CBRO_00011891 | rabl3; GTF2E1 |
| HiC_scaffold_52 | 22551701 | FDR | G | C | intergenic | CBRO_00011922-CBRO_00011923 | ALS2-Serp2 |
| HiC_scaffold_52 | 31021517 | FDR | C | T | intergenic | CBRO_00012051-CBRO_00012052 | Tmeff2-slc39a10 |
| **HiC_scaffold_53** | **11317840** | **Bonferroni** | **A** | **G** | **intergenic** | **CBRO_00005178-CBRO_00005179** | **Fucolectin-1-Fucolectin-5** |
| HiC_scaffold_53 | 11326035 | FDR | C | T | intergenic | CBRO_00005178-CBRO_00005179 | Fucolectin-1-Fucolectin-5 |
| HiC_scaffold_53 | 11326410 | FDR | G | A | intergenic | CBRO_00005178-CBRO_00005179 | Fucolectin-1-Fucolectin-5 |
| HiC_scaffold_53 | 11331079 | FDR | A | G | intergenic | CBRO_00005178-CBRO_00005179 | Fucolectin-1-Fucolectin-5 |
| HiC_scaffold_53 | 15966447 | FDR | G | A | upstream; downstream; intergenic | CBRO_00005235; CBRO_00005234; CBRO_00005234-CBRO_00005235 | Tmem222; WDTC1; WDTC1-Tmem222 |
| HiC_scaffold_53 | 17413090 | FDR | A | G | missense | CBRO_00005274 | Mag |
| HiC_scaffold_53 | 20715576 | FDR | C | A | intergenic | CBRO_00005380-CBRO_00005381 | Scrt2-Ino80c |
| HiC_scaffold_53 | 20715623 | FDR | G | A | intergenic | CBRO_00005380-CBRO_00005381 | Scrt2-Ino80c |
| HiC_scaffold_53 | 20715851 | FDR | A | G | intergenic | CBRO_00005380-CBRO_00005381 | Scrt2-Ino80c |
| HiC_scaffold_53 | 27386094 | FDR | G | T | intronic | CBRO_00005625 | Arhgef1 |
| HiC_scaffold_53 | 27396961 | FDR | T | A | intronic | CBRO_00005625 | Arhgef1 |
| HiC_scaffold_53 | 27398605 | FDR | T | G | downstream; intergenic | CBRO_00005625; CBRO_00005625-CBRO_00005626 | Arhgef1; Arhgef1-CD79A |
| HiC_scaffold_53 | 33282501 | FDR | A | G | intergenic | CBRO_00005732-CBRO_00005733 | mios-GLCCI1 |
| HiC_scaffold_53 | 39228193 | FDR | T | C | intergenic | CBRO_00005830-CBRO_00005831 | UNKNOWN-GnRHR2 |

| | | | | | | | |
|---|---|---|---|---|---|---|---|
| **HiC_scaffold_53** | **39228264** | **Bonferroni** | **C** | **T** | **intergenic** | **CBRO_00005830-CBRO_00005831** | **UNKNOWN-GnRHR2** |
| HiC_scaffold_53 | 39228942 | FDR | A | T | intergenic | CBRO_00005830-CBRO_00005831 | UNKNOWN-GnRHR2 |
| HiC_scaffold_53 | 39279263 | FDR | G | T | intronic | CBRO_00005832 | IGDCC3 |
| HiC_scaffold_53 | 39770914 | FDR | A | T | intronic | CBRO_00005849 | Cpne4 |
| HiC_scaffold_611 | 5621 | FDR | A | T | intergenic | CHR_START-CBRO_00020243 | CHR_START-fzdz-a |
| HiC_scaffold_611 | 5625 | FDR | G | T | intergenic | CHR_START-CBRO_00020243 | CHR_START-fzdz-a |
| HiC_scaffold_611 | 5634 | FDR | T | A | intergenic | CHR_START-CBRO_00020243 | CHR_START-fzdz-a |
| HiC_scaffold_1053 | 3494 | FDR | A | G | downstream; intergenic | CBRO_00020503; CHR_START-CBRO_00020503 | UBE2G2; CHR_START-UBE2G2 |
| HiC_scaffold_1133 | 9946 | FDR | A | G | intergenic | . | . |
| HiC_scaffold_1371 | 7318 | FDR | C | T | upstream; intergenic | CBRO_00021026; CHR_START-CBRO_00021026 | UNKNOWN; CHR_START-UNKNOWN |
| **HiC_scaffold_1848** | **40119** | **Bonferroni** | **C** | **A** | **intergenic** | **.** | **.** |
| **HiC_scaffold_1848** | **40465** | **Bonferroni** | **T** | **A** | **intergenic** | **.** | **.** |
| **HiC_scaffold_1848** | **40590** | **Bonferroni** | **T** | **C** | **intergenic** | **.** | **.** |
| HiC_scaffold_1848 | 40877 | FDR | T | C | intergenic | . | . |
| HiC_scaffold_1848 | 41351 | FDR | T | C | intergenic | . | . |
| HiC_scaffold_2220 | 10128 | FDR | G | T | intergenic | . | . |
| **HiC_scaffold_4461** | **12939** | **Bonferroni** | **T** | **A** | **intergenic** | **.** | **.** |
| HiC_scaffold_4665 | 13941 | FDR | C | T | intergenic | . | . |
| HiC_scaffold_6275 | 6000 | FDR | C | A | intergenic | . | . |
| HiC_scaffold_6337 | 5745 | FDR | T | G | intronic | CBRO_00021217 | PKP3 |
| HiC_scaffold_6769 | 2796 | FDR | G | A | intergenic | . | . |
| HiC_scaffold_6963 | 5970 | FDR | C | A | intergenic | . | . |
| HiC_scaffold_6963 | 6101 | FDR | A | G | intergenic | . | . |
| HiC_scaffold_9280 | 3448 | FDR | G | A | intergenic | . | . |
| HiC_scaffold_9949 | 52 | FDR | C | T | intergenic | . | . |
| HiC_scaffold_10928 | 3575 | FDR | G | A | downstream; intergenic | CBRO_00021896; CHR_START-CBRO_00021896 | CYP2A10; CHR_START-CYP2A10 |
| HiC_scaffold_11921 | 5560 | FDR | A | T | intergenic | . | . |
| HiC_scaffold_12068 | 2929 | FDR | G | T | intergenic | . | . |

| | | | | | | | |
|---|---|---|---|---|---|---|---|
| **HiC_scaffold_12778** | **1456** | **Bonferroni** | **T** | **A** | **missense** | **CBRO_00022026** | **COL8A1** |
| HiC_scaffold_17578 | 180 | FDR | T | G | intergenic | . | . |
| **HiC_scaffold_18999** | **1084** | **Bonferroni** | **A** | **G** | **intergenic** | **.** | **.** |

**Table S4. SNPs found to be strongly associated with growth SnpEff** (107)**.** SNPs that were identified as being strongly associated with both growth and composite fitness are italicized, and those that remain significant after a Bonferroni correction are bolded.

| Scaffold | Position | Significance | REF | ALT | Variant Type | Gene Identifier | Gene Card |
|---|---|---|---|---|---|---|---|
| HiC_scaffold_4 | 8897671 | FDR | A | T | intergenic | CBRO_00012254-CBRO_00012255 | Megf10-UNKNOWN |
| HiC_scaffold_4 | 16057698 | FDR | C | A | intergenic | CBRO_00012386-CBRO_00012387 | CCND2-Mlycd |
| HiC_scaffold_4 | 29273446 | FDR | T | C | synonymous | CBRO_00012620 | CKAP5 |
| HiC_scaffold_4 | 29273458 | FDR | C | T | synonymous | CBRO_00012620 | CKAP5 |
| HiC_scaffold_5 | 18259775 | FDR | C | A | upstream; intergenic | CBRO_00001229; CBRO_00001229-CBRO_00001230 | AP1S2; AP1S2-phka2 |
| *HiC_scaffold_5* | *18306419* | *FDR* | *C* | *G* | *upstream; intergenic* | *CBRO_00001232; CBRO_00001231-CBRO_00001232* | *xlrs1; PPEF2-xlrs1* |
| *HiC_scaffold_5* | *18306428* | *FDR* | *A* | *T* | *upstream; intergenic* | *CBRO_00001232; CBRO_00001231-CBRO_00001232* | *xlrs1; PPEF2-xlrs1* |
| *HiC_scaffold_5* | *18307019* | *FDR* | *G* | *T* | *intronic* | *CBRO_00001232* | *xlrs1* |
| *HiC_scaffold_5* | *18307030* | *FDR* | *G* | *A* | *intronic* | *CBRO_00001232* | *xlrs1* |
| HiC_scaffold_5 | 36619253 | FDR | T | C | intergenic | CBRO_00001583-CBRO_00001584 | Chst12-ZDHHC13 |
| *HiC_scaffold_7* | *13815058* | *FDR* | *A* | *G* | *synonymous; downstream* | *CBRO_00009805; CBRO_00009804* | *Aloxe3; UNKNOWN* |
| HiC_scaffold_7 | 13823565 | FDR | T | C | intronic | CBRO_00009806 | Fbxo30 |
| HiC_scaffold_7 | 13824467 | FDR | A | G | missense | CBRO_00009806 | Fbxo30 |
| HiC_scaffold_7 | 19371997 | FDR | C | T | upstream; intergenic | CBRO_00009922; CBRO_00009921-CBRO_00009922 | ELOVL4; TENT5A-ELOVL4 |
| HiC_scaffold_7 | 19372002 | FDR | T | G | upstream; intergenic | CBRO_00009922; CBRO_00009921-CBRO_00009922 | ELOVL4; TENT5A-ELOVL4 |
| HiC_scaffold_8 | 20265076 | FDR | T | C | upstream; intergenic | CBRO_00010647; CBRO_00010647-CBRO_00010648 | Srcin1; Srcin1-Srcin1 |
| HiC_scaffold_8 | 20265098 | FDR | G | C | upstream; intergenic | CBRO_00010647; CBRO_00010647-CBRO_00010648 | Srcin1; Srcin1-Srcin1 |
| HiC_scaffold_8 | 20278571 | FDR | G | A | intergenic | CBRO_00010647-CBRO_00010648 | Srcin1-Srcin1 |
| HiC_scaffold_9 | 15585466 | FDR | C | G | missense | CBRO_00004552 | Tmem260 |
| HiC_scaffold_9 | 18453213 | FDR | A | G | intergenic | CBRO_00004639-CBRO_00004640 | Bub1b-PAK6 |
| HiC_scaffold_9 | 28127377 | FDR | C | T | intergenic | CBRO_00004857-CBRO_00004858 | METTL21E-RASA3 |
| HiC_scaffold_10 | 193812 | FDR | C | G | intergenic | CBRO_00018931-CBRO_00018932 | Spsb4-UNKNOWN |

| | | | | | | | |
|---|---|---|---|---|---|---|---|
| HiC_scaffold_11 | 25632195 | FDR | C | T | intergenic | CBRO_00013717-CBRO_00013718 | CDH10-Cdh6 |
| HiC_scaffold_11 | 25632258 | FDR | C | T | intergenic | CBRO_00013717-CBRO_00013718 | CDH10-Cdh6 |
| HiC_scaffold_11 | 25632641 | FDR | A | G | intergenic | CBRO_00013717-CBRO_00013718 | CDH10-Cdh6 |
| HiC_scaffold_14 | 14624430 | FDR | T | C | intergenic | CBRO_00014084-CBRO_00014085 | KDM6B-FGF11 |
| HiC_scaffold_18 | 26970449 | FDR | C | T | intronic | CBRO_00013239 | CSAD |
| *HiC_scaffold_27* | *8137335* | *FDR* | *G* | *T* | *intronic* | *CBRO_00005998* | *SMARCA4* |
| HiC_scaffold_27 | 21919164 | FDR | G | T | synonymous | CBRO_00006396 | SSTR2 |
| HiC_scaffold_29 | 2136546 | FDR | A | T | upstream; intergenic | CBRO_00016347; CBRO_00016347-CBRO_00016348 | RAPGEF6; RAPGEF6-ACSL6 |
| HiC_scaffold_29 | 2147361 | FDR | C | T | intergenic | CBRO_00016347-CBRO_00016348 | RAPGEF6-ACSL6 |
| HiC_scaffold_31 | 6226140 | FDR | A | C | intronic | CBRO_00017224 | ranbp9 |
| HiC_scaffold_34 | 7439419 | FDR | G | T | intergenic | CBRO_00001828-CBRO_00001829 | rnf152-CAMTA1 |
| HiC_scaffold_34 | 30571660 | FDR | C | A | intronic | CBRO_00002374 | SHMT2 |
| HiC_scaffold_40 | 4693917 | FDR | G | A | intronic | CBRO_00016589 | SLC37A1 |
| HiC_scaffold_40 | 4694015 | FDR | T | C | synonymous | CBRO_00016589 | SLC37A1 |
| HiC_scaffold_40 | 4723358 | FDR | A | G | intronic | CBRO_00016591 | UBXN4 |
| HiC_scaffold_40 | 4732538 | FDR | T | C | intronic | CBRO_00016591 | UBXN4 |
| HiC_scaffold_40 | 4734825 | FDR | G | T | intronic | CBRO_00016591 | UBXN4 |
| HiC_scaffold_40 | 4780518 | FDR | G | C | intronic | CBRO_00016592 | ITGB2 |
| HiC_scaffold_40 | 5016538 | FDR | C | A | upstream; intergenic | CBRO_00016599; CBRO_00016599-CBRO_00016600 | RRP1B; RRP1B-ITGB2 |
| HiC_scaffold_43 | 26869231 | FDR | C | G | synonymous | CBRO_00008677 | lrpprc |
| HiC_scaffold_43 | 27800569 | FDR | C | T | downstream; intergenic | CBRO_00008685; CBRO_00008685-CBRO_00008686 | timp3; timp3-ETV6 |
| HiC_scaffold_44 | 19344526 | FDR | C | T | intergenic | CBRO_00007178-CBRO_00007179 | ATP11C-sox3 |
| HiC_scaffold_46 | 16495639 | FDR | G | A | intronic | CBRO_00007743 | PHLPP1 |
| HiC_scaffold_46 | 16510323 | FDR | G | A | intronic | CBRO_00007743 | PHLPP1 |
| HiC_scaffold_46 | 16512668 | FDR | T | A | intronic | CBRO_00007743 | PHLPP1 |
| **HiC_scaffold_46** | **16512886** | **Bonferroni** | **T** | **A** | **intronic** | **CBRO_00007743** | **PHLPP1** |
| HiC_scaffold_46 | 16513809 | FDR | T | C | synonymous | CBRO_00007743 | PHLPP1 |
| HiC_scaffold_52 | 19031083 | FDR | T | A | intergenic | CBRO_00011872-CBRO_00011873 | NRP2-MREG |

| | | | | | | | |
|---|---|---|---|---|---|---|---|
| HiC_scaffold_52 | 19031216 | FDR | A | T | intergenic | CBRO_00011872-CBRO_00011873 | NRP2-MREG |
| ***HiC_scaffold_1848*** | ***40119*** | ***Bonferroni*** | ***C*** | ***A*** | ***intergenic*** | **.** | **.** |
| ***HiC_scaffold_1848*** | ***40465*** | ***Bonferroni*** | ***T*** | ***A*** | ***intergenic*** | **.** | **.** |
| *HiC_scaffold_1848* | *40590* | *FDR* | *T* | *C* | *intergenic* | . | . |
| *HiC_scaffold_1848* | *40877* | *FDR* | *T* | *C* | *intergenic* | . | . |
| *HiC_scaffold_1848* | *41351* | *FDR* | *T* | *C* | *intergenic* | . | . |
| **HiC_scaffold_7644** | **5971** | **Bonferroni** | **T** | **G** | **intergenic** | **.** | **.** |
| HiC_scaffold_12681 | 4019 | FDR | T | C | upstream; intergenic | CBRO_00022068; CBRO_00022068-CHR_END | UNKNOWN; UNKNOWN-CHR_END |

1187 **Table S5. Gene ontology term enrichment for genes associated with growth.**

| Functional Category | Enrichment FDR | Genes in list | Total genes | Genes |
|---|---|---|---|---|
| Negative regulation of intracellular signal transduction | 0.0259 | 6 | 537 | PPEF2, RNF152, RASA3, RANBP9, PHLPP1, TIMP3 |
| Phosphorus metabolic process | 0.0259 | 17 | 3597 | PHLPP1, CCND2, PAK6, PPEF2, SHMT2, MLYCD, RRP1B, ITGB2, SRCIN1, PHKA2, ELOVL4, BUB1B, RANBP9, TIMP3, CAMTA1, ACSL6, RASA3 |
| Phosphate-containing compound metabolic process | 0.0259 | 17 | 3570 | PHLPP1, CCND2, PAK6, PPEF2, SHMT2, MLYCD, RRP1B, ITGB2, SRCIN1, PHKA2, ELOVL4, BUB1B, RANBP9, TIMP3, CAMTA1, ACSL6, RASA3 |
| Serine family amino acid catabolic process | 0.0259 | 2 | 17 | SHMT2, CSAD |
| Organic acid biosynthetic process | 0.0259 | 6 | 466 | ELOVL4, SHMT2, MLYCD, CHST12, ALOXE3, CSAD |
| Regulation of phosphate metabolic process | 0.0259 | 11 | 1870 | PHLPP1, CCND2, PAK6, PPEF2, SHMT2, RRP1B, ITGB2, SRCIN1, RANBP9, TIMP3, CAMTA1 |
| Nucleoside bisphosphate biosynthetic process | 0.0259 | 3 | 82 | MLYCD, ELOVL4, ACSL6 |
| Ribonucleoside bisphosphate biosynthetic process | 0.0259 | 3 | 82 | MLYCD, ELOVL4, ACSL6 |
| Purine nucleoside bisphosphate biosynthetic process | 0.0259 | 3 | 82 | MLYCD, ELOVL4, ACSL6 |
| Long-chain fatty-acyl-CoA biosynthetic process | 0.0259 | 2 | 19 | ELOVL4, ACSL6 |
| Thioester biosynthetic process | 0.0259 | 3 | 66 | MLYCD, ELOVL4, ACSL6 |
| Positive regulation by host of viral transcription | 0.0259 | 2 | 18 | SMARCA4, RRP1B |
| Sulfur compound biosynthetic process | 0.0259 | 5 | 207 | MLYCD, CHST12, ELOVL4, CSAD, ACSL6 |
| Regulation of phosphorus metabolic process | 0.0259 | 11 | 1872 | PHLPP1, CCND2, PAK6, PPEF2, SHMT2, RRP1B, ITGB2, SRCIN1, RANBP9, TIMP3, CAMTA1 |
| Acyl-CoA biosynthetic process | 0.0259 | 3 | 66 | MLYCD, ELOVL4, ACSL6 |
| Hypothalamus development | 0.0291 | 2 | 22 | NRP2, SOX3 |
| Sulfur compound metabolic process | 0.0312 | 5 | 393 | MLYCD, CHST12, ELOVL4, CSAD, ACSL6 |
| Long-chain fatty-acyl-CoA metabolic process | 0.0343 | 2 | 26 | ELOVL4, ACSL6 |
| Regulation of mitochondrial translation | 0.0343 | 2 | 26 | LRPPRC, SHMT2 |
| Limbic system development | 0.0405 | 3 | 115 | NRP2, KDM6B, SOX3 |
| Acyl-CoA metabolic process | 0.0406 | 3 | 119 | MLYCD, ELOVL4, ACSL6 |
| Thioester metabolic process | 0.0406 | 3 | 119 | MLYCD, ELOVL4, ACSL6 |
| Protein phosphorylation | 0.0412 | 11 | 2093 | PHLPP1, CCND2, PAK6, PPEF2, ITGB2, SRCIN1, PHKA2, BUB1B, RANBP9, TIMP3, RASA3 |
| Modulation by host of viral transcription | 0.0412 | 2 | 33 | SMARCA4, RRP1B |
| Carboxylic acid biosynthetic process | 0.0412 | 5 | 465 | ELOVL4, SHMT2, MLYCD, CHST12, ALOXE3 |
| Modulation of transcription in other organism involved in symbiotic interaction | 0.0412 | 2 | 34 | SMARCA4, RRP1B |
| Modulation by host of symbiont transcription | 0.0412 | 2 | 33 | SMARCA4, RRP1B |
| Cellular protein modification process | 0.0495 | 17 | 4434 | PHLPP1, CCND2, PAK6, PPEF2, RNF152, ITGB2, SPSB4, SRCIN1, PHKA2, FBXO30, KDM6B, BUB1B, RANBP9, TIMP3, CAMTA1, SHMT2, RASA3 |
| Protein modification process | 0.0495 | 17 | 4434 | PHLPP1, CCND2, PAK6, PPEF2, RNF152, ITGB2, SPSB4, SRCIN1, PHKA2, FBXO30, KDM6B, BUB1B, RANBP9, TIMP3, CAMTA1, SHMT2, RASA3 |

1188

**Table S6. Gene ontology term enrichment for genes associated with composite fitness.**

| Functional Category | Enrichment FDR | Genes in list | Total genes | Genes |
|---|---|---|---|---|
| Anterograde trans-synaptic signaling | 0.0060 | 13 | 746 | GRIN2C, SHISA9, ALS2, KIF1B, ASIC1, GNAI2, TACR1, ADCY8, LRFN2, ABR, RAPGEF2, ASIC2, PIP5K1C |
| Synaptic signaling | 0.0060 | 13 | 762 | GRIN2C, SHISA9, ALS2, KIF1B, ASIC1, GNAI2, TACR1, ADCY8, LRFN2, ABR, RAPGEF2, ASIC2, PIP5K1C |
| Trans-synaptic signaling | 0.0060 | 13 | 756 | GRIN2C, SHISA9, ALS2, KIF1B, ASIC1, GNAI2, TACR1, ADCY8, LRFN2, ABR, RAPGEF2, ASIC2, PIP5K1C |
| Chemical synaptic transmission | 0.0060 | 13 | 746 | GRIN2C, SHISA9, ALS2, KIF1B, ASIC1, GNAI2, TACR1, ADCY8, LRFN2, ABR, RAPGEF2, ASIC2, PIP5K1C |
| Regulation of I-kappaB kinase/NF-kappaB signaling | 0.0179 | 7 | 241 | NEK6, SLC35B2, MALT1, NLRP12, NLRC3, DDX1, PIM2 |
| Regulation of trans-synaptic signaling | 0.0185 | 9 | 468 | GRIN2C, SHISA9, ASIC1, GNAI2, TACR1, ADCY8, LRFN2, ABR, RAPGEF2 |
| Regulation of cell communication | 0.0185 | 32 | 3903 | NEK6, SLC35B2, MALT1, NLRP12, PPEF2, GRIN2C, NLRC3, SLC39A10, SHISA9, ALS2, RAPGEF2, SMARCA4, MAGI2, RGS11, ARHGEF1, DDX1, PIM2, ASIC1, GNAI2, TACR1, ADCY8, LRFN2, ABR, PTGDR2, CCK, GPR68, MIOS, SCRT2, PSMB7, ARHGAP29, PIP5K1C, GRK5 |
| Regulation of signaling | 0.0185 | 32 | 3952 | NEK6, SLC35B2, MALT1, NLRP12, PPEF2, GRIN2C, NLRC3, SLC39A10, SHISA9, ALS2, RAPGEF2, SMARCA4, MAGI2, RGS11, ARHGEF1, DDX1, PIM2, ASIC1, GNAI2, TACR1, ADCY8, LRFN2, ABR, PTGDR2, CCK, GPR68, MIOS, SCRT2, PSMB7, ARHGAP29, PIP5K1C, GRK5 |
| Modulation of chemical synaptic transmission | 0.0185 | 9 | 467 | GRIN2C, SHISA9, ASIC1, GNAI2, TACR1, ADCY8, LRFN2, ABR, RAPGEF2 |
| Sensory perception of sour taste | 0.0185 | 2 | 5 | ASIC2, ASIC1 |
| Regulation of biological quality | 0.0185 | 34 | 4319 | GRIN2C, KCNH8, SLC39A10, SHISA9, PRKDC, TACR1, SMARCA4, KCND3, ABCA4, TRIM71, KMT2E, TFRC, PIM2, MAG, ASIC2, ASIC1, GNAI2, LRRC4B, HSD17B7, WDTC1, ADCY8, LRFN2, ABR, ALOXE3, CSMD1, CCK, SRCIN1, ALS2, GPR68, RAPGEF2, NEB, PSMB7, NFKBIE, PIP5K1C |
| I-kappaB kinase/NF-kappaB signaling | 0.0185 | 7 | 280 | NEK6, SLC35B2, MALT1, NLRP12, NLRC3, DDX1, PIM2 |
| Positive regulation of catalytic activity | 0.0185 | 17 | 1514 | PPM1K, ALS2, RAPGEF2, MAGI2, SRCIN1, RGS11, ARHGEF1, GNAI2, GTF3C4, RIN2, ARHGAP29, ABR, CCK, SLC39A10, MALT1, ADCY8, NLRP12 |
| Regulation of protein tyrosine phosphatase activity | 0.0216 | 2 | 6 | GNAI2, SLC39A10 |
| Multicellular organismal response to stress | 0.0216 | 4 | 74 | ALS2, ASIC1, TACR1, CCK |
| Positive regulation of molecular function | 0.0270 | 19 | 1901 | PPM1K, MALT1, ALS2, RAPGEF2, SMARCA4, MAGI2, SRCIN1, RGS11, ARHGEF1, GNAI2, GTF3C4, RIN2, ARHGAP29, ADCY8, ABR, CCK, SLC39A10, MED25, NLRP12 |
| Cell-cell signaling | 0.0311 | 18 | 1774 | GRIN2C, SHISA9, ALS2, KIF1B, ASIC1, GNAI2, TACR1, ADCY8, LRFN2, ABR, GRK5, GPR68, SMARCA4, RAPGEF2, MAGI2, ASIC2, PSMB7, PIP5K1C |
| Tachykinin receptor signaling pathway | 0.0314 | 2 | 8 | TACR1, GRK5 |
| Cell proliferation | 0.0355 | 20 | 2165 | TFRC, PIM2, RAPGEF2, CD79A, GNAI2, TACR1, COL8A1, MALT1, SATB1, PTGDR2, CCK, SLC39A10, TRIM71, PRKDC, MED25, KLF9, GRK5, NLRC3, MAGI2, ARHGEF1 |
| Behavioral fear response | 0.0355 | 3 | 39 | ALS2, ASIC1, CCK |
| Response to pH | 0.0355 | 3 | 41 | ASIC1, ASIC2, GPR68 |
| Behavioral defense response | 0.0355 | 3 | 40 | ALS2, ASIC1, CCK |
| Fear response | 0.0355 | 3 | 41 | ALS2, ASIC1, CCK |
| Positive regulation of hydrolase activity | 0.0401 | 11 | 833 | ALS2, RAPGEF2, MAGI2, RGS11, ARHGEF1, RIN2, ARHGAP29, ABR, CCK, SLC39A10, NLRP12 |
| NcRNA transcription | 0.0457 | 4 | 110 | GTF3C4, SMARCA4, POLR2E, GTF2E1 |
| Hexose mediated signaling | 0.0457 | 2 | 13 | SMARCA4, ADCY8 |
| Sugar mediated signaling pathway | 0.0457 | 2 | 13 | SMARCA4, ADCY8 |
| Glucose mediated signaling pathway | 0.0457 | 2 | 13 | SMARCA4, ADCY8 |
| Positive regulation of cell communication | 0.0457 | 18 | 1937 | NEK6, SLC35B2, MALT1, GRIN2C, SLC39A10, ALS2, RAPGEF2, SMARCA4, NLRP12, DDX1, PIM2, GNAI2, TACR1, ADCY8, PTGDR2, GPR68, MIOS, PSMB7 |
| Positive regulation of signaling | 0.0457 | 18 | 1945 | NEK6, SLC35B2, MALT1, GRIN2C, SLC39A10, ALS2, RAPGEF2, SMARCA4, NLRP12, DDX1, PIM2, GNAI2, TACR1, ADCY8, PTGDR2, GPR68, MIOS, PSMB7 |

**Table S7. List of the 31 morphological traits measured for this study, and standard length; corresponding landmark ID's match those shown in Figure S8.**

| Trait Index | Trait Description | Trait Shorthand | Points |
|---|---|---|---|
| 1 | Nasal protrusion | nose | 3-4 |
| 2 | Nasal length | foresnout | 2-5 |
| 3 | Orbit to anal fin insertion | bellylen | 6-15 |
| 4 | Lateral facial length | snoutlen | 2-6 |
| 5 | Upper jaw to pectoral girdle | jaw2pect | 2-14 |
| 6 | Lateral skull length | pmx2add | 2-11 |
| 7 | Premaxilla length | pmxlen | 2-9 |
| 8 | Lower mandible length | jawlen | 1-9 |
| 9 | Jaw joint to orbit | foreeyewidth | 6-9 |
| 10 | Horizontal orbit diameter | eyewidth | 6-8 |
| 11 | Vertical orbit diameter | eyeht | 7-10 |
| 12 | Head height | headht | 7-9 |
| 13 | Suspensorium length | suspensorium | 9-11 |
| 14 | Adductor height | adductorht | 11-12 |
| 15 | Subopercle to pectoral girdle | ad2pect | 11-14 |
| 16 | Pectoral fin insertion width | pectinsertion | 13-14 |
| 17 | Anal to caudal distance | analtocaudal | 15-16 |
| 18 | Caudal peduncle height | caudalpedht | 16-18 |
| 19 | Dorsal to caudal distance | dorsaltocaudal | 18-19 |
| 20 | Body depth | bodydepth | 15-19 |
| 21 | Nasal protrusion angle | nasalangle | 7-5-3 |
| 22 | Premaxilla to orbit angle | topeyeangle | 7-2-10 |
| 23 | Premaxilla to adductor angle | lowereyeangle | 7-2-11 |
| 24 | Dorsal facial length | dorsalsnoutlen | 23-24, 25-26 |
| 25 | Adductor to premaxilla | eyetosnout | 21-24, 25-28 |
| 26 | Neurocranium to premaxilla | headlen | 24-20, 25-29 |
| 27 | Orbit to premaxilla | innereyetosnout | 22-24, 25-27 |
| 28 | Interorbital width | cranialwidth | 22-27 |
| 29 | Orbital neurocranium width | hindeyewidth | 21-28 |
| 30 | Max. neurocranium width | headwidth | 20-29 |
| 31 | Standard length (SL) | SL | 2-17 |

**Table S8. Generalized additive models fitted to composite fitness.** Model fit was assessed using AICc, and Akaike Weights represent proportional model support. A thin plate spline for the two linear discriminant axes s(LD1, LD2) is always included, as is a fixed effect of either experiment (i.e. Martin & Wainwright 2013, Martin and Gould 2020) or Lake (Crescent Pond/Little Lake) or an interaction between the two. In the last two models, Experiment and Lake are included as splines, modeled using a factor smooth (bs = "fs"). The best fit model had 5 estimated degrees of freedom.

| Model | AICc | ΔAICc | Akaike Weights |
|---|---|---|---|
| *Composite ~ s(LD1, LD2) + Experiment + Lake* | *99.114* | *0.000* | *0.825* |
| Composite ~ s(LD1, LD2) + Experiment * Lake | 102.210 | 3.096 | 0.175 |
| Composite ~ s(LD1, LD2) + s(LD1) + s(LD2) + Experiment + Lake | 131.456 | 32.342 | < 0.001 |
| Composite ~ s(LD1, LD2) + s(LD1) + s(LD2) + Experiment * Lake | 135.894 | 36.781 | < 0.001 |
| Composite ~ s(LD1, LD2) + s(LD1, Experiment, bs = "fs") + s(LD2, Experiment, bs = "fs") + Lake | 230.428 | 131.314 | < 0.001 |
| Composite ~ s(LD1, LD2) + s(LD1, Lake, bs = "fs") + s(LD2, Lake, bs = "fs") + Experiment | 230.868 | 131.754 | < 0.001 |

**Table S9. Generalized additive models fitted to growth.** Model fit was assessed using AICc, and Akaike Weights represent proportional model support. A thin plate spline for the two linear discriminant axes s(LD1, LD2) is always included, as is a fixed effect of either experiment (i.e. Martin & Wainwright 2013, Martin and Gould 2020) or Lake (Crescent Pond/Little Lake) or an interaction between the two. In the last two models, Experiment and Lake are included as splines, modeled using a factor smooth (bs = "fs"). The best fit model had 8.93 estimated degrees of freedom.

| Model | AICc | ΔAICc | Akaike Weights |
|---|---|---|---|
| *Growth ~ s(LD1, LD2) + Experiment * Lake* | *-44.658* | *0.000* | *1* |
| Growth ~ s(LD1, LD2) + Experiment + Lake | 3.904 | 48.562 | < 0.001 |
| Growth ~ s(LD1, LD2) + s(LD1) + s(LD2) + Experiment * Lake | 46.249 | 90.907 | < 0.001 |
| Growth ~ s(LD1, LD2) + s(LD1) + s(LD2) + Experiment + Lake | 89.121 | 133.779 | < 0.001 |
| Growth ~ s(LD1, LD2) + s(LD1, Lake, bs = "fs") + s(LD2, Lake, bs = "fs") + Experiment | 690.379 | 735.038 | < 0.001 |
| Growth ~ s(LD1, LD2) + s(LD1, Experiment, bs = "fs") + s(LD2, Experiment, bs = "fs") + Lake | 693.748 | 738.406 | < 0.001 |

**Table S10. Generalized additive models fitted to survival.** Model fit was assessed using AICc, and Akaike Weights represent proportional model support. A thin plate spline for the two linear discriminant axes s(LD1, LD2) is always included, as is a fixed effect of either experiment (i.e. Martin & Wainwright 2013, Martin and Gould 2020) or Lake (Crescent Pond/Little Lake) or an interaction between the two. In the last two models, Experiment and Lake are included as splines, modeled using a factor smooth (bs = "fs"). The best fit model had 5 estimated degrees of freedom.

| Model | AICc | ΔAICc | Akaike Weights |
|---|---|---|---|
| *Survival ~ s(LD1, LD2) + Experiment + Lake* | *141.057* | *0.000* | *0.849* |
| Survival ~ s(LD1, LD2) + Experiment * Lake | 144.504 | 3.447 | 0.151 |
| Survival ~ s(LD1, LD2) + s(LD1) + s(LD2) + Experiment + Lake | 173.399 | 32.342 | < 0.001 |
| Survival ~ s(LD1, LD2) + s(LD1) + s(LD2) + Experiment * Lake | 178.189 | 37.132 | < 0.001 |
| Survival ~ s(LD1, LD2) + s(LD1, Experiment, bs = "fs") + s(LD2, Experiment, bs = "fs") + Lake | 273.547 | 132.490 | < 0.001 |
| Survival ~ s(LD1, LD2) + s(LD1, Lake, bs = "fs") + s(LD2, Lake, bs = "fs") + Experiment | 273.694 | 132.637 | < 0.001 |

**Table S11. Generalized additive models fitted to growth including SNPs most strongly associated with composite fitness.** Model fit was assessed using AICc, and Akaike Weights represent proportional model support. The best fit model for composite fitness using morphology alone (see Table S8) was used as the base model. The SNPs that were most strongly associated with composite fitness (following a Bonferroni correction) were included as fixed effects, modeled as splines using a factor smooth, treating genotype as an ordered factor. Note that three SNPs were excluded due to their close proximity to other SNPs that were more strongly associated. All SNPs were considered individually, as well as all SNPs together. We were unable to assess all possible combinations of SNPs due to the vast number of potential models given the number of SNPs under consideration; rather, we fit one final model that only included SNPs found to be significant in the full model. In turn this model led to a substantial improvement in AICc. The best fit model had 20.29 estimated degrees of freedom.

| **Model** | **AICc** | **ΔAICc** | **Akaike Weights** |
|---|---|---|---|
| *Composite Fitness ~ s(LD1, LD2) + Experiment + Lake + s(Site1) + s(Site2) + s(Site6) + s(Site7) + s(Site8) + s(Site9) + s(Site10)* | *4.586* | *0.000* | *0.999* |
| Composite Fitness ~ s(LD1, LD2) + Experiment + Lake + s(Site1) + s(Site2) + s(Site3) + s(Site4) + s(Site5) + s(Site6) + s(Site7) + s(Site8) + s(Site9) + s(Site10) | 40.876 | 36.290 | < 0.001 |
| Composite Fitness ~ s(LD1, LD2) + Experiment + Lake + s(Site3) | 55.588 | 51.001 | < 0.001 |
| Composite Fitness ~ s(LD1, LD2) + Experiment + Lake + s(Site7) | 58.386 | 53.800 | < 0.001 |
| Composite Fitness ~ s(LD1, LD2) + Experiment + Lake + s(Site4) | 65.453 | 60.867 | < 0.001 |
| Composite Fitness ~ s(LD1, LD2) + Experiment + Lake + s(Site2) | 71.245 | 66.658 | < 0.001 |
| Composite Fitness ~ s(LD1, LD2) + Experiment + Lake + s(Site5) | 72.329 | 67.743 | < 0.001 |
| Composite Fitness ~ s(LD1, LD2) + Experiment + Lake + s(Site1) | 73.671 | 69.085 | < 0.001 |
| Composite Fitness ~ s(LD1, LD2) + Experiment + Lake + s(Site8) | 74.413 | 69.827 | < 0.001 |
| Composite Fitness ~ s(LD1, LD2) + Experiment + Lake + s(Site9) | 74.680 | 70.094 | < 0.001 |
| Composite Fitness ~ s(LD1, LD2) + Experiment + Lake + s(Site10) | 88.977 | 84.391 | < 0.001 |
| Composite Fitness ~ s(LD1, LD2) + Experiment + Lake + s(Site6) | 90.427 | 85.841 | < 0.001 |
| Composite Fitness ~ s(LD1, LD2) + Experiment + Lake | 99.114 | 94.527 | < 0.001 |

Note: Site1 = HiC_Scaffold_1:43866598, Site2 = HiC_Scaffold_53:11317840, Site3 = HiC_Scaffold_46:35151009, Site4 = HiC_Scaffold_8:20263964, Site5 = 37:18591438, Site5 = HiC_Scaffold_37:18591438, Site6 = HiC_Scaffold_24:15964553, Site7 = HiC_Scaffold_1848:40590, Site8 = HiC_Scaffold_4461:12939, Site9 = HiC_Scaffold_12778:1456, Site10 = HiC_Scaffold_18999:1084

**Table S12. Generalized additive models fitted to growth including SNPs most strongly associated with growth.** Model fit was assessed using AICc, and Akaike Weights represent proportional model support. The best fit model for growth using morphology alone (see Table S9) was used as the base model. Each of the four SNPs that were most strongly associated with growth (following a Bonferroni correction) were included as fixed effects, modeled as splines using a factor smooth, treating genotype as an ordered factor. All SNPs were considered individually, as well as all possible combinations. This was only feasible due to the small number of SNPs assessed (four). The best fit model had 7.97 estimated degrees of freedom.

| Model | AICc | ΔAICc | Akaike Weights |
|---|---|---|---|
| Growth ~ s(LD1, LD2) + Experiment * Lake + s(Site3) + s(Site4) | -67.649 | 0.000 | 0.490 |
| Growth ~ s(LD1, LD2) + Experiment * Lake + s(Site3) | -65.634 | 2.015 | 0.179 |
| Growth ~ s(LD1, LD2) + Experiment * Lake + s(Site1) | -64.161 | 3.488 | 0.086 |
| Growth ~ s(LD1, LD2) + Experiment * Lake + s(Site1) + s(Site3) | -63.926 | 3.723 | 0.076 |
| Growth ~ s(LD1, LD2) + Experiment * Lake + s(Site1) + s(Site2) | -63.861 | 3.788 | 0.074 |
| Growth ~ s(LD1, LD2) + Experiment * Lake + s(Site2) + s(Site4) | -63.503 | 4.146 | 0.062 |
| Growth ~ s(LD1, LD2) + Experiment * Lake + s(Site2) | -61.849 | 5.800 | 0.027 |
| Growth ~ s(LD1, LD2) + Experiment * Lake + s(Site1) + s(Site4) | -58.044 | 9.604 | 0.004 |
| Growth ~ s(LD1, LD2) + Experiment * Lake + s(Site4) | -56.068 | 11.581 | 0.001 |
| Growth ~ s(LD1, LD2) + Experiment * Lake + s(Site1) + s(Site3) + s(Site4) | -54.878 | 12.770 | < 0.001 |
| Growth ~ s(LD1, LD2) + Experiment * Lake + s(Site1) + s(Site2) + s(Site4) | -54.509 | 13.140 | < 0.001 |
| Growth ~ s(LD1, LD2) + Experiment * Lake + s(Site2) + s(Site3) | -47.602 | 20.047 | < 0.001 |
| Growth ~ s(LD1, LD2) + Experiment * Lake | -44.658 | 22.990 | < 0.001 |
| Growth ~ s(LD1, LD2) + Experiment * Lake + s(Site1) + s(Site2) + s(Site3) | -41.689 | 25.960 | < 0.001 |
| Growth ~ s(LD1, LD2) + Experiment * Lake + s(Site1) + s(Site2) + s(Site3) + s(Site4) | -29.801 | 37.847 | < 0.001 |

Note: Site1 = HiC_Scaffold_46:16512886, Site2 = HiC_Scaffold_1848:40119, Site3 = HiC_Scaffold_1848:40465, Site4 = HiC_Scaffold_7644:5971

**Table S13. Summary statistics for fitness networks constructed using adaptive loci.** Results for networks using all three measures of fitness (composite fitness, survival, and growth) are reported. Networks were constructed from random draws of five SNPs from either Standing genetic variation (SGV), introgression, or *de novo* mutations. The scaled number of accessible paths was calculated by dividing the number of accessible paths between generalists and specialists by the number of nodes present in a given fitness network.

| Fitness Metric | Trajectory | Source | Number of Nodes in Network | | | Number of Edges in Network | | | Number of Accessible Paths | | | Scaled Number of Accessible Paths | | | Distance of Shortest Accesible Path | | |
|---|---|---|---|---|---|---|---|---|---|---|---|---|---|---|---|---|---|
| | | | Median | Mean | SE | Median | Mean | SE | Median | Mean | SE | Median | Mean | SE | Median | Mean | SE |
| Composite | AtoM | SGV | 59.000 | 59.233 | 10.955 | 110.000 | 110.254 | 28.461 | 1.000 | 2.585 | 8.488 | 0.019 | 0.043 | 0.128 | 3.000 | 3.185 | 1.048 |
| | | Introgression | 28.000 | 28.026 | 7.456 | 43.000 | 44.459 | 16.704 | 1.000 | 1.890 | 6.686 | 0.043 | 0.069 | 0.220 | 3.000 | 2.914 | 0.892 |
| | | SGV + Introgression | 51.000 | 50.180 | 12.763 | 92.000 | 92.442 | 30.504 | 1.000 | 5.404 | 75.895 | 0.026 | 0.087 | 0.930 | 3.000 | 3.107 | 0.945 |
| | AtoP | SGV | 61.000 | 61.324 | 9.101 | 116.000 | 117.164 | 24.262 | 1.000 | 4.015 | 21.691 | 0.019 | 0.063 | 0.293 | 4.000 | 3.978 | 1.316 |
| | | Introgression | 46.000 | 46.785 | 11.442 | 77.000 | 80.066 | 28.504 | 1.000 | 1.664 | 2.741 | 0.026 | 0.036 | 0.047 | 3.000 | 3.248 | 1.025 |
| | | *De novo* | 48.000 | 47.373 | 9.243 | 83.000 | 83.082 | 24.048 | 1.000 | 2.039 | 5.624 | 0.026 | 0.042 | 0.098 | 3.000 | 3.495 | 1.052 |
| | | SGV + Introgression | 57.000 | 56.858 | 12.003 | 107.000 | 105.897 | 31.286 | 1.000 | 3.589 | 19.955 | 0.020 | 0.059 | 0.295 | 4.000 | 3.701 | 1.088 |
| | | SGV + *De novo* | 58.000 | 57.200 | 9.633 | 108.500 | 107.732 | 25.493 | 1.000 | 4.396 | 40.886 | 0.020 | 0.076 | 0.728 | 4.000 | 3.768 | 1.159 |
| Survival | AtoM | SGV | 62.000 | 61.752 | 9.036 | 136.000 | 136.282 | 29.143 | 1.000 | 309.508 | 4922.357 | 0.022 | 4.189 | 65.732 | 3.000 | 3.502 | 1.469 |
| | | Introgression | 27.500 | 27.920 | 7.145 | 46.000 | 48.345 | 17.452 | 1.000 | 2.491 | 7.478 | 0.043 | 0.089 | 0.240 | 3.000 | 2.922 | 0.952 |
| | | SGV + Introgression | 51.000 | 50.655 | 12.569 | 103.000 | 104.784 | 35.887 | 1.000 | 31.986 | 284.777 | 0.029 | 0.477 | 3.852 | 3.000 | 3.264 | 1.204 |
| | AtoP | SGV | 61.000 | 61.313 | 9.191 | 131.500 | 134.025 | 28.533 | 3.000 | 358.756 | 3156.552 | 0.054 | 5.721 | 51.543 | 5.000 | 5.163 | 2.077 |
| | | Introgression | 47.000 | 47.954 | 11.559 | 92.000 | 94.270 | 33.744 | 1.000 | 15.053 | 113.473 | 0.031 | 0.244 | 1.630 | 4.000 | 4.081 | 1.626 |
| | | *De novo* | 48.000 | 47.875 | 9.159 | 96.000 | 95.836 | 28.763 | 1.000 | 99.206 | 1933.358 | 0.031 | 1.550 | 29.317 | 4.000 | 4.058 | 1.690 |
| | | SGV + Introgression | 58.000 | 57.379 | 11.275 | 124.000 | 123.244 | 35.495 | 2.000 | 153.381 | 1199.043 | 0.038 | 2.255 | 17.255 | 5.000 | 4.861 | 1.948 |
| | | SGV + *De novo* | 58.000 | 57.572 | 9.406 | 127.000 | 124.970 | 29.966 | 2.000 | 143.683 | 1432.083 | 0.045 | 2.121 | 20.358 | 4.000 | 4.696 | 1.848 |
| Growth | AtoM | SGV | 38.000 | 38.166 | 6.678 | 48.000 | 47.959 | 12.495 | 1.000 | 1.142 | 0.443 | 0.027 | 0.031 | 0.012 | 2.000 | 2.347 | 0.655 |
| | | Introgression | 17.000 | 17.670 | 4.154 | 16.000 | 16.227 | 5.546 | 1.000 | 1.011 | 0.120 | 0.059 | 0.061 | 0.021 | 2.000 | 2.151 | 0.440 |
| | | SGV + Introgression | 31.000 | 31.104 | 7.998 | 35.000 | 36.299 | 13.914 | 1.000 | 1.111 | 0.376 | 0.033 | 0.038 | 0.016 | 2.000 | 2.265 | 0.553 |
| | AtoP | SGV | 38.000 | 37.975 | 6.154 | 52.000 | 51.120 | 12.469 | 1.000 | 1.316 | 0.749 | 0.028 | 0.035 | 0.020 | 2.000 | 2.861 | 1.143 |
| | | Introgression | 27.500 | 28.513 | 7.232 | 31.000 | 33.080 | 12.378 | 1.000 | 1.115 | 0.359 | 0.037 | 0.042 | 0.016 | 2.000 | 2.248 | 0.453 |
| | | *De novo* | 32.000 | 31.402 | 5.488 | 38.000 | 38.112 | 9.874 | 1.000 | 1.104 | 0.339 | 0.032 | 0.036 | 0.011 | 2.000 | 2.329 | 0.624 |
| | | SGV + Introgression | 33.000 | 34.295 | 7.648 | 44.500 | 43.807 | 14.444 | 1.000 | 1.205 | 0.590 | 0.031 | 0.037 | 0.018 | 2.000 | 2.500 | 0.816 |
| | | SGV + *De novo* | 36.000 | 35.389 | 5.713 | 45.000 | 45.326 | 11.109 | 1.000 | 1.154 | 0.519 | 0.029 | 0.033 | 0.015 | 2.000 | 2.571 | 0.812 |

**Table S14. Results of pairwise comparisons using a non-parametric Kruskal-Wallis test for measures of network size (number of nodes and number of edges), using the samples for composite fitness and survival.** *P*-values corrected for multiple tests using the false discovery rate. Medians, means, and SE for each group reported in Table S13.

| | | Number of Nodes in Network | | Number of Edges in Network | |
|---|---|---|---|---|---|
| | Pairwise Comparison | Generalist To Molluscivore | Generalist to Scale-eater | Generalist To Molluscivore | Generalist to Scale-eater |
| Composite Fitness & Survival | SGV - Introgression | < 0.0001 | < 0.0001 | < 0.0001 | < 0.0001 |
| | SGV - SGV + Introgression | < 0.0001 | < 0.0001 | < 0.0001 | < 0.0001 |
| | Introgression - SGV + Introgression | < 0.0001 | < 0.0001 | < 0.0001 | < 0.0001 |
| | SGV - *De novo* | - | < 0.0001 | - | < 0.0001 |
| | SGV - SGV + *De novo* | - | < 0.0001 | - | < 0.0001 |
| | *De novo* - SGV + *De novo* | - | < 0.0001 | - | < 0.0001 |
| | *De novo* - SGV + Introgression | - | < 0.0001 | - | < 0.0001 |
| | *De novo* - Introgression | - | 0.6921 | - | 0.1128 |
| | Introgression - SGV + *De novo* | - | < 0.0001 | - | < 0.0001 |
| | SGV + *De novo* - SGV + Introgression | - | 0.3068 | - | 0.0831 |

**Table S15. Results of pairwise comparisons using a non-parametric Kruskal-Wallis test for measures of network size (number of nodes and number of edges), using the samples for growth.** *P*-values corrected for multiple tests using the false discovery rate. Medians, means, and SE for each group reported in Table S13.

| | | Number of Nodes in Network | | Number of Edges in Network | |
|---|---|---|---|---|---|
| | Pairwise Comparison | Generalist To Molluscivore | Generalist to Scale-eater | Generalist To Molluscivore | Generalist to Scale-eater |
| Growth | SGV - Introgression | < 0.0001 | < 0.0001 | < 0.0001 | < 0.0001 |
| | SGV - SGV + Introgression | < 0.0001 | < 0.0001 | < 0.0001 | < 0.0001 |
| | Introgression - SGV + Introgression | < 0.0001 | < 0.0001 | < 0.0001 | < 0.0001 |
| | SGV - *De novo* | - | < 0.0001 | - | < 0.0001 |
| | SGV - SGV + *De novo* | - | 0.0014 | - | 0.0002 |
| | *De novo* - SGV + *De novo* | - | < 0.0001 | - | < 0.0001 |
| | *De novo* - SGV + Introgression | - | 0.0002 | - | 0.0001 |
| | *De novo* - Introgression | - | < 0.0001 | - | < 0.0001 |
| | Introgression - SGV + *De novo* | - | < 0.0001 | | < 0.0001 |
| | *SGV + De novo* - SGV + Introgression | - | 0.0590 | - | 0.1498 |

**Table S16. Results of pairwise comparisons using a non-parametric Kruskal-Wallis test for differences in the relative number of accessible paths between generalists and specialists in networks constructed using different sources of genetic variation using either composite fitness, growth, or survival as our measure of fitness.** *P*-values corrected for multiple tests using the false discovery rate. Medians, means, and SE for each group reported in Table S13.

| | Pairwise Comparison | Generalist To Molluscivore | Generalist to Scale-eater |
|---|---|---|---|
| Composite Fitness | SGV - Introgression | < 0.0001 | < 0.0001 |
| | SGV - SGV + Introgression | < 0.0001 | 0.7060 |
| | Introgression - SGV + Introgression | < 0.0001 | < 0.0001 |
| | SGV - *De novo* | - | < 0.0001 |
| | SGV - SGV + *De novo* | - | 0.0679 |
| | *De novo* - SGV + *De novo* | - | < 0.0001 |
| | *De novo* - SGV + Introgression | - | < 0.0001 |
| | *De novo* - Introgression | - | 0.0911 |
| | Introgression - SGV + *De novo* | - | < 0.0001 |
| | *SGV + De novo* - SGV + Introgression | - | 0.1232 |
| | Pairwise Comparison | Generalist To Molluscivore | Generalist to Scale-eater |
| Growth | SGV - Introgression | < 0.0001 | < 0.0001 |
| | SGV - SGV + Introgression | < 0.0001 | 0.0145 |
| | Introgression - SGV + Introgression | < 0.0001 | < 0.0001 |
| | SGV - *De novo* | - | < 0.0001 |
| | SGV - SGV + *De novo* | - | 0.5854 |
| | *De novo* - SGV + *De novo* | - | < 0.0001 |
| | *De novo* - SGV + Introgression | - | 0.0996 |
| | *De novo* - Introgression | - | 0.0001 |
| | Introgression - SGV + *De novo* | - | < 0.0001 |
| | *SGV + De novo* - SGV + Introgression | - | 0.0385 |
| | Pairwise Comparison | Generalist To Molluscivore | Generalist to Scale-eater |
| Survival | SGV - Introgression | < 0.0001 | 0.0425 |
| | SGV - SGV + Introgression | 0.0004 | 0.3872 |
| | Introgression - SGV + Introgression | < 0.0001 | 0.0468 |
| | SGV - *De novo* | - | 0.0757 |
| | SGV - SGV + *De novo* | - | 0.7967 |
| | *De novo* - SGV + *De novo* | - | 0.0148 |
| | *De novo* - SGV + Introgression | - | 0.1450 |
| | *De novo* - Introgression | - | 0.5277 |
| | Introgression - SGV + *De novo* | - | 0.0036 |
| | *SGV + De novo* - SGV + Introgression | - | 0.3122 |

**Table S17. Results of pairwise comparisons using a non-parametric Kruskal-Wallis test for differences in the length of the shortest accessible paths between generalists and specialists in networks constructed using different sources of genetic variation using either composite fitness, growth, or survival as our measure of fitness.** *P*-values corrected for multiple tests using the false discovery rate. Medians, means, and SE for each group reported in Table S13.

| | Pairwise Comparison | Generalist To Molluscivore | Generalist to Scale-eater |
|---|---|---|---|
| Composite Fitness | SGV - Introgression | < 0.0001 | < 0.0001 |
| | SGV - SGV + Introgression | 0.0002 | 0.0020 |
| | Introgression - SGV + Introgression | 0.3294 | < 0.0001 |
| | SGV - *De novo* | - | < 0.0001 |
| | SGV - SGV + *De novo* | - | 0.0232 |
| | *De novo* - SGV + *De novo* | - | < 0.0001 |
| | *De novo* - SGV + Introgression | - | 0.0024 |
| | *De novo* - Introgression | - | 0.0002 |
| | Introgression - SGV + *De novo* | - | < 0.0001 |
| | SGV + *De novo* - SGV + Introgression | - | 0.3535 |
| | Pairwise Comparison | Generalist To Molluscivore | Generalist to Scale-eater |
| Growth | SGV - Introgression | < 0.0001 | < 0.0001 |
| | SGV - SGV + Introgression | 0.0182 | 0.0073 |
| | Introgression - SGV + Introgression | < 0.0001 | 0.0215 |
| | SGV - *De novo* | - | < 0.0001 |
| | SGV - SGV + *De novo* | - | 0.0309 |
| | *De novo* - SGV + *De novo* | - | 0.0003 |
| | *De novo* - SGV + Introgression | - | 0.0775 |
| | *De novo* - Introgression | - | 0.3384 |
| | Introgression - SGV + *De novo* | - | 0.0001 |
| | SGV + *De novo* - SGV + Introgression | - | 0.3562 |
| | Pairwise Comparison | Generalist To Molluscivore | Generalist to Scale-eater |
| Survival | SGV - Introgression | < 0.0001 | < 0.0001 |
| | SGV - SGV + Introgression | 0.0028 | 0.1279 |
| | Introgression - SGV + Introgression | < 0.0001 | < 0.0001 |
| | SGV - *De novo* | - | < 0.0001 |
| | SGV - SGV + *De novo* | - | 0.0152 |
| | *De novo* - SGV + *De novo* | - | < 0.0001 |
| | *De novo* - SGV + Introgression | - | < 0.0001 |
| | *De novo* - Introgression | - | 0.4422 |
| | Introgression - SGV + *De novo* | - | < 0.0001 |
| | SGV + *De novo* - SGV + Introgression | - | 0.1454 |